

Artificial Intelligence in *Gastroenterology*

Artif Intell Gastroenterol 2021 April 28; 2(2): 10-68



A**I****G**

Artificial Intelligence in Gastroenterology

Contents**Bimonthly Volume 2 Number 2 April 28, 2021****REVIEW**

- 10** Artificial intelligence in rectal cancer
Yakar M, Etiz D
- 27** Artificial intelligence in gastrointestinal radiology: A review with special focus on recent development of magnetic resonance and computed tomography
Chang KP, Lin SH, Chu YW

MINIREVIEWS

- 42** Clinical value of artificial intelligence in hepatocellular carcinoma: Current status and prospect
Yi PS, Hu CJ, Li CH, Yu F
- 56** Artificial intelligence for pancreatic cancer detection: Recent development and future direction
Laoveeravat P, Abhyankar PR, Brenner AR, Gabr MM, Habr FG, Atsawarungrangkit A

ABOUT COVER

Editorial Board Member of *Artificial Intelligence in Gastroenterology*, Xavier Delgado, MD, PhD, Associate Professor, Chairman, Chief Doctor, Lecturer, Surgeon, Surgical Oncologist, Department of Surgery, Centre Médico Chirurgical Volta, La Chaux de Fonds 2300, Switzerland. ex.delgado@yahoo.com

AIMS AND SCOPE

The primary aim of *Artificial Intelligence in Gastroenterology* (AIG, *Artif Intell Gastroenterol*) is to provide scholars and readers from various fields of artificial intelligence in gastroenterology with a platform to publish high-quality basic and clinical research articles and communicate their research findings online.

AIG mainly publishes articles reporting research results obtained in the field of artificial intelligence in gastroenterology and covering a wide range of topics, including artificial intelligence in gastrointestinal cancer, liver cancer, pancreatic cancer, hepatitis B, hepatitis C, nonalcoholic fatty liver disease, inflammatory bowel disease, irritable bowel syndrome, and *Helicobacter pylori* infection.

INDEXING/ABSTRACTING

There is currently no indexing.

RESPONSIBLE EDITORS FOR THIS ISSUE

Production Editor: *Jia-Hui Li*, Production Department Director: *Xiang Li*, Editorial Office Director: *Jin-Lei Wang*.

NAME OF JOURNAL

Artificial Intelligence in Gastroenterology

ISSN

ISSN 2644-3236 (online)

LAUNCH DATE

July 28, 2020

FREQUENCY

Bimonthly

EDITORS-IN-CHIEF

Rajvinder Singh, Ferruccio Bonino

EDITORIAL BOARD MEMBERS

<https://www.wjgnet.com/2644-3236/editorialboard.htm>

PUBLICATION DATE

April 28, 2021

COPYRIGHT

© 2021 Baishideng Publishing Group Inc

INSTRUCTIONS TO AUTHORS

<https://www.wjgnet.com/bpg/gerinfo/204>

GUIDELINES FOR ETHICS DOCUMENTS

<https://www.wjgnet.com/bpg/GerInfo/287>

GUIDELINES FOR NON-NATIVE SPEAKERS OF ENGLISH

<https://www.wjgnet.com/bpg/gerinfo/240>

PUBLICATION ETHICS

<https://www.wjgnet.com/bpg/GerInfo/288>

PUBLICATION MISCONDUCT

<https://www.wjgnet.com/bpg/gerinfo/208>

ARTICLE PROCESSING CHARGE

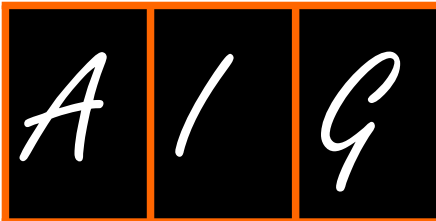
<https://www.wjgnet.com/bpg/gerinfo/242>

STEPS FOR SUBMITTING MANUSCRIPTS

<https://www.wjgnet.com/bpg/GerInfo/239>

ONLINE SUBMISSION

<https://www.f6publishing.com>



Artificial intelligence in rectal cancer

Melek Yakar, Durmus Etiz

ORCID number: Melek Yakar 0000-0002-9042-9489; Durmus Etiz 0000-0002-2225-0364.

Author contributions: Yakar M and Etiz D collected data and wrote the manuscript; Etiz D formatted and revised the article.

Conflict-of-interest statement: No conflict of interest has been declared by the authors.

Open-Access: This article is an open-access article that was selected by an in-house editor and fully peer-reviewed by external reviewers. It is distributed in accordance with the Creative Commons Attribution NonCommercial (CC BY-NC 4.0) license, which permits others to distribute, remix, adapt, build upon this work non-commercially, and license their derivative works on different terms, provided the original work is properly cited and the use is non-commercial. See: <http://creativecommons.org/licenses/by-nc/4.0/>

Manuscript source: Invited manuscript

Specialty type: Oncology

Country/Territory of origin: Turkey

Peer-review report's scientific quality classification

Grade A (Excellent): 0

Grade B (Very good): 0

Melek Yakar, Durmus Etiz, Department of Radiation Oncology, Eskisehir Osmangazi University Faculty of Medicine, Eskisehir 26040, Turkey

Melek Yakar, Durmus Etiz, Eskisehir Osmangazi University Center of Research and Application for Computer Aided Diagnosis and Treatment in Health, Eskisehir 26040, Turkey

Corresponding author: Melek Yakar, MD, Assistant Professor, Department of Radiation Oncology, Eskisehir Osmangazi University Faculty of Medicine, No. 4 Odunpazari, Eskisehir 26040, Turkey. mcakcay@ogu.edu.tr

Abstract

Accurate and rapid diagnosis is essential for correct treatment in rectal cancer. Determining the optimal treatment plan for a patient with rectal cancer is a complex process, and the oncological results and toxicity are not the same in every patient with the same treatment at the same stage. In recent years, the increasing interest in artificial intelligence in all fields of science has also led to the development of innovative tools in oncology. Artificial intelligence studies have increased in many steps from diagnosis to follow-up in rectal cancer. It is thought that artificial intelligence will provide convenience in many ways from personalized treatment to reducing the workload of the physician. Prediction algorithms can be standardized by sharing data between centers, diversifying data, and creating big data.

Key Words: Rectal cancer; Artificial intelligence; Deep learning; Machine learning

©The Author(s) 2021. Published by Baishideng Publishing Group Inc. All rights reserved.

Core Tip: There is a growing interest in the application of artificial intelligence in healthcare to improve disease diagnosis, management, and the development of effective treatments. Considering the large number of patients diagnosed with rectum cancer and a significant amount of data, artificial intelligence is an important tool to improve diagnosis and treatment, follow-up in rectal cancer, develop personalized medicine, improve the quality of life of patients, and reduce unnecessary health expenses.

Citation: Yakar M, Etiz D. Artificial intelligence in rectal cancer. *Artif Intell Gastroenterol* 2021; 2(2): 10-26

Grade C (Good): C
 Grade D (Fair): D, D
 Grade E (Poor): E

Received: January 23, 2021

Peer-review started: January 23, 2021

First decision: February 10, 2021

Revised: March 3, 2021

Accepted: March 15, 2021

Article in press: March 15, 2021

Published online: April 28, 2021

P-Reviewer: Atsawarungruangkit A, Chen P, Shen F, Wang RF

S-Editor: Wang JL

L-Editor: Filipodia

P-Editor: Li JH



URL: <https://www.wjgnet.com/2644-3236/full/v2/i2/10.htm>

DOI: <https://dx.doi.org/10.35712/aig.v2.i2.10>

INTRODUCTION

Artificial intelligence (AI) is the computer science that tries to imitate human-like intelligence in machines by using computer software and algorithms to perform certain tasks without direct human stimuli^[1,2]. Machine learning (ML) is a subset of AI that uses data-driven algorithms that learn to imitate human behavior based on the previous example or experience^[3]. Deep learning (DL) is an ML technique that uses deep neural networks to create a model. Increasing computing power and reducing financial barriers led to the emergence of the DL field^[4].

AI has entered our lives as support in every field. In medicine, it helps clinical processes and management of medical data and information. AI applications assist physicians in diagnosis, research, treatment, and prognosis evaluation of the disease^[5]. Cancer is the most common cause of death in developed countries, and it is estimated that the number of cases will increase even more in aging populations^[6,7]. Therefore, cancer research will continue to be the top priority for saving lives in the next decade.

In oncology, there are typical clinical questions such as ‘Which patients have the highest risk of toxicity?’ and ‘What is the probability of local control and survival in this patient?’. Although clinical studies exist as the gold standard for answers to these questions, clinical studies are costly, slow, and limited to reachable patients. By using the available data, future clinical studies can be better planned, and new findings can be obtained. Evidence-based medicine is based on randomized controlled trials designed with a large patient population. However, the number of clinical and biological parameters that need to be investigated to obtain precise results is increasing day by day^[8].

New and separate approaches are required for all patient subpopulations. Clinicians should use all diagnostic tools (radiological imaging, metabolic imaging, blood and genetic testing, *etc.*) to decide on the appropriate combination of therapy (radiotherapy, chemotherapy, targeted therapy, and immunotherapy). In oncology, AI, a new methodology that provides information using the large data available, has begun to be used to support clinical decisions^[9]. It is important to combine a large and heterogeneous amount of data and create accurate models. Today, AI in oncology has entered our lives in early detection, diagnosis, treatment, and patient follow-up.

Although AI can take place in every step from patient consultation to patient follow-up in rectal cancer and can contribute to the clinician and the society, there are still many challenges and problems to be solved. Big data sets should be created for AI first, and these data sets should be improved. The development of prediction tools with a wide variety of variables and models limits the comparability of existing studies and the use of standards. Prediction algorithms can be standardized by sharing data between centers, diversifying data, and creating big data. In addition, the models can be made clinically applicable by updating the models by entering new data into the models. Today, the accuracy and quality of the data is also of great importance, as no AI algorithm can fix the problems in training data.

Colorectal cancer is the fourth most common type of cancer worldwide, with approximately 800000 new cases diagnosed each year and accounting for approximately 10% of all cancers^[10]. Determining the optimal treatment plan for a patient with rectal cancer is a complex process. In addition to decisions regarding the purpose of rectal cancer surgery, the possible functional consequences of treatment, including the possibility of preserving normal bowel function and genitourinary function, should be considered. Achieving treatment goals and minimal impact on the quality of life can be challenging at the same time, especially for patients with distal rectal cancer. Careful patient selection in terms of specific treatment options and the use of sequential multimodality therapy combining chemoradiotherapy (CRT), chemotherapy (ChT), and surgical treatment are recommended for most patients^[11].

In this review, the role of AI in the diagnosis, treatment, and follow-up of rectal cancer is discussed.

AI IN DIAGNOSIS OF RECTAL CANCER

AI in the detection of lymph node metastasis

Rectal cancers constitute the majority of gastrointestinal tumors. Among the metastatic spreading routes of rectal cancer, lymph node (LN) metastasis is the most important due to its high risk of local recurrence, which leads to poor prognosis^[12]. LN metastasis is an important factor in treatment selection and in predicting prognosis. Preoperative evaluation of metastatic LNs is critical in determining the optimal treatment strategies of rectal cancer cases. Magnetic resonance (MR) imaging is widely used in clinical practice for the diagnosis of metastatic LNs in rectal cancer. MR is considered superior to computed tomography (CT) for better separation of soft tissue. Radiologists often evaluate their shape, boundaries, and signal intensities to identify metastatic LN^[13]. However, correct evaluation in a short time is a great challenge, especially when considering clinics with a high number of cases. Also, when the same MR image is evaluated by different radiologists, very different results can be obtained, which weakens the sensitivity of LN staging^[14-17]. As a result, it is often difficult to accurately determine the presence of LN metastasis. In recent years, the development of DL technology has greatly improved image recognition capability, making it possible to identify specific target areas within an image and allow images to be classified according to specified target features^[18].

According to some studies, although the AI system is more successful than senior physicians in the diagnosis of solid tumors, such as lung, breast, prostate, and thyroid cancer, few studies have yet been reported on the determination of metastatic LN^[19-25]. In the literature, there are studies in which LN metastases have been detected with AI in some cancers such as lung, oral cavity, breast, stomach, and thyroid cancer^[26-30].

In the study conducted by Ding *et al.*^[18] enrolling 414 cases diagnosed with rectal cancer by collecting data from six centers, MR images of the cases were evaluated. Faster region-based convolutional neural network (Faster R-CNN), a new AI algorithm, was evaluated in the study. Patients who underwent surgery with a diagnosis of rectal cancer, whose patient data could be accessed, who did not receive preoperative RT or ChT, and who had MR images at the stage of diagnosis, were included in the study. Radiologist-based diagnosis and pathologist-based diagnosis were compared with the Faster R-CNN system. The number of metastatic LNs diagnosed between two of the three groups was evaluated using the pair-wise correlation analysis. A statistically significant correlation was found in the comparison of both groups [radiologist - Faster R-CNN ($P < 0.001$), pathologist - radiologist ($P = 0.011$), and pathologist - Faster R-CNN ($P < 0.001$). In Faster R-CNN, radiologist, and pathologist LN staging, consistency control was performed between groups, and the highest consistency was found among the Faster R-CNN - radiologist diagnosis ($P = 0.018$). Among the Faster R-CNN - pathologist diagnosis, the P value was 0.039. Among the radiologist - pathologist diagnosis, the P value was 0.043^[18].

In another study by Ding *et al.*^[13], Faster R-CNN was evaluated for metastatic LN prediction, and it aimed to create mathematical nomograms for preoperative metastatic LN prediction. In the prediction of metastatic LN with Faster R-CNN, the MR images of 545 rectal cancer cases who did not receive preoperative RT or ChT were divided into training and validation groups at the rate of 2:1. While creating the nomogram, 183 cases were used as an outcome variable for the presence of LN metastasis, and 153 cases were used as validation for the level of LN metastasis (N1 or N2). Variables were age, gender, preoperatively differentiate grade, metastatic LN obtained by MR, metastatic LN obtained by postoperative pathology, carcinoembryonic antigen (CEA), carbohydrate antigen 19-9. Important variables in predicting metastatic LN positivity with Faster R-CNN in univariate analysis were tumor differentiation grade and CEA level ($P < 0.05$) and age and tumor differentiation gradient in multivariate analysis ($P < 0.001$). Variables determined as important variables in multivariate analysis in MR-based and Faster R-CNN-based metastatic LN prediction were used in nomogram formation; in the MR-based nomogram and the Faster R-CNN-based nomogram, area under curve (AUC) and 95% confidence interval (CI) were found to be 0.856 (0.808-0.905) and 0.862 (0.816-0.909), respectively. According to this study, the Faster R-CNN nomogram appears to be suitable and reliable for predicting the presence of metastatic lymph nodes preoperatively^[13].

Lu *et al.*^[31] evaluated 28080 MR images of 351 rectal cancer cases with Faster R-CNN in their study. Radiologist diagnosis and Faster R-CNN diagnosis were compared using receiver operating characteristic curves (ROC), and the Faster R-CNN ROC was found to be 0.912. It was accepted as a more effective and more objective method. According to the study, the diagnosis was made in 20 s per case with Faster R-CNN, while radiologists made the diagnosis in 600 s per case^[31].

The diagnosis of metastatic LN in rectal cancer is very important for treatment decisions and prognosis. The diagnosis of metastatic LN by MR is largely based on the subjective interpretation of the radiologist. Therefore, it lacks objectivity and reproducibility, although it has a variable diagnostic accuracy. Therefore, using AI systems in the diagnosis phase can contribute to the ability of radiologists to diagnose metastatic LN correctly and in a shorter time and to make a more accurate treatment decision with more accurate tumor, node, metastasis (TNM) staging.

AI in the detection of t stage and tumor differentiation

Choosing the most appropriate treatment is important in rectal cancer. A correct preoperative stage is important for the surgical and neoadjuvant CRT decision. Generally, pathological type, tumor differentiation, infiltration depth, and presence of lymph node metastasis determine the prognosis of the tumor. Therefore, understanding the pathological features of the tumor is very important for the clinical treatment decision^[32]. Radiomic analysis is a tool developed to assess tumor heterogeneity. Radiomics is a noninvasive method that includes high-quality image acquisition, high-throughput quantitative feature extraction, high-dimensional feature extraction, and diagnostic, prognostic, or predictive model generation. Radiomic models using medical images and clinical data have potential in making clinical decision^[33]. The MRI-based radiomic model has been used to differentiate cancer from benign tissue and reflect the histological features of rectal cancer^[34].

In the study conducted by Ma *et al.*^[35] with 152 rectal cancer cases, it aimed to predict the pathological characteristics of the tumor from the MR-based radiomic model. Tumor delineation was performed using 3T MR and high resolution T2-weighted images, and 1029 radiomic features were extracted. Multilayer perceptron, logistic regression (LR), support vector machine (SVM), decision tree (DT), random forest, and K-nearest neighbor (KNN) have been trained and used five-fold cross-validation to create prediction models. The best performance of the radiomics model for the degree of differentiation, T stage, and N stage was obtained by SVM (AUC, 0.862; 95%CI: 0.750–0.967; sensitivity, 83.3%; specificity, 85.0%), multilayer perceptron (AUC, 0.809; 95%CI: 0.690–0.905; sensitivity, 76.2%; specificity, 74.1%), and random forest (AUC, 0.746; 95%CI: 0.622–0.872; sensitivity, 79.3%; specificity, 72.2%). This study demonstrated that the high-resolution T2-weighted images-based radiomics model could serve as pretreatment biomarkers in predicting pathological features of rectal cancer^[35].

AI in detection of distant metastasis

Although advances in treatment strategies and multidisciplinary treatment modalities have reduced local recurrences, distant metastasis continues to be the main cause of treatment failure in patients with rectal cancer^[6]. The most common metastasis site is the liver, and liver metastasis develops in 26.5% of cases within 5 years from diagnosis^[36]. At the stage of diagnosis, there is no liver metastasis in staging, but metachronous liver metastasis (MLM) that develops after initial staging and treatment is thought to be caused by occult metastases and micrometastases^[37,38].

The main treatment strategy for early detected MLM is surgical resection, providing better prognosis and survival as well as a chance for cure compared to other treatments. However, a significant portion of patients with MLM may have lost their surgical chances by the time it is detected^[39]. Although studies are reporting that some variables increase the risk of MLM, there is still no definite marker that can be used to predict the cases that will develop MLM^[40]. Radiomics, which have come to the forefront recently, are obtained by using automated high-throughput extraction of many quantitative properties, offering the chance to capture intratumoral heterogeneity in a noninvasive manner^[41].

Liang *et al.*^[42] predicted MLM by using MR radiomics with ML in a total of 108 rectal cancer cases with 54 MLM and 54 nonmetastatic patients. Radiomics were obtained from venous phase and T2-weighted MR images, and 2058 radiomic properties were evaluated by two separate ML techniques (SVM; LR). After determining the optimal radiomic properties, four groups of models were created: A model containing five radiomic features from T2 weighted MR images (Model_{T2}), a model containing eight radiomic features from venous phase images (Model_{VP}), a model containing the sum of these radiomics, *i.e.* 13 radiomics (Model_{combined}), and a model containing 22 optimal radiomics (Model_{optimal}). Model_{optimal} was determined as the best prediction model with the LR algorithm, and its accuracy, sensitivity, specificity, and AUC were 0.80, 0.83, 0.76, and 0.87, respectively^[42].

Peritoneal carcinomatosis (PC) has a poor prognosis and is considered a terminal stage. PC is present at diagnosis in 5%-10% of the cases diagnosed with colorectal cancer and in 25%-44% of recurrent disease. While a median survival of 33 mo can be achieved with cytoreductive surgery and hyperthermic intraperitoneal ChT, it is < 10 mo if incomplete cytoreductive surgery and diffuse PC are present^[43]. Survival rates can also be high with minimally invasive surgery if PC can be detected early. To predict synchronous PC cases, Yuan *et al*^[44] evaluated 19814 tomography images obtained from 54 PC and 76 non-PC cases in training, and 7837 images obtained from 40 cases as the test group. Using the ResNet-three dimensional (3D) algorithm + SVM algorithm, an accuracy rate of 94.1% was obtained, AUC: 0.92 (0.91-0.94), sensitivity 93.7%, specificity 94.4%, positive predictive value 93.7%, and the negative predictive value was found to be 94.4%. The performance of the algorithm was determined to be better than routine contrast-enhanced CT (AUC: 0.791 *vs* AUC: 0.92)^[44].

Distant metastasis detection can be made more accurately in the earlier period by supporting the physician with the prediction models having high accuracy and this can reduce the cost of treatment while increasing survival rates.

AI IN RECTAL CANCER TREATMENT AND RESPONSE TO TREATMENT

Contouring in radiotherapy

Contouring is an important step that is routinely performed in RT to determine the treatment target and organs at risk (OAR). In a typical clinical workflow, the radiation oncologist needs to contour this target volume and OAR on the simulation images. Contouring is generally performed on CT and less commonly on MR images in clinics where MR guided RT is applied. This contouring process can take hours per patient^[45]. AI can be used both to minimize the differences between physicians and to shorten the duration of this step in RT planning.

Target volume contouring: MR plays an important role in the diagnosis and treatment of rectal cancer^[46]. It guides the physician in identifying the primary tumor, especially in RT planning. Also, MR-based planning increases local control and complete response rates, with the potential to facilitate individualized treatment plans for dose escalation^[47,48]. Also, defining and contouring gross tumor volume (GTV) is time-consuming, and differences in target volume contouring among physicians may cause variability in treatment and different oncological results^[49]. Although the application of Atlas-based automatic segmentation algorithms can reduce the identification time, these methods have low performance in rectal cancer^[50]. The main advantage of DL methods is that they automatically create the most suitable model from the training data sets. In recent years, DL methods have also started to be used in RT steps. Tumor contouring with CNNs has been extensively studied in lung and head and neck cancers and a reduction in contouring time per patient of up to 10 min was observed compared to the contouring time of the physician^[51-53].

In rectum cancer, contouring of GTV and clinical target volume (CTV) were performed using MR and CT images. Wang *et al*^[54] created a DL-based autosegmentation algorithm for GTV delineation using MR (3 Tesla, T2-weighted) images of 93 locally advanced rectal cancer cases. The model was trained in two phases that are tumor recognition and tumor segmentation. Data is divided into 90% training and 10% validation groups for 10-fold cross-validation. Hausdorff distance (HD), average surface distance (ASD), Dice index (DSC), and Jaccard index (JSC) were used to compare and evaluate automatic and manual contouring. For the validation data set, DSC, JSC, HD and ASD (mean \pm SD) were 0.74 ± 0.14 , 0.60 ± 0.16 , 20.44 ± 13.35 , and 3.25 ± 1.69 mm, respectively. In the manual contouring of two radiation oncologists, DSC, JSC, HD and ASD (mean \pm SD) were 0.71 ± 0.13 , 0.57 ± 0.15 , 14.91 ± 7.62 , and 2.67 ± 1.46 mm, respectively. There was no statistically significant difference between the DL-based autosegmentation and manual contouring in terms of DSC ($P = 0.42$), JSC ($P = 0.35$), HD ($P = 0.079$), and ASD ($P = 0.16$) values. Before postprocess (erosion and dilation), that is, correction of contours and removing small isolated points, a statistically significant difference ($P = 0.0027$) was found only in HD. According to this study, results close to manual contouring can be obtained with DL-based algorithms using T2-weighted MR images^[54].

In another study by Trebeschi *et al*^[55], tumor contouring was performed using multiparametric MR images. The study included 140 locally advanced rectal cancer cases, and each case was contoured by two experienced radiologists. In this study, the CNN algorithm was used to function as a voxel classifier. CNN was trained using the

voxel values of the region with and without tumor in MR. In the independent validation data set, the DSC value was determined as 0.68 and 0.70 according to CNN and both radiologists. The AUC value for both radiologists was found to be 0.99. This study showed that DL can perform the correct localization and segmentation of rectal cancer in MRI in most patients^[55].

Song *et al*^[56] evaluated CTV contouring with CNN in 199 rectal cancer cases. For training, validation, and testing, 98 cases, 38 cases, and 63 cases were used, respectively. While volumetric DCS showed the volumetric overlap between automatic segmentation and manual contouring, surface DCS showed the overlap between automatic segmentation and manual contouring surfaces. Two CNN techniques were used in the present study that were DeepLabv3 + and ResUNet, and the volumetric DSC and surface DCS of CTV were 0.88 *vs* 0.87 ($P = 0.0005$) and 0.79 *vs* 0.78 ($P = 0.008$), respectively. According to this study, high quality and shorter CTV contouring can be performed with CNNs^[56]. Target volume contouring studies with AI in rectum cancer are summarized in [Table 1](#).

Contouring of OAR: In radiotherapy, it is necessary to make the contouring of OAR correctly to protect them and to evaluate the toxicity correctly. To fully benefit from the advantages of technological developments in RT planning and devices, OAR must be defined correctly. This step can become a rate limiting step in clinics with a high number of patients. Also, there may be differences among the practitioners, and due to significant anatomical changes (edema, tumor response, weight loss, *etc.*) during the treatment, it may be necessary to make a new plan with new contouring during the treatment. AI, particularly CNN, is a potential tool to reduce the physician's workload and set a standard in contouring. In recent years, DL methods have been widely used in medical applications, and CNN has been used in contouring OAR in head-neck, lung, and prostate cancer^[57-59]. There are also studies on this subject in rectal cancer.

OAR contouring was also evaluated in the study performed by Song *et al*^[56] for CTV contouring. As OAR, small intestine, bladder, and femoral heads were contoured. With ResUNet, both volumetric and surface DSC values in femoral head contouring and surface DSC values in bladder contouring were found to be statistically more significant, and contouring performance was better. Higher volumetric and surface DSC were obtained with DeepLabv3 + for the small intestine^[56].

Men *et al*^[60] conducted a segmentation study using deep dilated CNN based DL technique in both CTV and OAR (bladder, femoral heads, small intestine, and colon). CT images of 278 rectal cancer cases were included in the study. Images of 218 randomly selected cases were used for training, and images of the remaining 60 cases were used for validation. In this study, DSC was also evaluated and for CTV, bladder, left femoral head, right femoral head, small intestine, and colon as 87.7%, 93.4%, 92.1%, 92.3%, 65.3%, and 61.8%. CTV and OAR contouring time per case was found to be 45 s on average^[60].

In another study conducted by Men *et al*^[61], the effect of the patient's position on segmentation accuracy was investigated with CNN. The study included 50 supine and 50 prone cases with planning CT, and three different models were trained: Patients in the same position, patients in different positions, and patients in both positions. Performance evaluation regarding segmentation was performed using DSC and HD for CTV, bladder, and femurs. While the model trained in different positions compared to the model trained in the same position was statistically significantly better for CTV and bladder ($P < 0.05$), it was found to be $P > 0.05$ in femur segmentation. DSC values were 0.84 *vs* 0.74, 0.88 *vs* 0.85, and 0.91 *vs* 0.91 for CTV, bladder, and femurs, respectively. The accuracy rates for the model trained in both positions were similar ($P > 0.05$). The DSC was 0.84, 0.88, and 0.91 for CTV, bladder, and femur, respectively. According to this study, while the patient position is important for CTV and bladder in segmentation with the CNN model, it was not found to be an important factor for the femur^[61]. Studies are summarized in [Table 1](#).

In RT, while providing effective treatment for the tumor, protection of OAR is very important in terms of acute and late side effects. For this, it is an important step to define the tumor volume and OAR correctly and accurately. However, this step requires intensive labor and time and can be rate-limiting. Creating models with DL and using them in clinical practice will ensure standardization among physicians in contouring and accelerate this step.

Radiotherapy planning

Treatment planning is an important step in the RT workflow. Treatment planning has become more sophisticated over the past few decades with the help of computer science, allowing for the minimization of normal tissue damage while providing

Table 1 Target volume and organs at risk contouring with artificial intelligence

Ref.	Number of patients	Imaging method	Contouring	Artificial intelligence method	Results
Wang <i>et al</i> ^[54] , 2018	93	MR (3 Tesla, T2-weighted)	GTV, CTV	CNN	Between deep learning-based autosegmentation and manual contouring DSC ($P = 0.42$), JSC ($P = 0.35$), HD ($P = 0.079$), and ASD ($P = 0.16$); Before postprocess process only in HD ($P = 0.0027$).
Trebeschi <i>et al</i> ^[55] , 2017	140	Multiparametric MRI (1.5 Tesla, T2-weighted)	GTV	CNN	According to CNN and both radiologists in independent validation data set DSC: 0.68 and 0.70; For both radiologists AUC: 0.99.
Song <i>et al</i> ^[56] , 2020	199	CT (3 mm section thickness)	CTV and OAR	CNNs (DeepLabv3+ and ResUNet)	CTV segmentation better with DeepLabv3+ than ResUNet (volumetric DSC, 0.88 <i>vs</i> 0.87, $P = 0.0005$; surface DSC, 0.79 <i>vs</i> 0.78, $P = 0.008$); DeepLabv3+ model segmentation was better in the small intestine, with the ResUNet model, bladder and femoral heads segmentation results were better. In both models, the OAR manual correction time was 4 min.
Men <i>et al</i> ^[60] , 2017	278	CT (5 mm section thickness)	CTV and OAR	CNN (DDCNN)	DSC values; CTV: 87.7%, bladder: 93.4%, left femoral head: 92.1%, right femoral head: 92.3%, small intestine: 65.3%, colon 61.8%.
Men <i>et al</i> ^[61] , 2018	100	CT (3 mm section thickness)	CTV and OAR	CNN	CTV and bladder contouring were better in the model trained in the same position than the model trained in a different position ($P < 0.05$). No statistically significant difference between femoral heads ($P > 0.05$). No statistical difference between accuracy rates in CTV, bladder, and femoral heads segmentation in the model trained in both positions ($P > 0.05$).

AUC: Area under the curve; ASD: Average surface distance; CNN: Convolutional neural network; CT: Computed tomography; CTV: Clinical target volume; DDCNN: Deep dilated convolutional neural network; DSC: Dice similarity coefficient; GTV: Gross tumor volume; HD: Hausdorff distance; JSC: Jaccard index; MRI: Magnetic resonance imaging; OAR: Organs at risk.

adequate tumor dose. As a result, treatment planning has become more labor-intensive and takes hours and sometimes even days for planners. In RT planning, many algorithms have been developed to support planners, and these algorithms focus on automating the planning process and/or optimizing dosimetric changes. These algorithms have contributed to the improvement of treatment planning efficiency and quality^[62]. Planning workflow starts with determining dosimetric requirements regarding target volume and OARs and makes decisions about basic planning parameters, including beam energy, number, and angles, *etc.*, based on the needs of each case. While creating a minimally acceptable plan can be quick, improving a plan is much more difficult. Also, the plan may need to be improved according to the mid-plan result evaluation of the physicians, which causes increased effort and time. Automatic treatment planning systems, from simple automation to AI, are gradually taking their place in planning systems.

The knowledge-based planning system helps to use the previous planning information in the database with ML methods in obtaining the best dose distribution for target volume and OAR. Knowledge-based treatment planning algorithms use geometric and dosimetric information to estimate doses for new patients using the information found in training data. The dose volume histogram prediction model was created by using a knowledge-based treatment planning system, using 80 plans in training, and evaluating 70 plans in the test with simultaneous integrated boost and VMAT techniques. Using this model, the multileaf collimator sequences of 70 clinically validated plans were re-optimized. While doing this, parameters such as field geometry and photon energy were not changed. Dosimetric results were evaluated by comparing dose volume histogram data as homogeneity index, conformal index, hot spots (volumes taking more than 107% of the prescribed dose), mean dose, femoral heads, and bladder mean ($D_{mean_{mesane}}$, $D_{mean_{femoralhead}}$) and 50% of the dose ($D_{50\%bladder}$, $D_{50\%femoralhead}$). Similar conformal index was obtained when comparing the original plan (1.00 ± 0.05 for planning target volume (PTV)_{boost} and 1.03 ± 0.02 for PTV) and the knowledge-based plan (0.99 ± 0.04 for PTV_{boost} and 1.03 ± 0.02 for PTV). Better homogeneity index values were obtained in the knowledge-based plan (0.05 ± 0.01 for PTV_{boost} and 0.26 ± 0.01 for PTV) compared to the original plan (0.06 ± 0.01 for PTV_{boost} and 0.26 ± 0.01 for PTV) ($P < 0.05$). It has been shown that $V_{107\%}$ values in the original plan were higher than the knowledge-based plan. The knowledge-based plan achieved a statistically significant decrease in $D_{50\%femoralhead}$, $D_{mean_{femoralhead}}$, $D_{50\%}$

bladder^r and $D_{\text{mean}_{\text{mesane}}}$ values. According to this study, the knowledge-based planning system provided a statistically significant advantage in some dosimetric data compared to the original plans^[63].

Zhou *et al.*^[64] aimed to develop a DL model for intensity-modulated RT, which provides an estimation of 3D voxel-wise dose distribution. Of the 122 post-op intensity-modulated RT treated cases, the plans of 100 cases were used for training-validation, and the plans of 22 cases were used for testing. To estimate 3D dose distributions, a 3D-DL model named U-Res-Net_B was created^[60]. No statistically significant difference was found between the original plans and the DL model named U-Res-Net_B in terms of dosimetric parameters (homogeneity index, conformal index, V50, and V45 for PTV and OARs). The DSC value of the model was higher than 0.9 for most isodose volumes, and the ratio of 3D gamma passing ranged from 0.81 to 0.90 for PTV and OAR. This study has developed a DL model by considering beam configuration input; this model has shown that it has potential in terms of automated planning for easier clinical evaluation of more comprehensive cases^[64].

Evaluation of chemoradiotherapy response

In locally advanced rectal cancer, neoadjuvant CRT improves local control, disease-free survival, and sphincter preservation rates^[65]. However, tumor regression patterns after neoadjuvant CRT vary widely, from the pathological complete response (pCR) to disease progression. Although cases with pCR have the best survival and tumor control, neoadjuvant CRT can provide pCR in only 10%-30% of cases in locally advanced rectal cancer^[66]. Some studies have shown that cases with pCR have low recurrence rates, and therefore less invasive alternative surgical treatments, such as sphincter-sparing local excision or a watch-and-wait approach, may be more appropriate^[67-70]. Therefore, it is very important to determine the cases that are likely to have a complete clinical response before surgery.

MR, which enables the evaluation of the therapeutic response noninvasively, is promising in the early prediction of pCR. MR images taken at different times of the CRT, including before, during, and after treatment, can be analyzed separately or in combination to provide anatomical and functional information. With the advancement of MR imaging technology, several different sequences can be included in the MR protocol within a reasonable imaging time (< 30 min), and this multiparametric MR can provide comprehensive information to facilitate quantitative radiomic analysis for prediction of tumor response^[71]. Radiomics extracts hundreds of quantitative image features and then uses advanced statistical analysis to classify different groups. Nie *et al.*^[72] predicted patients with pCR after CRT was completed with 80%-90% prediction accuracy of pretreatment multiparametric MRI-based radiomic analysis.

Shi *et al.*^[71] predicted the treatment response with DL from the radiomics they obtained from the MR images taken before treatment and in the middle of treatment (3-4 wk after the start of treatment) in CRT cases with a diagnosis of locally advanced rectal cancer. Of the 51 cases included in the study, 45 cases pre-treatment, 41 cases mid-treatment, and 35 cases both pre-treatment and mid-treatment MR images were available, and the MR protocol was specified as T2, diffusion-weighted imaging with b-values of 0 and 800 s/mm² and dynamic contrast-enhanced. In the surgical specimen performed after CRT, the response of the case depending on the tumor regression grade was determined. Total tumor volume and mean apparent diffusion coefficient (ADC) were measured on MRI. Using Haralick's Gray Level Co-occurrence Matrix was used to distinguish cases with and without pCR, cases with and without good response by applying radiomics using texture, and histogram parameters and CNN. Tumor volume decreased in mid-treatment MRI compared to before, and ADC increased. In predicting the cases with and without pCR with their radiomic features, AUC values were found to be 0.80, 0.82, and 0.86 when the pre-treatment MR, mid-treatment MR, and both MR, respectively, were evaluated together. In cases that respond well and those that do not, these rates were 0.91, 0.92, and 0.93, respectively. When MRIs before and during treatment were evaluated together, AUC was found to be 0.83 in DL prediction of cases with and without pCR^[71].

A study conducted by Fu *et al.*^[73] aimed to obtain and compare handcrafted and DL-based radiomic features from pre-treatment diffusion-weighted imaging-MR images. Forty-three cases that underwent CRT with the diagnosis of locally advanced rectal cancer were included in the study. MRI was taken before treatment in all patients, and total mesorectal excision was applied 6-12 wk after the CRT. GTV from MR images was contoured by an experienced radiation oncologist. Postsurgical cases were grouped as responsive ($n = 22$) and unresponsive ($n = 21$). Handcrafted and DL-based radiomic features were extracted from diffusion-weighted imaging ADC map using traditional computer-aided diagnostic methods and pretrained CNN, respectively. The

ROC curve (AUC) of the model created with handcrafted radiomic features was 0.64, while that of the DL-based model was 0.73. Its statistical significance was found to be better ($P < 0.05$). According to this study, radiomic features obtained from MR images and the algorithm created using DL were shown to be better in predicting CRT response^[73].

In another study by Shayesteh *et al*^[74], 98 cases diagnosed with rectal cancer were included in the study, and MRI was performed 1 wk before the CRT. Radiomics such as density, shape, and texture features were extracted from MR images. For training and validation, 53 and 45 cases, respectively, were used. SVM, Bayesian network, neural network, and KNN algorithms were used one by one and together for predicting response to CRT. Prediction performance was evaluated by AUC. When the algorithms were evaluated separately, the best result was obtained with the Bayesian network algorithm, and the AUC and accuracy rate were 0.75 and 80.9%, respectively. When the algorithms (SVM, neural network, Bayesian network, KNN) were evaluated together, the AUC and accuracy rate were 0.97 and 92.8%, respectively. According to this study, the prediction process can be improved when algorithms are used together^[74].

In another study conducted with 89 cases diagnosed with locally advanced rectal cancer, 66 cases were included in the training group and 23 cases were included in the test group, and resistance prediction to CRT was evaluated. Radiomics obtained from pre-treatment MR, ADC images, and clinical features of the cases were evaluated with the Random Forest Classifier (RFC) algorithm. Of 133 radiomic features and nine clinical features (entropy_{mean}, inverse variance energy_{mean}, small area emphasis, ADC_{min}, ADC_{mean}, sd Ga02, small gradient emphasis, age, and size) were determined as ten important variables. With the RFC algorithm, cases resistant to CRT were estimated with an accuracy rate of 91.3% (88.9% sensitivity and 92.8% specificity, AUC: 0.83)^[75]. According to this study in predicting the response to CRT, when the radiomic and clinical parameters are evaluated together, predictions with high accuracy rates can be obtained. If these resistant cases can be predicted, treatment strategies can be changed, and oncological outcomes can be improved.

In another study conducted with 55 cases diagnosed with locally advanced rectal cancer, radiomics obtained from MRI images taken before, during, and after CRT were evaluated by the RFC algorithm for treatment response prediction. Images of 28 cases from 55 cases were used in the training, and images of 27 cases were used to evaluate the performance of the algorithm. pCR was obtained in 16 cases from all cases, and good results were obtained with the RFC algorithm in predicting pCR with AI (AUC: 0.86, 95% CI: 0.70-0.94). In the prediction of unresponsive cases, AUC was 0.83 (95% CI: 0.71-0.92) with the RFC algorithm^[76].

In the study conducted by Bibault *et al*^[77] with 95 cases diagnosed with T2-4N0-1 rectal cancer, radiomics (1683 radiomic features per case) obtained from CT images before CRT were evaluated together with clinical and treatment data, and the response prediction was made with AI. While radiomics were used with deep neural network and SVM, prediction models were created using only TNM staging in linear regression. pCR was obtained in a total of 23 cases. In prediction with deep neural network, SVM, and LR algorithms, the accuracy rates were 80.0%, 71.5%, and 69.5%, respectively^[77]. In another study, artificial neural network, Naïve Bayes Classifier, KNN, SVM, and multiple LR models were evaluated in the response prediction of 270 locally advanced rectal cancer patients who underwent CRT. The most important factors affecting pCR were post CRT CEA level, the time between CRT and surgery, ChT regimen, clinical nodal status, and nodal stage. The accuracy rates for artificial neural network, KNN, SVM, Naïve Bayes Classifier, and multiple LR were 88%, 80%, 71%, 80%, and 77%, respectively^[78]. Studies evaluating the CRT response with AI in rectal cancer are summarized in [Table 2](#).

Shen *et al*^[79] predicted response to CRT in 169 rectal cancer cases using positron emission tomography (PET)-CT radiomics. A total of 68 features were excluded from the metabolic active tumor site. Estimation was made with the RF algorithm, and the ROC algorithm was used to evaluate the performance. After CRT, pCR was obtained in 22 (13%) cases, and 42 radiomics features were included in the algorithm. Accordingly, the sensitivity, specificity, positive predictive value, negative predictive value, and accuracy were 81.8%, 97.3%, 81.8%, 97.3%, and 95.3%, respectively^[79].

While the correct classification of cases in which pCR is provided helps to identify less invasive therapeutic strategies such as mucosectomy or wait-and-watch, early prediction of cases that do not respond to CRT will also allow these cases to be directed to more effective treatments.

Table 2 Studies of chemoradiotherapy response prediction with artificial intelligence

Ref.	Number of patients	Parameters evaluated	Imaging method	Technique used	Results
Shi <i>et al</i> ^[71] , 2019	51 (90% cases for training and the remaining 10% for testing)	Tumor volume, mean ADC, radiomic	MRI (Pre-CRT and mid-CRT) (T2-DWI, DCE)	CNN	(1) pCR response prediction: (a) Pre-CRT with MR AUC: 0.80; (b) Mid-CRT with MR AUC: 0.82; and (c) Pre- and mid-CRT MR together AUC: 0.86; and (2) Good response to CRT: predicting yes/no: (a) Pre-CRT with MR AUC: 0.91; (b) Mid-CRT with MR AUC: 0.92; and (c) Pre- and mid-CRT MR together AUC: 0.93.
Fu <i>et al</i> ^[73] , 2020	43	Radiomic	MRI (Pre-CRT, DWI)	Handcrafted traditional computer-aided diagnostic method <i>vs</i> deep learning	Deep learning model with handcrafted model CRT response prediction AUC values: 0.64 <i>vs</i> 0.73 ($P < 0.05$)
Shayesteh <i>et al</i> ^[74] , 2019	98 (53 training and 45 validation set)	Radiomic	MRI (1 wk before CRT) (3 Tesla, T2W-weighted)	Machine learning (SVM, BN, NN, KNN)	AUC for the BN algorithm: 74%, accuracy: 79%; When four algorithms were used together, AUC: 97.8% and accuracy rate 92.8%.
Yang <i>et al</i> ^[75] , 2019	89 (66 training and 23 testing)	Radiomic and clinical features	MRI (Pre-CRT) (3 Tesla, T2W, 3 mm section thickness)	RFC	Predicting the accuracy of tumor resistance with RFC 91.3%, AUC: 0.83.
Ferrari <i>et al</i> ^[76] , 2019	55 (28 training, 27 validation)	Radiomic	MR (Pre, Mid, Post RT) (3 Tesla, T2W, 2 mm section thickness)	RFC	(1) Prediction of cases with pCR by RFC; AUC: 0.86; and (2) Prediction of unresponsive cases with RFC; AUC 0.83.
Bibault <i>et al</i> ^[77] , 2018	95	Radiomic, clinical variables	CT	DNN, SVM, LR	CRT response prediction accuracy rates; DNN: 80%; SVM: 71.5% LR: 69.5%.
Huang <i>et al</i> ^[78] , 2020	270 (236 training, 34 validation)	Clinical variables	-	ANN, KNN, SVM, NBC, MLR	pCR prediction accuracy rates and AUC values; ANN: 88%, 0.84 KNN: 80%, 0.74 SVM: 71%, 0.76 NBC: 80%, 0.63 MLR: 83%, 0.77.

ADC: Apparent diffusion coefficient; ANN: Artificial neural network; AUC: Area under the curve; BN: Bayesian network; CNN: Convolutional neural network; CRT: Chemoradiotherapy; CT: Computed tomography; DCE: Dynamic contrast-enhanced; DNN: Deep neural network; DWI: Diffusion-weighted imaging; KNN: K-nearest neighbors; LR: Linear regression; MLR: Multiple logistic regression; MRI: Magnetic resonance imaging; NBC: Naïve bayes classifier; NN: Neural network; pCR: Pathological complete response; RFC: Random forest classifier; SVM: Support vector machine.

Prediction of KRAS mutation in rectal cancer

Kirsten rat sarcoma (KRAS) mutations, which occur in approximately 30%–40% of colorectal cancer, have been indicated as a highly specific negative biomarker for the antibody-targeted therapies to the epidermal growth factor receptor^[80]. Metastatic colorectal cancers with KRAS mutations are resistant to anti-epidermal growth factor receptor targeted therapy. Therefore, the KRAS mutation test has been recommended by the National Comprehensive Cancer Network guidelines to guide targeted therapy for cases diagnosed with metastatic colorectal cancer^[81].

Determination of the KRAS mutation is usually made by pathological examination of the tumor tissue. However, intratumor heterogeneity or heterogeneity of KRAS mutation that can occur between different tumor regions limits histological approaches^[82]. Moreover, the inability to determine mutation status due to poor DNA quality of biopsy samples, difficult to access tissue samples from metastatic colorectal cancers, repeated tumor sampling, and relatively high costs also limit the feasibility of molecular tests to monitor targeted therapy^[83]. Therefore, a relatively simple and noninvasive method for KRAS mutations can be helpful for personalized treatment strategies.

In a study by Cui *et al*^[84], 304 cases with rectal cancer diagnosis from center I (training dataset, $n = 231$; internal validation dataset, $n = 91$) and 86 cases from center II were included as an external validation dataset. It aimed to predict KRAS mutation from T2-weighted image-based radiomics. Subsequently, three classification methods, *i.e.* LR, decision tree, and SVM algorithm, were applied to develop the radiomics signature for KRAS prediction in the training dataset. The predictive performance was evaluated by ROC analysis. A total of seven radiomics properties were accepted as important variables for KRAS prediction, and the best predictor was determined as the SVM. The AUC was found to be 0.722 (95%CI: 0.654–0.790)^[84].

AI IN FOLLOW-UP IN RECTAL CANCER

Treatment toxicity

Effective toxicity estimation and evaluation schemes are required to limit RT-related side effects. High-tech devices and planning systems provide submillimetric precision. However, while giving the desired dose to the target volume, the OARs in its immediate neighborhood may be affected, leading to RT-induced toxicity. Acute toxicity occurs during treatment or within 3 mo of completion of treatment and usually, full recovery takes weeks to months. Late side effects such as fibrosis or RT-induced oncogenesis are generally irreversible and considered progressive over time. When planning RT, its potential benefits should be weighed against the possibility of damaging healthy organs and tissues to maximize the curative response while minimizing the possibility of normal tissue complications. On the other hand, the target volume should not be compromised to preserve OARs. In addition to complex dosimetric data, AI provides the clinician with the ability to predict complications by integrating higher-level information such as detailed clinical and comorbidity data into a more comprehensive and quantitative model^[85].

Dosimetric parameters include dose volume histogram parameters and threshold doses such as maximum point doses. Nondosimetric factors include other variables such as age, gender, and histopathology. Normal tissue complication probability and tumor control probability prediction models focused on using dosimetric parameters alone^[86,87]. Also, the necessity of using nondosimetric parameters has been emphasized in the Quantitative Analysis of Normal Tissue Effects in the Clinic^[88]. Data-driven approaches, on the other hand, aim to determine the model that best fits the input data (called properties or independent variables) and output data (called the response or dependent variable). Toxicity predictors can be examined roughly in three parts as dosimetric, clinical, and image-based.

In rectum cancer RT, toxicity can be predicted in advance with AI-based models, and appropriate dose-area restrictions, additional treatment planning (simultaneous CT, *etc.*), and prophylactic medical support treatments can be reviewed. There are AI studies that predicted rectal toxicity in prostate and cervical cancer radiotherapy, but there are no studies predicting toxicity with AI in rectal cancer radiotherapy^[89-91]. Oyaga-Iriarte *et al*^[92] conducted a study to predict irinotecan toxicity in metastatic colorectal cancer with ML models, and leukopenia was estimated with 76% accuracy, neutropenia 75%, and diarrhea 91%.

The development of prediction tools with a wide variety of variables and models limits the comparability and standard use of existing toxicity studies. Toxicity estimation algorithms can be standardized by sharing data between centers and creating big data. The application of such models is valuable in many different ways for both patients and clinicians.

Survival

In oncological treatments, forecasting is very important in the treatment decision-making process because accurate survival prediction is critical in making palliative/curative treatment decisions. Also, the prediction of remaining life expectancy can be an incentive for patients to live a fuller or more fulfilling life. Survival statistics assist oncologists in making treatment decisions, but these are data from large and heterogeneous groups and are not well suited to predict what will happen to a specific patient. AI algorithms for the prediction of RT and ChT response have received considerable attention recently. In cases diagnosed with cancer, predicting survival is important in improving treatment and providing information to patients and clinicians. Considering the data set of rectal cancer patients with specific demographic, tumor, and treatment information, it is an important issue whether the patient's survival or recurrence can be predicted by any parameter. Today, many hospitals store data in digital media. By evaluating these large data sets with AI techniques, it may be possible to predict treatment outcomes of patients, plan personalized medicine, improve corporate performance, and regulate health insurance.

In a study conducted by Zhao *et al*^[93], survival prediction was made with an ML method in cases with metastatic rectal cancer, and 4098 cases were used in training and 3107 cases were used as test data. A survival prediction nomogram was created. While creating the prediction model, lasso (least absolute shrinkage and selection operator), an ML technique that can lead to superior performance compared to traditional multivariate regression, was used. The model was designed to predict 3-year overall survival. The ML model formed the basis of the nomogram. Important

variables used in the nomogram were age, Charlson-Deyo score, tumor grade, pre-op CEA, liver metastasis, bone metastasis, brain metastasis, lung metastasis, peritoneal metastasis, presence of primary surgery, surgery for the metastatic area, the number of metastatic lymph nodes, and the presence of ChT. The c-index was used to evaluate the performance of the ML technique. Internally validated c-index values were 0.816 (95% CI: 0.813-0.818), 0.789 (95% CI: 0.786-0.790), and 0.778 (95% CI: 0.775-0.780) for 1-, 2-, and 3-year survival, respectively. External validated c-index was 0.811, 0.779, and 0.778 for 1-, 2-, and 3-year survival, respectively^[93]. There was great variation in overall survival times in cases diagnosed with metastatic rectal cancer. Accurate models with ML methods can assist patients and clinicians in setting expectations and clinical decisions in this challenging patient group.

Pham *et al*^[94] used AI to discover DNp73 expression in terms of 5-year overall survival and prognosis in their study with 143 cases diagnosed with rectal cancer. Ten different CNN algorithms were used, and each immunochemical image was resized. For the algorithm, 90% of these images were used in training and 10% as test data, and the accuracy rates of ten algorithms varied between 90%-96%^[94].

Li *et al*^[95] conducted a study with 84 patients diagnosed with locally advanced rectal cancer and predicted survival with radiomics obtained from PET, CT, and PET-CT images with CNN. They compared the CNN method evaluated in the study with the Cox proportional-hazards model and random survival forests method. C-index was used in the performance evaluation of the methods. C-indexes of models created with radiomics obtained from PET, CT, and PET-CT images for Cox proportional-hazards, random survival forests, and CNN were 0.53-0.58-0.60 *vs* 0.58-0.61-0.58 and 0.62-0.60-0.64 respectively, and the best performance was obtained when CNN and PET-CT were used together^[95].

In the study conducted by Oliveira *et al*^[96] to predict the 1-, 2-, 3-, 4-, and 5-year survival of cases with rectal and colon cancer, they evaluated 2221 cases in the test for colon cancer, 20061 cases in training, 551 cases in the test for rectal cancer, and 4962 cases in training. Important variables for colon cancer were determined as age, CEA, CS site-specific factor 2, TNM stage, localization of the primary tumor, and regional lymph nodes. For rectal cancer, important variables were age, tumor extension, tumor size, TNM staging, surgery of the primary tumor, and gender. ML performance was evaluated by the accuracy rate and AUC. Accuracy rates and AUC for predicting survival for colon cancer for 1-, 2-, 3-, 4-, and 5-years were 95.6% (AUC: 0.980), 96.2% (0.984), 96.4% (0.988), 96.6% (0.988), and 96.4% (0.985), respectively, and their mean was 96.2% (0.984). Accuracy rates and AUC for predicting 1-, 2-, 3-, 4-, and 5-year survival for rectal cancer were 94.4% (AUC: 0.957), 94.4% (0.960), 94.0% (0.961), 93.8% (0.963), and 94.5% (0.971), respectively, with a mean of 94.1% (0.960)^[96].

Accurate survival prediction in cancer patients remains a problem due to the increasing heterogeneity and complexity of cancer, treatment options, and different patient characteristics (age, Karnofsky Performance Status Scale, comorbid diseases, *etc.*). If reliable predictions can be achieved with AI, it can help with personalized care and medicine. Studies on AI-based survival prediction are increasing day by day in the literature, and there is still no standard algorithm.

CONCLUSION

In recent years, the increasing interest in AI in all fields of science has led to the development of innovative tools in oncology. The development of prediction tools with a wide variety of variables and models limits the comparison of existing studies and the use of standards.

In order to improve long-term prognosis, it is important to predict the overall survival of patients with a diagnosis of rectal cancer and progression of the disease receiving multimodal treatment. With the evaluation of clinical, radiological, genetic, dosimetric, and epidemiological factors using AI, it is possible to perform accurate predictions to achieve personalized treatment. Given high treatment costs, potential serious toxicity, harms of early progression, and low survival in cases of ineffective treatment, predictive systems with AI are promising. Multicenter studies with large data sets can provide algorithms with higher accuracy rates.

AI technology develops day by day in the realization of human behaviors in oncology and offers more efficient, faster, and lower cost solutions. Both AI and robotic potential are enormous in the follow-up and treatment of rectal cancer. AI and robotics are on the way to becoming a part of our health ecosystem.

REFERENCES

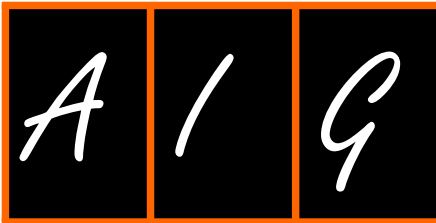
- 1 Meyer P, Noblet V, Mazzara C, Lallement A. Survey on deep learning for radiotherapy. *Comput Biol Med* 2018; **98**: 126-146 [PMID: 29787940 DOI: 10.1016/j.compbiomed.2018.05.018]
- 2 LeCun Y, Bengio Y, Hinton G. Deep learning. *Nature* 2015; **521**: 436-444 [PMID: 26017442 DOI: 10.1038/nature14539]
- 3 Jarrett D, Stride E, Vallis K, Gooding MJ. Applications and limitations of machine learning in radiation oncology. *Br J Radiol* 2019; **92**: 20190001 [PMID: 31112393 DOI: 10.1259/bjr.20190001]
- 4 Boldrini L, Bibault JE, Masciocchi C, Shen Y, Bittner MI. Deep Learning: A Review for the Radiation Oncologist. *Front Oncol* 2019; **9**: 977 [PMID: 31632910 DOI: 10.3389/fonc.2019.00977]
- 5 Makedon F, Karkaletsis V, Maglogiannis I. Overview: Computational analysis and decision support systems in oncology. *Oncol Rep* 2006; **15** Spec no.: 971-974 [PMID: 16525686 DOI: 10.3892/or.15.4.971]
- 6 Siegel RL, Miller KD, Jemal A. Cancer statistics, 2019. *CA Cancer J Clin* 2019; **69**: 7-34 [PMID: 30620402 DOI: 10.3322/caac.21551]
- 7 DeSantis CE, Miller KD, Dale W, Mohile SG, Cohen HJ, Leach CR, Goding Sauer A, Jemal A, Siegel RL. Cancer statistics for adults aged 85 years and older, 2019. *CA Cancer J Clin* 2019; **69**: 452-467 [PMID: 31390062 DOI: 10.3322/caac.21577]
- 8 Bibault JE, Giraud P, Burgun A. Big Data and machine learning in radiation oncology: State of the art and future prospects. *Cancer Lett* 2016; **382**: 110-117 [PMID: 27241666 DOI: 10.1016/j.canlet.2016.05.033]
- 9 Kohane IS, Drazen JM, Campion EW. A glimpse of the next 100 years in medicine. *N Engl J Med* 2012; **367**: 2538-2539 [PMID: 23268669 DOI: 10.1056/NEJMe1213371]
- 10 Tepper J. Gunderson and Tepper's Clinical Radiation Oncology. 5th edition. Elsevier, 2020
- 11 Baxter NN, Garcia-Aguilar J. Organ preservation for rectal cancer. *J Clin Oncol* 2007; **25**: 1014-1020 [PMID: 17350952 DOI: 10.1200/JCO.2006.09.7840]
- 12 Ishihara S, Kawai K, Tanaka T, Kiyomatsu T, Hata K, Nozawa H, Morikawa T, Watanabe T. Oncological Outcomes of Lateral Pelvic Lymph Node Metastasis in Rectal Cancer Treated With Preoperative Chemoradiotherapy. *Dis Colon Rectum* 2017; **60**: 469-476 [PMID: 28383446 DOI: 10.1097/DCR.0000000000000752]
- 13 Ding L, Liu G, Zhang X, Liu S, Li S, Zhang Z, Guo Y, Lu Y. A deep learning nomogram kit for predicting metastatic lymph nodes in rectal cancer. *Cancer Med* 2020; **9**: 8809-8820 [PMID: 32997900 DOI: 10.1002/cam4.3490]
- 14 Beets-Tan RG, Beets GL, Vliegen RF, Kessels AG, Van Boven H, De Bruine A, von Meyenfeldt MF, Baeten CG, van Engelshoven JM. Accuracy of magnetic resonance imaging in prediction of tumour-free resection margin in rectal cancer surgery. *Lancet* 2001; **357**: 497-504 [PMID: 11229667 DOI: 10.1016/s0140-6736(00)04040-x]
- 15 Matsuoka H, Nakamura A, Masaki T, Sugiyama M, Nitatori T, Ohkura Y, Sakamoto A, Atomi Y. Optimal diagnostic criteria for lateral pelvic lymph node metastasis in rectal carcinoma. *Anticancer Res* 2007; **27**: 3529-3533 [PMID: 17972513]
- 16 Cho EY, Kim SH, Yoon JH, Lee Y, Lim YJ, Kim SJ, Baek HJ, Eun CK. Apparent diffusion coefficient for discriminating metastatic from non-metastatic lymph nodes in primary rectal cancer. *Eur J Radiol* 2013; **82**: e662-e668 [PMID: 24016824 DOI: 10.1016/j.ejrad.2013.08.007]
- 17 Kim JH, Beets GL, Kim MJ, Kessels AG, Beets-Tan RG. High-resolution MR imaging for nodal staging in rectal cancer: are there any criteria in addition to the size? *Eur J Radiol* 2004; **52**: 78-83 [PMID: 15380850 DOI: 10.1016/j.ejrad.2003.12.005]
- 18 Ding L, Liu GW, Zhao BC, Zhou YP, Li S, Zhang ZD, Guo YT, Li AQ, Lu Y, Yao HW, Yuan WT, Wang GY, Zhang DL, Wang L. Artificial intelligence system of faster region-based convolutional neural network surpassing senior radiologists in evaluation of metastatic lymph nodes of rectal cancer. *Chin Med J (Engl)* 2019; **132**: 379-387 [PMID: 30707177 DOI: 10.1097/CM9.0000000000000095]
- 19 Gardezi SJS, Elazab A, Lei B, Wang T. Breast Cancer Detection and Diagnosis Using Mammographic Data: Systematic Review. *J Med Internet Res* 2019; **21**: e14464 [PMID: 31350843 DOI: 10.2196/14464]
- 20 Chen CM, Chou YH, Han KC, Hung GS, Tiu CM, Chiou HJ, Chiou SY. Breast lesions on sonograms: computer-aided diagnosis with nearly setting-independent features and artificial neural networks. *Radiology* 2003; **226**: 504-514 [PMID: 12563146 DOI: 10.1148/radiol.2262011843]
- 21 Wang J, Yang X, Cai H, Tan W, Jin C, Li L. Discrimination of Breast Cancer with Microcalcifications on Mammography by Deep Learning. *Sci Rep* 2016; **6**: 27327 [PMID: 27273294 DOI: 10.1038/srep27327]
- 22 Rajpurkar P, Irvin J, Ball RL, Zhu K, Yang B, Mehta H, Duan T, Ding D, Bagul A, Langlotz CP, Patel BN, Yeom KW, Shpanskaya K, Blankenberg FG, Seekins J, Amrhein TJ, Mong DA, Halabi SS, Zucker EJ, Ng AY, Lungren MP. Deep learning for chest radiograph diagnosis: A retrospective comparison of the CheXNeXt algorithm to practicing radiologists. *PLoS Med* 2018; **15**: e1002686 [PMID: 30457988 DOI: 10.1371/journal.pmed.1002686]
- 23 Huang P, Lin CT, Li Y, Tammemagi MC, Brock MV, Atkar-Khattra S, Xu Y, Hu P, Mayo JR, Schmidt H, Gingras M, Pasian S, Stewart L, Tsai S, Seely JM, Manos D, Burrowes P, Bhatia R, Tsao MS, Lam S. Prediction of lung cancer risk at follow-up screening with low-dose CT: a training and validation study of a deep learning method. *Lancet Digit Health* 2019; **1**: e353-e362 [PMID: 32864596 DOI: 10.1016/S2589-7500(19)30159-1]

- 24 **Li H**, Weng J, Shi Y, Gu W, Mao Y, Wang Y, Liu W, Zhang J. An improved deep learning approach for detection of thyroid papillary cancer in ultrasound images. *Sci Rep* 2018; **8**: 6600 [PMID: 29700427 DOI: 10.1038/s41598-018-25005-7]
- 25 **Reda I**, Shalaby A, Elmogy M, Elfotouh AA, Khalifa F, El-Ghar MA, Hosseini-Asl E, Gimelfarb G, Werghe N, El-Baz A. A comprehensive non-invasive framework for diagnosing prostate cancer. *Comput Biol Med* 2017; **81**: 148-158 [PMID: 28063376 DOI: 10.1016/j.combiomed.2016.12.010]
- 26 **Tau N**, Stundzia A, Yasufuku K, Hussey D, Metser U. Convolutional Neural Networks in Predicting Nodal and Distant Metastatic Potential of Newly Diagnosed Non-Small Cell Lung Cancer on FDG PET Images. *AJR Am J Roentgenol* 2020; **215**: 192-197 [PMID: 32348182 DOI: 10.2214/AJR.19.22346]
- 27 **Ariji Y**, Fukuda M, Kise Y, Nozawa M, Yanashita Y, Fujita H, Katsumata A, Ariji E. Contrast-enhanced computed tomography image assessment of cervical lymph node metastasis in patients with oral cancer by using a deep learning system of artificial intelligence. *Oral Surg Oral Med Oral Pathol Oral Radiol* 2019; **127**: 458-463 [PMID: 30497907 DOI: 10.1016/j.oooo.2018.10.002]
- 28 **Ehteshami Bejnordi B**, Veta M, Johannes van Diest P, van Ginneken B, Karssemeijer N, Litjens G, van der Laak JAWM; the CAMELYON16 Consortium, Hermsen M, Manson QF, Balkenhol M, Geessink O, Stathonikos N, van Dijk MC, Bult P, Beca F, Beck AH, Wang D, Khosla A, Gargeya R, Irshad H, Zhong A, Dou Q, Li Q, Chen H, Lin HJ, Heng PA, Haß C, Bruni E, Wong Q, Halici U, Öner MÜ, Cetin-Atalay R, Berseth M, Khvatkov V, Vylegzhanin A, Kraus O, Shaban M, Rajpoot N, Awan R, Sirinukunwattana K, Qaiser T, Tsang YW, Tellez D, Annuschein J, Hufnagl P, Valkonen M, Kartasalo K, Latonen L, Ruusuvoori P, Liimatainen K, Albarqouni S, Mungal B, George A, Demirci S, Navab N, Watanabe S, Seno S, Takenaka Y, Matsuda H, Ahmady Phoulady H, Kovalev V, Kalinovsky A, Liauchuk V, Bueno G, Fernandez-Carrobles MM, Serrano I, Deniz O, Racoceanu D, Venâncio R. Diagnostic Assessment of Deep Learning Algorithms for Detection of Lymph Node Metastases in Women With Breast Cancer. *JAMA* 2017; **318**: 2199-2210 [PMID: 29234806 DOI: 10.1001/jama.2017.14585]
- 29 **Gao Y**, Zhang ZD, Li S, Guo YT, Wu QY, Liu SH, Yang SJ, Ding L, Zhao BC, Lu Y. Deep neural network-assisted computed tomography diagnosis of metastatic lymph nodes from gastric cancer. *Chin Med J (Engl)* 2019; **132**: 2804-2811 [PMID: 31856051 DOI: 10.1097/CM9.0000000000000532]
- 30 **Lee JH**, Ha EJ, Kim JH. Application of deep learning to the diagnosis of cervical lymph node metastasis from thyroid cancer with CT. *Eur Radiol* 2019; **29**: 5452-5457 [PMID: 30877461 DOI: 10.1007/s00330-019-06098-8]
- 31 **Lu Y**, Yu Q, Gao Y, Zhou Y, Liu G, Dong Q, Ma J, Ding L, Yao H, Zhang Z, Xiao G, An Q, Wang G, Xi J, Yuan W, Lian Y, Zhang D, Zhao C, Yao Q, Liu W, Zhou X, Liu S, Wu Q, Xu W, Zhang J, Wang D, Sun Z, Zhang X, Hu J, Zhang M, Zheng X, Wang L, Zhao J, Yang S. Identification of Metastatic Lymph Nodes in MR Imaging with Faster Region-Based Convolutional Neural Networks. *Cancer Res* 2018; **78**: 5135-5143 [PMID: 30026330 DOI: 10.1158/0008-5472.CAN-18-0494]
- 32 **Benson AB**, Venook AP, Al-Hawary MM, Cederquist L, Chen YJ, Ciombor KK, Cohen S, Cooper HS, Deming D, Engstrom PF, Grem JL, Grothey A, Hochster HS, HOFFE S, Hunt S, Kamel A, Kirilcuk N, Krishnamurthi S, Messersmith WA, Meyerhardt J, Mulcahy MF, Murphy JD, Nurkin S, Saltz L, Sharma S, Shibata D, Skibber JM, Sofocleous CT, Stoffel EM, Stotsky-Himelfarb E, Willett CG, Wuthrick E, Gregory KM, Gurski L, Freedman-Cass DA. Rectal Cancer, Version 2.2018, NCCN Clinical Practice Guidelines in Oncology. *J Natl Compr Canc Netw* 2018; **16**: 874-901 [PMID: 30006429 DOI: 10.6004/jnccn.2018.0061]
- 33 **Gillies RJ**, Kinahan PE, Hricak H. Radiomics: Images Are More than Pictures, They Are Data. *Radiology* 2016; **278**: 563-577 [PMID: 26579733 DOI: 10.1148/radiol.2015151169]
- 34 **Gröne J**, Loch FN, Taupitz M, Schmidt C, Kreis ME. Accuracy of Various Lymph Node Staging Criteria in Rectal Cancer with Magnetic Resonance Imaging. *J Gastrointest Surg* 2018; **22**: 146-153 [PMID: 28900855 DOI: 10.1007/s11605-017-3568-x]
- 35 **Ma X**, Shen F, Jia Y, Xia Y, Li Q, Lu J. MRI-based radiomics of rectal cancer: preoperative assessment of the pathological features. *BMC Med Imaging* 2019; **19**: 86 [PMID: 31747902 DOI: 10.1186/s12880-019-0392-7]
- 36 **Akgül Ö**, Çetinkaya E, Ersöz Ş, Tez M. Role of surgery in colorectal cancer liver metastases. *World J Gastroenterol* 2014; **20**: 6113-6122 [PMID: 24876733 DOI: 10.3748/wjg.v20.i20.6113]
- 37 **Kruskal JB**, Thomas P, Kane RA, Goldberg SN. Hepatic perfusion changes in mice livers with developing colorectal cancer metastases. *Radiology* 2004; **231**: 482-490 [PMID: 15128993 DOI: 10.1148/radiol.2312030160]
- 38 **Cuenod C**, Leconte I, Siauve N, Resten A, Dromain C, Poulet B, Frouin F, Clément O, Fria G. Early changes in liver perfusion caused by occult metastases in rats: detection with quantitative CT. *Radiology* 2001; **218**: 556-561 [PMID: 11161178 DOI: 10.1148/radiology.218.2.r01fe10556]
- 39 **McNally SJ**, Parks RW. Surgery for colorectal liver metastases. *Dig Surg* 2013; **30**: 337-347 [PMID: 24051581 DOI: 10.1159/000351442]
- 40 **Zhu D**, Zhong Y, Wu H, Ye L, Wang J, Li Y, Wei Y, Ren L, Xu B, Xu J, Qin X. Predicting metachronous liver metastasis from colorectal cancer using serum proteomic fingerprinting. *J Surg Res* 2013; **184**: 861-866 [PMID: 23721930 DOI: 10.1016/j.jss.2013.04.065]
- 41 **Lambin P**, Leijenaar RTH, Deist TM, Peerlings J, de Jong EEC, van Timmeren J, Sanduleanu S, Larue RTHM, Even AJG, Jochems A, van Wijk Y, Woodruff H, van Soest J, Lustberg T, Roelofs E, van Elmpt W, Dekker A, Mottaghy FM, Wildberger JE, Walsh S. Radiomics: the bridge between medical imaging and personalized medicine. *Nat Rev Clin Oncol* 2017; **14**: 749-762 [PMID: 28018286 DOI: 10.1038/nrco.2017.166]

- 28975929 DOI: [10.1038/nrclinonc.2017.141](https://doi.org/10.1038/nrclinonc.2017.141)]
- 42 **Liang M**, Cai Z, Zhang H, Huang C, Meng Y, Zhao L, Li D, Ma X, Zhao X. Machine Learning-based Analysis of Rectal Cancer MRI Radiomics for Prediction of Metachronous Liver Metastasis. *Acad Radiol* 2019; **26**: 1495-1504 [PMID: [30711405](https://pubmed.ncbi.nlm.nih.gov/30711405/) DOI: [10.1016/j.acra.2018.12.019](https://doi.org/10.1016/j.acra.2018.12.019)]
 - 43 **Razenberg LG**, van Gestel YR, Creemers GJ, Verwaal VJ, Lemmens VE, de Hingh IH. Trends in cytoreductive surgery and hyperthermic intraperitoneal chemotherapy for the treatment of synchronous peritoneal carcinomatosis of colorectal origin in the Netherlands. *Eur J Surg Oncol* 2015; **41**: 466-471 [PMID: [25680955](https://pubmed.ncbi.nlm.nih.gov/25680955/) DOI: [10.1016/j.ejso.2015.01.018](https://doi.org/10.1016/j.ejso.2015.01.018)]
 - 44 **Yuan Z**, Xu T, Cai J, Zhao Y, Cao W, Fichera A, Liu X, Yao J, Wang H. Development and Validation of an Image-based Deep Learning Algorithm for Detection of Synchronous Peritoneal Carcinomatosis in Colorectal Cancer. *Ann Surg* 2020 [PMID: [32694449](https://pubmed.ncbi.nlm.nih.gov/32694449/) DOI: [10.1097/SLA.0000000000004229](https://doi.org/10.1097/SLA.0000000000004229)]
 - 45 **Hong TS**, Tomé WA, Harari PM. Heterogeneity in head and neck IMRT target design and clinical practice. *Radiother Oncol* 2012; **103**: 92-98 [PMID: [22405806](https://pubmed.ncbi.nlm.nih.gov/22405806/) DOI: [10.1016/j.radonc.2012.02.010](https://doi.org/10.1016/j.radonc.2012.02.010)]
 - 46 **Kaur H**, Choi H, You YN, Rauch GM, Jensen CT, Hou P, Chang GJ, Skibber JM, Ernst RD. MR imaging for preoperative evaluation of primary rectal cancer: practical considerations. *Radiographics* 2012; **32**: 389-409 [PMID: [22411939](https://pubmed.ncbi.nlm.nih.gov/22411939/) DOI: [10.1148/rg.322115122](https://doi.org/10.1148/rg.322115122)]
 - 47 **Engels B**, Platteaux N, Van den Begin R, Gevaert T, Sermeus A, Storme G, Verellen D, De Ridder M. Preoperative intensity-modulated and image-guided radiotherapy with a simultaneous integrated boost in locally advanced rectal cancer: report on late toxicity and outcome. *Radiother Oncol* 2014; **110**: 155-159 [PMID: [24239243](https://pubmed.ncbi.nlm.nih.gov/24239243/) DOI: [10.1016/j.radonc.2013.10.026](https://doi.org/10.1016/j.radonc.2013.10.026)]
 - 48 **Hernando-Requejo O**, López M, Cubillo A, Rodriguez A, Ciervide R, Valero J, Sánchez E, Garcia-Aranda M, Rodriguez J, Potdevin G, Rubio C. Complete pathological responses in locally advanced rectal cancer after preoperative IMRT and integrated-boost chemoradiation. *Strahlenther Onkol* 2014; **190**: 515-520 [PMID: [24715243](https://pubmed.ncbi.nlm.nih.gov/24715243/) DOI: [10.1007/s00066-014-0650-0](https://doi.org/10.1007/s00066-014-0650-0)]
 - 49 **Mavroidis P**, Giantsoudis D, Awan MJ, Nijkamp J, Rasch CR, Duppen JC, Thomas CR Jr, Okunieff P, Jones WE 3rd, Kachnic LA, Papanikolaou N, Fuller CD; Southwest Oncology Group Radiation Oncology Committee. Consequences of anorectal cancer atlas implementation in the cooperative group setting: radiobiologic analysis of a prospective randomized in silico target delineation study. *Radiother Oncol* 2014; **112**: 418-424 [PMID: [24996454](https://pubmed.ncbi.nlm.nih.gov/24996454/) DOI: [10.1016/j.radonc.2014.05.011](https://doi.org/10.1016/j.radonc.2014.05.011)]
 - 50 **Gambacorta MA**, Valentini C, Dinapoli N, Boldrini L, Caria N, Barba MC, Mattiucci GC, Pasini D, Minsky B, Valentini V. Clinical validation of atlas-based auto-segmentation of pelvic volumes and normal tissue in rectal tumors using auto-segmentation computed system. *Acta Oncol* 2013; **52**: 1676-1681 [PMID: [23336255](https://pubmed.ncbi.nlm.nih.gov/23336255/) DOI: [10.3109/0284186X.2012.754989](https://doi.org/10.3109/0284186X.2012.754989)]
 - 51 **Lin L**, Dou Q, Jin YM, Zhou GQ, Tang YQ, Chen WL, Su BA, Liu F, Tao CJ, Jiang N, Li JY, Tang LL, Xie CM, Huang SM, Ma J, Heng PA, Wee JTS, Chua MLK, Chen H, Sun Y. Deep Learning for Automated Contouring of Primary Tumor Volumes by MRI for Nasopharyngeal Carcinoma. *Radiology* 2019; **291**: 677-686 [PMID: [30912722](https://pubmed.ncbi.nlm.nih.gov/30912722/) DOI: [10.1148/radiol.2019182012](https://doi.org/10.1148/radiol.2019182012)]
 - 52 **Lustberg T**, van Soest J, Gooding M, Peressutti D, Aljabar P, van der Stoep J, van Elmpt W, Dekker A. Clinical evaluation of atlas and deep learning based automatic contouring for lung cancer. *Radiother Oncol* 2018; **126**: 312-317 [PMID: [29208513](https://pubmed.ncbi.nlm.nih.gov/29208513/) DOI: [10.1016/j.radonc.2017.11.012](https://doi.org/10.1016/j.radonc.2017.11.012)]
 - 53 **Guo Z**, Guo N, Gong K, Zhong S, Li Q. Gross tumor volume segmentation for head and neck cancer radiotherapy using deep dense multi-modality network. *Phys Med Biol* 2019; **64**: 205015 [PMID: [31514173](https://pubmed.ncbi.nlm.nih.gov/31514173/) DOI: [10.1088/1361-6560/ab440d](https://doi.org/10.1088/1361-6560/ab440d)]
 - 54 **Wang J**, Lu J, Qin G, Shen L, Sun Y, Ying H, Zhang Z, Hu W. Technical Note: A deep learning-based autosegmentation of rectal tumors in MR images. *Med Phys* 2018; **45**: 2560-2564 [PMID: [29663417](https://pubmed.ncbi.nlm.nih.gov/29663417/) DOI: [10.1002/mp.12918](https://doi.org/10.1002/mp.12918)]
 - 55 **Trebeschi S**, van Griethuysen JJM, Lambregts DMJ, Lahaye MJ, Parmar C, Bakers FCH, Peters NHGM, Beets-Tan RGH, Aerts HJWL. Deep Learning for Fully-Automated Localization and Segmentation of Rectal Cancer on Multiparametric MR. *Sci Rep* 2017; **7**: 5301 [PMID: [28706185](https://pubmed.ncbi.nlm.nih.gov/28706185/) DOI: [10.1038/s41598-017-05728-9](https://doi.org/10.1038/s41598-017-05728-9)]
 - 56 **Song Y**, Hu J, Wu Q, Xu F, Nie S, Zhao Y, Bai S, Yi Z. Automatic delineation of the clinical target volume and organs at risk by deep learning for rectal cancer postoperative radiotherapy. *Radiother Oncol* 2020; **145**: 186-192 [PMID: [32044531](https://pubmed.ncbi.nlm.nih.gov/32044531/) DOI: [10.1016/j.radonc.2020.01.020](https://doi.org/10.1016/j.radonc.2020.01.020)]
 - 57 **Ibragimov B**, Xing L. Segmentation of organs-at-risks in head and neck CT images using convolutional neural networks. *Med Phys* 2017; **44**: 547-557 [PMID: [28205307](https://pubmed.ncbi.nlm.nih.gov/28205307/) DOI: [10.1002/mp.12045](https://doi.org/10.1002/mp.12045)]
 - 58 **Zhu J**, Zhang J, Qiu B, Liu Y, Liu X, Chen L. Comparison of the automatic segmentation of multiple organs at risk in CT images of lung cancer between deep convolutional neural network-based and atlas-based techniques. *Acta Oncol* 2019; **58**: 257-264 [PMID: [30398090](https://pubmed.ncbi.nlm.nih.gov/30398090/) DOI: [10.1080/0284186X.2018.1529421](https://doi.org/10.1080/0284186X.2018.1529421)]
 - 59 **Savenije MHF**, Maspero M, Sikkens GG, van der Voort van Zyp JRN, T J Kotte AN, Bol GH, T van den Berg CA. Clinical implementation of MRI-based organs-at-risk auto-segmentation with convolutional networks for prostate radiotherapy. *Radiat Oncol* 2020; **15**: 104 [PMID: [32393280](https://pubmed.ncbi.nlm.nih.gov/32393280/) DOI: [10.1186/s13014-020-01528-0](https://doi.org/10.1186/s13014-020-01528-0)]
 - 60 **Men K**, Dai J, Li Y. Automatic segmentation of the clinical target volume and organs at risk in the planning CT for rectal cancer using deep dilated convolutional neural networks. *Med Phys* 2017; **44**: 6377-6389 [PMID: [28963779](https://pubmed.ncbi.nlm.nih.gov/28963779/) DOI: [10.1002/mp.12602](https://doi.org/10.1002/mp.12602)]
 - 61 **Men K**, Boimel P, Janopaul-Naylor J, Cheng C, Zhong H, Huang M, Geng H, Fan Y, Plastaras JP,

- Ben-Josef E, Xiao Y. A study of positioning orientation effect on segmentation accuracy using convolutional neural networks for rectal cancer. *J Appl Clin Med Phys* 2019; **20**: 110-117 [PMID: 30418701 DOI: 10.1002/acm2.12494]
- 62 **Wang C**, Zhu X, Hong JC, Zheng D. Artificial Intelligence in Radiotherapy Treatment Planning: Present and Future. *Technol Cancer Res Treat* 2019; **18**: 1533033819873922 [PMID: 31495281 DOI: 10.1177/1533033819873922]
- 63 **Wu H**, Jiang F, Yue H, Li S, Zhang Y. A dosimetric evaluation of knowledge-based VMAT planning with simultaneous integrated boosting for rectal cancer patients. *J Appl Clin Med Phys* 2016; **17**: 78-85 [PMID: 27929483 DOI: 10.1120/jacmp.v17i6.6410]
- 64 **Zhou J**, Peng Z, Song Y, Chang Y, Pei X, Sheng L, Xu XG. A method of using deep learning to predict three-dimensional dose distributions for intensity-modulated radiotherapy of rectal cancer. *J Appl Clin Med Phys* 2020; **21**: 26-37 [PMID: 32281254 DOI: 10.1002/acm2.12849]
- 65 **Sebag-Montefiore D**, Stephens RJ, Steele R, Monson J, Grieve R, Khanna S, Quirke P, Couture J, de Metz C, Myint AS, Bessell E, Griffiths G, Thompson LC, Parmar M. Preoperative radiotherapy versus selective postoperative chemoradiotherapy in patients with rectal cancer (MRC CR07 and NCIC-CTG C016): a multicentre, randomised trial. *Lancet* 2009; **373**: 811-820 [PMID: 19269519 DOI: 10.1016/S0140-6736(09)60484-0]
- 66 **Gérard JP**, Azria D, Gourgou-Bourgade S, Martel-Laffay I, Hennequin C, Etienne PL, Vendrely V, François E, de La Roche G, Bouché O, Mirabel X, Denis B, Mineur L, Berdah JF, Mahé MA, Bécouarn Y, Dupuis O, Lledo G, Montoto-Grillot C, Conroy T. Comparison of two neoadjuvant chemoradiotherapy regimens for locally advanced rectal cancer: results of the phase III trial ACCORD 12/0405-Prodigie 2. *J Clin Oncol* 2010; **28**: 1638-1644 [PMID: 20194850 DOI: 10.1200/JCO.2009.25.8376]
- 67 **Borschitz T**, Wachtlin D, Möhler M, Schmidberger H, Junginger T. Neoadjuvant chemoradiation and local excision for T2-3 rectal cancer. *Ann Surg Oncol* 2008; **15**: 712-720 [PMID: 18163173 DOI: 10.1245/s10434-007-9732-x]
- 68 **Renehan AG**, Malcomson L, Emsley R, Gollins S, Maw A, Myint AS, Rooney PS, Susnerwala S, Blower A, Saunders MP, Wilson MS, Scott N, O'Dwyer ST. Watch-and-wait approach versus surgical resection after chemoradiotherapy for patients with rectal cancer (the OnCoRe project): a propensity-score matched cohort analysis. *Lancet Oncol* 2016; **17**: 174-183 [PMID: 26705854 DOI: 10.1016/S1470-2045(15)00467-2]
- 69 **Ludwig KA**. Sphincter-sparing resection for rectal cancer. *Clin Colon Rectal Surg* 2007; **20**: 203-212 [PMID: 20011201 DOI: 10.1055/s-2007-984864]
- 70 **Marijnen CA**. Organ preservation in rectal cancer: have all questions been answered? *Lancet Oncol* 2015; **16**: e13-e22 [PMID: 25638548 DOI: 10.1016/S1470-2045(14)70398-5]
- 71 **Shi L**, Zhang Y, Nie K, Sun X, Niu T, Yue N, Kwong T, Chang P, Chow D, Chen JH, Su MY. Machine learning for prediction of chemoradiation therapy response in rectal cancer using pre-treatment and mid-radiation multi-parametric MRI. *Magn Reson Imaging* 2019; **61**: 33-40 [PMID: 31059768 DOI: 10.1016/j.mri.2019.05.003]
- 72 **Nie K**, Shi L, Chen Q, Hu X, Jabbour SK, Yue N, Niu T, Sun X. Rectal Cancer: Assessment of Neoadjuvant Chemoradiation Outcome based on Radiomics of Multiparametric MRI. *Clin Cancer Res* 2016; **22**: 5256-5264 [PMID: 27185368 DOI: 10.1158/1078-0432.CCR-15-2997]
- 73 **Fu J**, Zhong X, Li N, Van Dams R, Lewis J, Sung K, Raldow AC, Jin J, Qi XS. Deep learning-based radiomic features for improving neoadjuvant chemoradiation response prediction in locally advanced rectal cancer. *Phys Med Biol* 2020; **65**: 075001 [PMID: 32092710 DOI: 10.1088/1361-6560/ab7970]
- 74 **Shayesteh SP**, Alikhassi A, Fard Esfahani A, Miraie M, Geramifar P, Bitarafan-Rajabi A, Haddad P. Neo-adjuvant chemoradiotherapy response prediction using MRI based ensemble learning method in rectal cancer patients. *Phys Med* 2019; **62**: 111-119 [PMID: 31153390 DOI: 10.1016/j.ejmp.2019.03.013]
- 75 **Yang C**, Jiang ZK, Liu LH, Zeng MS. Pre-treatment ADC image-based random forest classifier for identifying resistant rectal adenocarcinoma to neoadjuvant chemoradiotherapy. *Int J Colorectal Dis* 2020; **35**: 101-107 [PMID: 31786652 DOI: 10.1007/s00384-019-03455-3]
- 76 **Ferrari R**, Mancini-Terracciano C, Voena C, Rengo M, Zerunian M, Ciardiello A, Grasso S, Mare' V, Paramatti R, Russomando A, Santacesaria R, Satta A, Solfaroli Camillocci E, Faccini R, Laghi A. MR-based artificial intelligence model to assess response to therapy in locally advanced rectal cancer. *Eur J Radiol* 2019; **118**: 1-9 [PMID: 31439226 DOI: 10.1016/j.ejrad.2019.06.013]
- 77 **Bibault JE**, Giraud P, Housset M, Durdax C, Taieb J, Berger A, Coriat R, Chaussade S, Dousset B, Nordlinger B, Burgun A. Deep Learning and Radiomics predict complete response after neo-adjuvant chemoradiation for locally advanced rectal cancer. *Sci Rep* 2018; **8**: 12611 [PMID: 30135549 DOI: 10.1038/s41598-018-30657-6]
- 78 **Huang CM**, Huang MY, Huang CW, Tsai HL, Su WC, Chang WC, Wang JY, Shi HY. Machine learning for predicting pathological complete response in patients with locally advanced rectal cancer after neoadjuvant chemoradiotherapy. *Sci Rep* 2020; **10**: 12555 [PMID: 32724164 DOI: 10.1038/s41598-020-69345-9]
- 79 **Shen WC**, Chen SW, Wu KC, Lee PY, Feng CL, Hsieh TC, Yen KY, Kao CH. Predicting pathological complete response in rectal cancer after chemoradiotherapy with a random forest using ¹⁸F-fluorodeoxyglucose positron emission tomography and computed tomography radiomics. *Ann Transl Med* 2020; **8**: 207 [PMID: 32309354 DOI: 10.21037/atm.2020.01.107]
- 80 **Isaksson LJ**, Pepa M, Zaffaroni M, Marvaso G, Alterio D, Volpe S, Corrao G, Augugliaro M,

- Starzyńska A, Leonardi MC, Orecchia R, Jereczek-Fossa BA. Machine Learning-Based Models for Prediction of Toxicity Outcomes in Radiotherapy. *Front Oncol* 2020; **10**: 790 [PMID: 32582539 DOI: 10.3389/fonc.2020.00790]
- 81 **Heinemann V**, von Weikersthal LF, Decker T, Kiani A, Vehling-Kaiser U, Al-Batran SE, Heintges T, Lerchenmüller C, Kahl C, Seipelt G, Kullmann F, Stauch M, Scheithauer W, Hielscher J, Scholz M, Müller S, Link H, Niederle N, Rost A, Höffkes HG, Moehler M, Lindig RU, Modest DP, Rossius L, Kirchner T, Jung A, Stintzing S. FOLFIRI plus cetuximab versus FOLFIRI plus bevacizumab as first-line treatment for patients with metastatic colorectal cancer (FIRE-3): a randomised, open-label, phase 3 trial. *Lancet Oncol* 2014; **15**: 1065-1075 [PMID: 25088940 DOI: 10.1016/S1470-2045(14)70330-4]
- 82 **Allegra CJ**, Rumble RB, Hamilton SR, Mangu PB, Roach N, Hantel A, Schilsky RL. Extended RAS Gene Mutation Testing in Metastatic Colorectal Carcinoma to Predict Response to Anti-Epidermal Growth Factor Receptor Monoclonal Antibody Therapy: American Society of Clinical Oncology Provisional Clinical Opinion Update 2015. *J Clin Oncol* 2016; **34**: 179-185 [PMID: 26438111 DOI: 10.1200/JCO.2015.63.9674]
- 83 **Watanabe T**, Kobunai T, Yamamoto Y, Matsuda K, Ishihara S, Nozawa K, Iinuma H, Shibuya H, Eshima K. Heterogeneity of KRAS status may explain the subset of discordant KRAS status between primary and metastatic colorectal cancer. *Dis Colon Rectum* 2011; **54**: 1170-1178 [PMID: 21825899 DOI: 10.1097/DCR.0b013e31821d37a3]
- 84 **Cui Y**, Liu H, Ren J, Du X, Xin L, Li D, Yang X, Wang D. Development and validation of a MRI-based radiomics signature for prediction of KRAS mutation in rectal cancer. *Eur Radiol* 2020; **30**: 1948-1958 [PMID: 31942672 DOI: 10.1007/s00330-019-06572-3]
- 85 **Sundström M**, Edlund K, Lindell M, Glimelius B, Birgisson H, Micke P, Botling J. KRAS analysis in colorectal carcinoma: analytical aspects of Pyrosequencing and allele-specific PCR in clinical practice. *BMC Cancer* 2010; **10**: 660 [PMID: 21122130 DOI: 10.1186/1471-2407-10-660]
- 86 **Burman C**, Kutcher GJ, Emami B, Goitein M. Fitting of normal tissue tolerance data to an analytic function. *Int J Radiat Oncol Biol Phys* 1991; **21**: 123-135 [PMID: 2032883 DOI: 10.1016/0360-3016(91)90172-z]
- 87 **Seppenwoolde Y**, Lebesque JV, de Jaeger K, Belderbos JS, Boersma LJ, Schilstra C, Henning GT, Hayman JA, Martel MK, Ten Haken RK. Comparing different NTCP models that predict the incidence of radiation pneumonitis. Normal tissue complication probability. *Int J Radiat Oncol Biol Phys* 2003; **55**: 724-735 [PMID: 12573760 DOI: 10.1016/s0360-3016(02)03986-x]
- 88 **Marks LB**, Yorke ED, Jackson A, Ten Haken RK, Constine LS, Eisbruch A, Bentzen SM, Nam J, Deasy JO. Use of normal tissue complication probability models in the clinic. *Int J Radiat Oncol Biol Phys* 2010; **76**: S10-S19 [PMID: 20171502 DOI: 10.1016/j.ijrobp.2009.07.1754]
- 89 **Tomatis S**, Rancati T, Fiorino C, Vavassori V, Fellin G, Cagna E, Mauro FA, Girelli G, Monti A, Baccolini M, Naldi G, Bianchi C, Menegotti L, Pasquino M, Stasi M, Valdagni R. Late rectal bleeding after 3D-CRT for prostate cancer: development of a neural-network-based predictive model. *Phys Med Biol* 2012; **57**: 1399-1412 [PMID: 22349550 DOI: 10.1088/0031-9155/57/5/1399]
- 90 **Chen J**, Chen H, Zhong Z, Wang Z, Hrycushko B, Zhou L, Jiang S, Albuquerque K, Gu X, Zhen X. Investigating rectal toxicity associated dosimetric features with deformable accumulated rectal surface dose maps for cervical cancer radiotherapy. *Radiat Oncol* 2018; **13**: 125 [PMID: 29980214 DOI: 10.1186/s13014-018-1068-0]
- 91 **Abdollahi H**, Mahdavi SR, Mofid B, Bakhshandeh M, Razzaghdoost A, Saadipoor A, Tanha K. Rectal wall MRI radiomics in prostate cancer patients: prediction of and correlation with early rectal toxicity. *Int J Radiat Biol* 2018; **94**: 829-837 [PMID: 29969358 DOI: 10.1080/09553002.2018.1492756]
- 92 **Oyaga-Iriarte E**, Insausti A, Sayar O, Aldaz A. Prediction of irinotecan toxicity in metastatic colorectal cancer patients based on machine learning models with pharmacokinetic parameters. *J Pharmacol Sci* 2019; **140**: 20-25 [PMID: 31105026 DOI: 10.1016/j.jphs.2019.03.004]
- 93 **Zhao B**, Gabriel RA, Vaida F, Lopez NE, Eisenstein S, Clary BM. Predicting Overall Survival in Patients with Metastatic Rectal Cancer: a Machine Learning Approach. *J Gastrointest Surg* 2020; **24**: 1165-1172 [PMID: 31468331 DOI: 10.1007/s11605-019-04373-z]
- 94 **Pham TD**, Fan C, Zhang H, Sun XF. Artificial intelligence-based 5-year survival prediction and prognosis of DNp73 expression in rectal cancer patients. *Clin Transl Med* 2020; **10**: e159 [PMID: 32898334 DOI: 10.1002/ctm2.159]
- 95 **Li H**, Boimel P, Janopaul-Naylor J, Zhong H, Xiao Y, Ben-Josef E, Fan Y. Deep Convolutional Neural Networks for Imaging Data Based Survival Analysis of Rectal Cancer. *Proc IEEE Int Symp Biomed Imaging* 2019; **2019**: 846-849 [PMID: 31929858 DOI: 10.1109/ISBI.2019.8759301]
- 96 **Oliveira T**, Silva A, Satoh K, Julian V, Leão P, Novais P. Survivability Prediction of Colorectal Cancer Patients: A System with Evolving Features for Continuous Improvement. *Sensors (Basel)* 2018; **18** [PMID: 30200676 DOI: 10.3390/s18092983]



Artificial intelligence in gastrointestinal radiology: A review with special focus on recent development of magnetic resonance and computed tomography

Kai-Po Chang, Shih-Huan Lin, Yen-Wei Chu

ORCID number: Kai-Po Chang [0000-0003-1730-9728](https://orcid.org/0000-0003-1730-9728); Shih-Huan Lin [0000-0002-9037-0683](https://orcid.org/0000-0002-9037-0683); Yen-Wei Chu [0000-0002-5525-4011](https://orcid.org/0000-0002-5525-4011).

Author contributions: Chu YW and Chang KP conceived the idea for the manuscript; Chang KP and Lin SH reviewed the literature and drafted the manuscript; Chu YW drafted and finally approved the manuscript.

Supported by Ministry of Science and Technology, No. 109-2321-B-005-024 and No. 109-2320-B-039-005; National Chung Hsing University and Chung-Shan Medical University, No. NCHU-CSMU 10911; China Medical University Hospital, No. DMR-109-258; and ChangHua Christian Hospital and National Chung Hsing University, No. NCHU-CCH-11006.

Conflict-of-interest statement: Authors declare no conflict of interests for this article.

Open-Access: This article is an open-access article that was selected by an in-house editor and fully peer-reviewed by external reviewers. It is distributed in accordance with the Creative Commons Attribution

Kai-Po Chang, Shih-Huan Lin, Yen-Wei Chu, PhD Program in Medical Biotechnology, National Chung Hsing University, Taichung 40227, Taiwan

Kai-Po Chang, Department of Pathology, China Medical University Hospital, Taichung 40447, Taiwan

Yen-Wei Chu, Institute of Genomics and Bioinformatics, National Chung Hsing University, Taichung 40227, Taiwan

Yen-Wei Chu, Institute of Molecular Biology, National Chung Hsing University, Taichung 40227, Taiwan

Yen-Wei Chu, Agricultural Biotechnology Center, National Chung Hsing University, Taichung 40227, Taiwan

Yen-Wei Chu, Biotechnology Center, National Chung Hsing University, Taichung 40227, Taiwan

Yen-Wei Chu, PhD Program in Translational Medicine, National Chung Hsing University, Taichung 40227, Taiwan

Yen-Wei Chu, Rong Hsing Research Center for Translational Medicine, Taichung 40227, Taiwan

Corresponding author: Yen-Wei Chu, PhD, Director, Professor, Institute of Genomics and Bioinformatics, National Chung Hsing University, Kuo Kuang Road, Taichung 40227, Taiwan. ywchu@nchu.edu.tw

Abstract

Artificial intelligence (AI), particularly the deep learning technology, have been proven influential to radiology in the recent decade. Its ability in image classification, segmentation, detection and reconstruction tasks have substantially assisted diagnostic radiology, and has even been viewed as having the potential to perform better than radiologists in some tasks. Gastrointestinal radiology, an important subspecialty dealing with complex anatomy and various modalities including endoscopy, have especially attracted the attention of AI researchers and engineers worldwide. Consequently, recently many tools have been developed for

NonCommercial (CC BY-NC 4.0) license, which permits others to distribute, remix, adapt, build upon this work non-commercially, and license their derivative works on different terms, provided the original work is properly cited and the use is non-commercial. See: <http://creativecommons.org/licenses/by-nc/4.0/>

Manuscript source: Invited manuscript

Specialty type: Gastroenterology and hepatology

Country/Territory of origin: Taiwan

Peer-review report's scientific quality classification

Grade A (Excellent): 0
Grade B (Very good): 0
Grade C (Good): C
Grade D (Fair): D
Grade E (Poor): 0

Received: January 27, 2021

Peer-review started: January 27, 2021

First decision: March 7, 2021

Revised: March 21, 2021

Accepted: April 20, 2021

Article in press: April 20, 2021

Published online: April 28, 2021

P-Reviewer: Lu G, Lui TK

S-Editor: Wang JL

L-Editor: A

P-Editor: Li JH



lesion detection and image construction in gastrointestinal radiology, particularly in the fields for which public databases are available, such as diagnostic abdominal magnetic resonance imaging (MRI) and computed tomography (CT). This review will provide a framework for understanding recent advancements of AI in gastrointestinal radiology, with a special focus on hepatic and pancreatobiliary diagnostic radiology with MRI and CT. For fields where AI is less developed, this review will also explain the difficulty in AI model training and possible strategies to overcome the technical issues. The authors' insights of possible future development will be addressed in the last section.

Key Words: Artificial intelligence; Deep learning; Image diagnosis; Radiology; Magnetic resonance imaging; Computed tomography

©The Author(s) 2021. Published by Baishideng Publishing Group Inc. All rights reserved.

Core Tip: Gastrointestinal radiology is a subspecialty that is important and complex, and is thus a popular subject in artificial intelligence (AI). Recently many deep-learning based diagnosis assistance tool have been developed in gastrointestinal radiology, particularly in diagnostic abdominal magnetic resonance imaging (MRI) and computed tomography (CT). Herein we will review recent advance of AI in gastrointestinal radiology, with a special focus on abdominal MRI and CT. Current difficulty in less-developed fields will be explained as well.

Citation: Chang KP, Lin SH, Chu YW. Artificial intelligence in gastrointestinal radiology: A review with special focus on recent development of magnetic resonance and computed tomography. *Artif Intell Gastroenterol* 2021; 2(2): 27-41

URL: <https://www.wjgnet.com/2644-3236/full/v2/i2/27.htm>

DOI: <https://dx.doi.org/10.35712/aig.v2.i2.27>

INTRODUCTION

The field of gastrointestinal radiology includes diagnostic radiology and interventional radiology. In the practice of diagnostic gastrointestinal radiology, various imaging tools are applied for the diagnosis of lesions in the abdominal cavity. These tools include X-ray used in abdominal plain film^[1], angiography and abdominal computed tomography (CT)^[2], magnetic resonance used in abdominal magnetic resonance imaging (MRI)^[3,4], and ultrasound used in abdominal sonography^[5]. For some diagnostic tasks, intravenous contrasts are used to enhance lesions for study. Contrast-enhanced, three-phase CT is the standard for examination of liver tumors and many other lesion types^[6]. Contrast-enhanced ultrasound and MRI, though less frequently used, have some clinical use in examination of pancreatic lesions and inflammatory bowel disease^[7-9]. Please refer to Ripollés *et al*^[7] for example of contrast-enhanced ultrasound for diagnosis for Crohn's disease.

Artificial intelligence (AI) have been influential in radiology recently, because it has potential to reduce workloads of radiologists, and diagnostic radiology tools stated above have provided feasible ground for machine learning model development. Potential of machine learning models to reduce radiologist workload come from its better stability, higher work efficiency, and better accuracy in some selected tasks^[10] than human workers. Deep learning has proven its suitability for different imaging methods, and radiology and has been widely used in image classification, segmentation, detection, and reconstruction tasks^[11]. There are some optimistic radiologists who are willing to let AI assist them in their work so that they can enhance their role in other places^[12,13]. Of course, there are also pessimistic radiologists who worry that the development of AI systems will replace radiologists^[14].

The most significant shortcoming of machine learning algorithms require a lot of data^[15]. At the same time, the lack of unified standard training data will lead to a decrease in the efficiency of AI learning, but it is difficult for doctors to label a large amount of accurate data in complex diseases. In addition, the algorithm may learn false correlations, which may also lead to overfitting. At the same time, it is difficult

for AI to explain the causality in the observation dataset. Semi-supervised learning is between supervised learning and unsupervised learning. In the training process, a small amount of labeled data and a large amount of unlabeled data are used at the same time. The development of semi-supervised learning algorithms is mainly because data labeling is very expensive or impossible in some fields^[16-18]. The development of semi-supervised learning can also simultaneously solve the problems of a large number of labeling and overfitting.

INTERVENTIONAL RADIOLOGY

Interventional radiology uses imaging techniques in diagnostic radiology to treat diseases or take specimens. The practice of interventional procedures in gastrointestinal radiology can be best exemplified by the treatment solid organ tumors. Among the most-frequently used non-surgical treatment procedures of hepatocellular carcinoma (HCC) are transcatheter arterial chemoembolization (TACE) and radiofrequency ablation (RFA). In TACE^[19], liver tumors are first highlighted by angiography, and then embolized by particles coated with chemotherapeutic drugs. In RFA^[20], the lesion is located by ultrasound rather than angiography and ablated by radiofrequency heating. In addition to liver cancer, any solid organ tumors with rich vasculature can be treated with this procedure. For example, pancreatic neuroendocrine tumors are frequently hypervascular, therefore are sometimes treated by embolization since last century^[21,22], especially in patients with multiple endocrine neoplasia type 1 syndrome, where multiple tumors may make resection unfeasible^[23]. are also widely applied in some of pancreatic tumors, such as neuroendocrine tumors. Application of RFA, which does not require rich vasculature, is even more versatile than TACE. There are reports of successful radiofrequency ablation on unresectable pancreatic cancer^[24,25], and even intra-abdominal sarcomas such as gastrointestinal stromal tumor^[26].

Interventional radiology also has broad application on non-tumor diseases, especially in vascular diseases. The best well-known example is emergent management of gastrointestinal bleeding, where the bleeding artery can be visualized by angiography, and embolized^[27,28]. A similar approach can be also applied to thrombotic diseases such as Budd-Chiari syndrome or celiac artery occlusion^[29,30]. In management of these disorders, the vessels are visualized and dilated with stents or dissolved with thrombolytic agents. Applications of interventional radiology are numerous and still developing, so a thorough review is out of scope of this article.

Both diagnostic and interventional gastrointestinal radiology can be done endoscopically. For example, in endoscopic ultrasound (EUS), the ultrasound probe is inserted through an endoscope to visualize lesions that are not easily accessible by abdominal sonography^[31,32]. Biopsy and other interventional procedures can then be done to the visualized lesion *via* the endoscope, as exemplified in publications by Williams *et al*^[33], and Kahaleh *et al*^[34]. Endoscopic radiological images are more difficult to be collected in large amount, because like in EUS, most image from endoscopic procedures are manually captured with custom angle of the endoscopist, rather than in an automatic and standard manner. Therefore, unlike in development of AI in regular diagnostic radiology, in which large scale public dataset, such as pancreas CT dataset from The Cancer Imaging Archive^[35-37], and Beyond the Cranial Vault Abdomen data set^[38,39], are readily available, most AI studies in endoscopic radiology still requires collection and processing of multihospital data. Moreover, lack of standardization and technical difficulty can make researchers reluctant or afraid to make image public. For example, in the study of computer-aided diagnosis of gastrointestinal stromal tumors by Li *et al*^[40], the authors made the research possible only after collecting data from 19 hospitals, and did not publish the dataset. To our knowledge, there is only one well-known, public database of endoscopic ultrasound, published in 2020^[41], and we hope that more database will be available in the following decade. In the present situation, due to less available resource, endoscopic radiology is less developed, so in this review article, we will focus on non-endoscopic radiological examination, particularly on CT and MRI.

DEEP LEARNING IN RADIOLOGY: ACHIEVING STATE OF THE ART IN LESION DETECTION

In the last five years, there have been marked progress in deep learning-assisted lesion detection for radiology, particularly in computed tomography. The progress can be exemplified by the DeepLesion tool developed by National Institutes of Health^[42], which claims to detect all types of lesion in computed tomography regardless of the organ, with a sensitivity of 81.1% and five false-positives per case. DeepLesion was published along with an immense dataset with 32120 CT slices. With this annotated database in hand as a powerful tool, researchers refined lesion detection algorithm at an accelerated pace. For example, with the DeepLesion dataset, researchers from Chinese Academy of Sciences were able to develop the MVP-Net tool^[43] by feature pyramid network, which claims to be 5.65% more sensitive than DeepLesion. With more developed advancements in deep learning algorithms and more databases available, we can expect that universal lesion detection in computed tomography will reach clinical use in reasonable time. An example of lesion detection in DeepLesion can be found in Yan *et al*^[42].

For MRI, recent advancements are much less pronounced. Due to complex and variable sequencing techniques used in MRI, such as perfusion weighted imaging and T2* used in stroke protocol^[44] and diffusion weighted imaging^[45] used in various organs, development of an universal, organ-neutral lesion detection algorithm is very difficult, if not impossible. Nonetheless, for individual organs, there is still marked progression. For example, using a deep learning algorithm, Amit *et al*^[46] developed a tool for lesion detection in breast MRI. Later, in 2019, with the application of deep learning on T1-weighted, fat-suppressed MR images, Kijowski *et al*^[47] further extended the technology to predict breast lesion type. Though not as effective as in breast lesion detection, the application of deep learning on musculoskeletal system MRI has achieved marked success for the detection of variable lesions, such as fracture, deformity, and metastatic disease. There are numerous studies about lesion detection on MRI in other organs, but it is beyond the scope of this review article.

Given the fact that there are on an average five false-positive lesions detected by DeepLesion, deep learning algorithms trained by radiographs are prone to over-detecting lesions. Researchers are aware of this problem and have tried to overcome it by various technologies. The most-used and earliest method applied is multi-view convolutional networks (CNN), wherein native 3D shapes are recognized from their rendered 2D views^[48]. By using multi-view CNN, Setio *et al*^[49], Kang *et al*^[50] and El-Regaily *et al*^[51] reported significant reduction of false-positive lesions in the lung with computed tomography, thus making this algorithm the most effective detection training tool for lung image. Recent results of the use of multi-view CNN in lung lesion detection are shown in Table 1.

In addition to lung computer tomography, multi-view CNN has been used with other imaging subjects as well. It is also used to increase specificity in mammographic image classification^[52] and longitudinal multiple sclerosis lesion segmentation^[53]. Besides multi-view CNN, masking techniques during neural network training are also used to reduce false positive lesions. For example, Zlocha *et al*^[54] used dense masks to improve the performance of RetinaNet^[55], and the researchers developing ULDor tool^[56] used pseudo mask to reduce false positivity in universal lesion detector.

Taken together, in recent years, deep learning for lesion detection in technology has shown great progress. In the next section, we will focus on how these technical advancements have benefited the diagnosis of gastrointestinal lesions.

DISEASE DIAGNOSIS AND PREDICTION IN GASTROENTEROLOGY

Cholangiographic diagnosis

One of the most advanced achievement in gastrointestinal radiology is the non-invasive evaluation of for the bile ducts. Before the era of image reconstruction and advanced endoscopy, visualization and diagnosis of lesions causing biliary disease usually required quite invasive procedures such as transhepatic cholangiography^[57]. In late 20th century, with the advancements in endoscopy, it was replaced by endoscopic methods like retrograde cholangiopancreatography (ERCP)^[58] and EUS cholangiography^[59,60]. For achieving both treatment and diagnosis, endoscopic procedure maybe necessary and appropriate, but for the sole purpose of diagnosis, such as visualization of lesions in primary sclerosing cholangitis (PSC)^[61] and

Table 1 Recent results in usage of multi-view convolutional networks in lung lesion detection

Dataset	Toolset	AUC	Ref.
LIDC	ConvNets (2D)	0.996	Setio <i>et al</i> ^[49] , 2016
LIDC	Inception-Resnet (3D)	0.99	Kang <i>et al</i> ^[50] , 2017
LIDC	MatConvNet (2D)	0.94	El-Regaily <i>et al</i> ^[51] , 2020

LIDC: Lexington Infectious Disease Consultants; AUC: Area under the curve.

choledochal cyst^[62], endoscopic procedure maybe too invasive and inconvenient for patients.

Therefore, in the last three decades, with the increasing demand of non-invasive procedures and the progress of digital image reconstruction technologies, some radiology visualization tools, such as magnetic resonance cholangiopancreatography (MRCP)^[63] and CT cholangiography^[64], have been developed and achieved clinical importance. For diagnostic problems, the precision of non-invasive examination has become comparable to that of endoscopic procedure. MRCP achieved diagnostic accuracy of up to 97% in the diagnosis of choledocholithiasis as early as 2000^[65]. In 2011, MRCP even rivaled the performance of pathologic examination, with an accuracy of 82.9% in predicting carcinomatous biliary obstruction^[66]. In the meantime, CT cholangiography also reached the status of standard care in some situations, such as preoperative biliary anatomy assessment when MRCP is inconclusive^[67].

These noninvasive diagnostic examinations are, of course, far from perfect. Despite early success, in some studies between 2010 and 2020, the sensitivity of MRCP for choledocholithiasis was reportedly inferior to that of EUS^[68]. This outcome may be attributed to subjectivity and inter-observer variability of interpretation, because, even though it is less demanding than ERCP, the radiological assessment of the bile duct and pancreas still requires high level of expertise to interpret^[69]. For more demanding tasks, such as detection and classification of pancreatic lesions^[70,71], the performance of noninvasive tests can be even more disappointing.

To cope with the problem of interpretation difficulty in noninvasive cholangiopancreatography, researchers began to use variable deep learning methods in an attempt to achieve more subjective and sensitive lesion detection in the bile ducts and pancreas. For example, Ringe *et al*^[72] developed a transfer learning-based system for automated detection of PSC, achieving a sensitivity of 95%. If this system is used clinically, radiologists can avoid all-manual interpretation for difficult PSC detection, thus reducing possible the inter-observer disagreement. Some of researchers also used deep learning to improve image reconstruction and segmentation in the pancreatobiliary region, to reduce pitfall in traditional MRCP and CT cholangiography. For example, Tang *et al*^[73] used deep learning to improve highlighting of perampullary regions in MRI, which can be difficult with traditional MRCP method. Al-Oudat *et al*^[74] used Denoising Convolutional Neural Networks for better construction of intrahepatic biliary segmentation in MRI image.

Besides its utility in noninvasive examination, deep learning can also benefit imaging difficulty in endoscopic procedure. By a segmentation algorithm trained by D-LinkNet34 and U-Net, Huang *et al*^[75] developed a system to evaluate stone removal difficulty of ERCP. By training on a deep learning model using ultrasound images and videos, Zhang *et al*^[76] developed a system to recognize pancreas segments and stations in EUS. With globally increasing computing power and maturing deep learning technology, we can expect radiological pancreaticobiliary system assessment to continuously improve in the future.

Detection and classification of solid organ tumor

Imaging studies, such as abdominal contrasted CT scan and contrast enhanced ultrasound, are crucial for the evaluation of solid organ tumor diagnosis, such as liver cancer, pancreatic cancer, and other solid organ tumors. The best example is screening for HCC in patients with cirrhosis^[77]. Image diagnosis of liver tumor is crucial and effective to the point that HCC can be diagnosed by three-phase contrasted CT^[78] alone, without the need of a biopsy^[79]. Despite being less accurate, image diagnosis is helpful in more difficult-to-diagnose tumor types, such as focal nodular hyperplasia and hepatocellular adenoma^[80-82]. CT diagnosis is also crucial and sensitive for pancreas cancer diagnosis^[83] and prediction of malignant change in cystic lesion^[84].

The first problem in image diagnosis is that, even with state-of-the-art, highly sensitive technique, it can have less than ideal specificity. For example, image appearance of intrahepatic cholangiocarcinoma (ICC) can mimic HCC both in contrast-enhanced CT^[85] and contrast-enhanced ultrasound^[86]. Since the long-term outcome and treatment strategy are significantly different between HCC and ICC^[87,88], this can be a severe misdiagnosis that impacts prognosis. Some vascular tumors like epithelioid hemangioendothelioma^[89,90] and sclerosed hemangioma^[91] may also mimic epithelial malignancy, making the image diagnosis even less specific. Moreover, because of a large volume of abdominal CT and MRI done for liver cancer screening, the workload is quite a lot for radiologists^[92,93]. Pancreatic cancer is more problematic, since inflammatory process such as autoimmune pancreatitis can mimic adenocarcinoma, causing diagnostic difficulty in CT and MRI^[94,95]. Less prevalent tumor types, such as acinar cell carcinoma of pancreas, can be even more challenging^[96]. Therefore, there is strong demand for automatic tumor classification algorithm for abdominal imaging, to improve the accuracy of tumor classification and reduce radiologists' workload.

Of the two purposes stated above, the most recent development was on assisted lesion detection to relieve radiologists' workload. Using watershed transform and Gaussian mixture, Das *et al.*^[97] developed a tool that they claimed can detect hemangioma, HCC and metastatic carcinoma with a classification accuracy of 99.38%; however, they did not consider ICC in their differential diagnosis, therefore, this tool can be used only for screening, and not for final tumor diagnosis. Vorontsov *et al.*^[98] used fully convolutional network for the detection of liver metastatic colorectal cancer, with a sensitivity of up to 85%. There are several other developed for liver tumor detection and segmentation with variable success^[99,100]. For automatic pancreatic cancer detection, there are also variable success. Li *et al.*^[101] developed a computer aided diagnosis model by Dual threshold principal component analysis for pancreas cancer on PET/CT image, with an accuracy of up to 87.72%. By using faster region-based CNN on CT image, Liu *et al.*^[102] built a diagnosis system which detected pancreatic cancer with an area under the curve (AUC) of 0.9632. These studies are only some examples of AI detection of digestive system cancer in medical images. For a more detailed discussion, readers can refer to the other review article focused on this subject^[103].

Few researchers have published results about detailed tumor classification based on abdominal imaging. By training convolution CNN with both MRI image and clinical data, Zhen *et al.*^[104]'s model achieved AUC of up to 0.985 in the classification of malignant tumors as hepatocellular carcinoma, metastatic carcinoma or other primary malignancies. Yasaka *et al.*^[105] attempted automatic classification of liver tumor into five classes (HCC, other malignancy, indeterminate masses, and two classes of benign lesions) using CNN, and achieved an accuracy of 0.84. Scope of these classification tools are summarized in Table 2. Due to limited literature available, it is too early to predict whether automatic radiological tumor classification will be comparable to pathologic diagnosis, but the recent results seem promising, and would be a good subject for further research.

Intelligent assistance on endoscopic radiology

Endoscopic radiological procedures, such as EUS and ERCP, can be very difficult to perform and interpret, and require a lot of training to achieve competence^[106], particularly if combined with interventional procedures like ampullectomy or biopsy^[107,108]. Artificial intelligence assistance to reduce difficulty and allow for a reasonable learning curve is therefore desired for these procedures.

Due to the limited availability of public image database of EUS and ERCP, the development of AI models for these modalities is, as stated in a previous review article, still in its infancy^[109]. There are, however, already some promising results in assistance of endoscopic radiological procedure. The most pronounced progress is with depth assessment in EUS. EUS imaging for evaluation of tumor depth is crucial in predicting the safety of endoscopic submucosal dissection^[110]; however, the image diagnosis can be subjective, and requires much expertise. Cho *et al.*^[111] developed a tool using deep learning that predicts tumor depth in EUS with a claimed AOC of 0.887. For less sophisticated tasks such as detection of pancreatic cancer in EUS, the result is even better, with a claimed AOC of 0.940^[112]. Therefore, it is evident that deep learning-assisted diagnosis can be a reliable tool.

In summary, AI has proven helpful in radiological diagnosis. Although few of the tools described above have reached clinical use, with current development, we can expect AI-assisted diagnosis to advance further in few years, and it may eventually become relevant to everyday clinical practice.

Table 2 Classification scope for recent deep learning-based tumor classification tools

Ref.	HCC	ICC	Metastatic carcinoma	Other malignancy	Benign tumors
Das <i>et al</i> ^[97] , 2019	O	X	O	X	O
Vorontsov <i>et al</i> ^[98] , 2019	X	X	O	X	X
Zhen <i>et al</i> ^[104] , 2020	O	O	O	O	X
Yasaka <i>et al</i> ^[105] , 2018	O	O	O	O	O

HCC: Hepatocellular carcinoma; ICC: Intrahepatic cholangiocarcinoma. X: Yes; O: No.

MAIN CHALLENGES AND PITFALLS OF THE APPLICATION OF AI IN RADIOLOGY

Although AI has made a lot of contributions in radiology, there are still some challenges and pitfalls, and AI experts should be cautious when working with radiologists. One of the biggest challenges is the availability of data. Ordinary deep learning algorithms will be learned through millions of training datasets, but it is difficult for the medical field to have such a large amount of data, and even if there are a large number of training datasets, there is currently no unified classification standard^[113,114]. If the training dataset is too small, multiple neuron training through deep learning will easily lead to overfitting^[115,116] and will show poor accuracy in independent tests. How to choose the right amount of model depth to adapt to a smaller training dataset will be the biggest challenge for AI engineers. In addition, generative adversarial networks^[117] is also very suitable for small training datasets. At the same time, the establishment of a large number of training databases can also effectively help improve the efficiency of AI. Physicians and engineers work together to establish an open database and set uniform standards, which can also enhance AI applicability in radiology and pathology.

In addition, some diseases (usually rare diseases) have a problem of extreme disparity in the classification ratio, which is called imbalanced data. Imbalanced data training is more difficult, which usually leads to high accuracy but poor results, because the machine only needs to guess more. The classification, you can get a good-looking accuracy. Although there are good solutions already available^[118], these are still important challenges for using AI with rare diseases.

Finally, when an AI model that can be used clinically is to be developed, proper verification settings must be ensured in the experimental verification of the model. Lack of sufficient verification can lead to untrustworthy models^[119]. It is common that the training dataset and the test dataset are not extensive at the time of collection, thus resulting in poor results in practical applications.

FUTURE OF AI IN GASTROINTESTINAL RADIOLOGY

With advanced deep learning algorithm, computers can assist clinicians to make an accurate diagnostic decision by providing the right information. For difficulties in endoscopic and interventional procedure, however, information alone is of little help. Complete automation of a manual procedure must be assisted by both deep learning and robotics. For example, there have been marked advancements in robot-assisted endoscopy devices^[120]. If these robots can be combined with an intelligent system that detect lesions *via* ultrasound^[112], then it would have a potential to automatically take procure a biopsy sample from the lesion, or perform a surgical procedure, thus eliminating the difficulties of endoscopic and surgical technique.

The other factor that would augment the power of intelligent system is the development of radiological technology itself. The best example would be combination of radiology and endoscopic robotic capsule^[121,122]. Recently, with the assistance of neural network, trajectory control and image visualization of endoscopic robotic capsules have been more automatic than they were previously^[123]. In the future, if the size of ultrasound probe or other radiological device can be reduced to nanoscale, with an intelligent robotic capsule and intelligent ultrasound probe, fully automated detection and management of any lesion accessible by endoscopic capsules would be possible. Possible path to fully automatic diagnosis and intervention in

gastroenterology by combining artificial intelligence with various technologies is shown in [Figure 1](#).

The problems inherent to AI itself, that is, data acquisition and annotation, will also be solved by recent technical developments in deep learning models. The best sample would be using unsupervised learning or semi-supervised learning^[16,18] to decrease or eliminate the need for radiologist annotation, making development of models faster. For research topics with large public database and well-developed models, such as abdominal CT, transfer learning with pre-trained model and included clinical data can also make training easier, more precise, and faster^[124]. In addition to improvement of deep learning model itself, the advancement of advanced deep learning algorithm will enable in-vivo live visualization of lesion detection in endoscope^[125], which will be a powerful, clinically applicable function. LeNet-5 architecture can be found in publication by Lecun *et al*^[126].

However, areas with less data availability, such as EUS, cannot be advanced with AI technology alone. For developments of these areas, international collaboration for collection of multi-center image database and clinical data must be done to overcome data scarcity and facilitate precise training and evaluation of models. These multi-center database of image and clinical data will not only benefit model training, but also validation of previous models. Because multi-center data can be more unbiased than data from single source, validation or re-training by multi-center data may improve precision of models by eliminating sampling bias.

With future advancement in data science, deep learning algorithm and medical robotics, AI can play important role in gastrointestinal radiology in the future and may lead a medial revolution.

CONCLUSION

As demonstrated in the assistance of liver tumor diagnosis and cholangiography, AI has the potential to reduce radiology workload and improve diagnostic specificity, thus making radiologic diagnoses faster and more reliable. In some tasks like the detection of a malignant stricture, we can even hope for machine diagnosis to surpass human diagnosis, making fully automated diagnosis possible. Conversely, for fields where training data collection is more difficult, such as endoscopic ultrasound, training deep learning models would still be slow using today's technology.

To overcome the problem of lack of technical advancement due to limited data in these areas, particularly in endoscopic procedure, two approaches maybe used. The first solution is to use algorithms that are designed to increase data availability in small medical dataset, such as generative adversarial network and transfer learning. The other suggestion is to build public, global endoscopic image library for model training. In conclusion, though a lot have to be done to make AI universally successful in gastrointestinal radiology, the researchers and developers actually already have the facility to deal with the difficult aspects of this task. Therefore, it is reasonable to expect more scientific advancements and clinical use of AI in the coming decade.

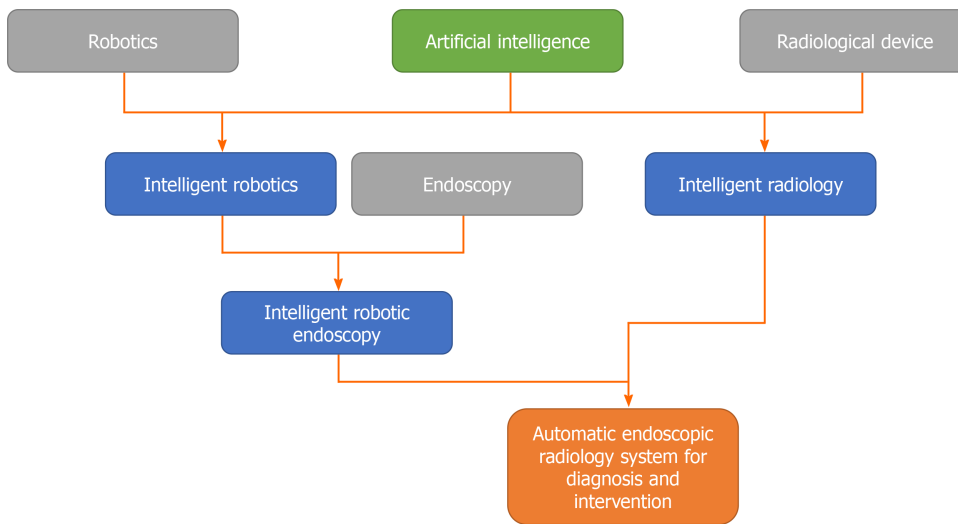


Figure 1 Illustration of a possible path to automatic diagnostic and interventional system in gastroenterology.

REFERENCES

- 1 **Gans SL**, Stoker J, Boermeester MA. Plain abdominal radiography in acute abdominal pain; past, present, and future. *Int J Gen Med* 2012; **5**: 525-533 [PMID: 22807640 DOI: 10.2147/IJGM.S17410]
- 2 **Tsapaki V**, Rehani M, Saini S. Radiation safety in abdominal computed tomography. *Semin Ultrasound CT MR* 2010; **31**: 29-38 [PMID: 20102693 DOI: 10.1053/j.sult.2009.09.004]
- 3 **Hussain SM**, Wielopolski PA, Martin DR. Abdominal magnetic resonance imaging at 3.0 T: problem or a promise for the future? *Top Magn Reson Imaging* 2005; **16**: 325-335 [PMID: 16785848 DOI: 10.1097/01.rmr.0000224689.06501.16]
- 4 **Attenberger UI**, Morelli J, Budjan J, Henzler T, Sourbron S, Bock M, Riffel P, Hernando D, Ong MM, Schoenberg SO. Fifty Years of Technological Innovation: Potential and Limitations of Current Technologies in Abdominal Magnetic Resonance Imaging and Computed Tomography. *Invest Radiol* 2015; **50**: 584-593 [PMID: 26039773 DOI: 10.1097/RLI.000000000000173]
- 5 **Spaulding KA**. A review of sonographic identification of abdominal blood vessels and juxtavascular organs. *Vet Radiol Ultrasound* 1997; **38**: 4-23 [PMID: 9238765 DOI: 10.1111/j.1740-8261.1997.tb01597.x]
- 6 **Dietrich CF**, Maddalena ME, Cui XW, Schreiber-Dietrich D, Ignee A. Liver tumor characterization-review of the literature. *Ultraschall Med* 2012; **33** Suppl 1: S3-10 [PMID: 22723026 DOI: 10.1055/s-0032-1312897]
- 7 **Ripollés T**, Martínez-Pérez MJ, Paredes JM, Vizuete J, García-Martínez E, Jiménez-Restrepo DH. Contrast-enhanced ultrasound in the differentiation between phlegmon and abscess in Crohn's disease and other abdominal conditions. *Eur J Radiol* 2013; **82**: e525-e531 [PMID: 23838329 DOI: 10.1016/j.ejrad.2013.05.043]
- 8 **Ziech ML**, Hummel TZ, Smets AM, Nievelstein RA, Lavini C, Caan MW, Nederveen AJ, Roelofs JJ, Bipat S, Benninga MA, Kindermann A, Stoker J. Accuracy of abdominal ultrasound and MRI for detection of Crohn disease and ulcerative colitis in children. *Pediatr Radiol* 2014; **44**: 1370-1378 [PMID: 24903659 DOI: 10.1007/s00247-014-3010-4]
- 9 **Faccioli N**, Dietrich CF, Foti G, Santi E, Comai A, D'Onofrio M. Activity-Based Cost Analysis of Including Contrast-Enhanced Ultrasound (CEUS) in the Diagnostic Pathway of Focal Pancreatic Lesions Detected by Abdominal Ultrasound. *Ultraschall Med* 2019; **40**: 618-624 [PMID: 30895585 DOI: 10.1055/a-0869-7861]
- 10 **Obermeyer Z**, Emanuel EJ. Predicting the Future - Big Data, Machine Learning, and Clinical Medicine. *N Engl J Med* 2016; **375**: 1216-1219 [PMID: 27682033 DOI: 10.1056/NEJMp1606181]
- 11 **Litjens G**, Kooi T, Bejnordi BE, Setio AAA, Ciompi F, Ghafoorian M, van der Laak JAWM, van Ginneken B, Sánchez CI. A survey on deep learning in medical image analysis. *Med Image Anal* 2017; **42**: 60-88 [PMID: 28778026 DOI: 10.1016/j.media.2017.07.005]
- 12 **Pesapane F**, Codari M, Sardanelli F. Artificial intelligence in medical imaging: threat or opportunity? *Eur Radiol Exp* 2018; **2**: 35 [PMID: 30353365 DOI: 10.1186/s41747-018-0061-6]
- 13 **European Society of Radiology (ESR)**. Impact of artificial intelligence on radiology: a EuroAIM survey among members of the European Society of Radiology. *Insights Imaging* 2019; **10**: 105 [PMID: 31673823 DOI: 10.1186/s13244-019-0798-3]
- 14 **Collado-Mesa F**, Alvarez E, Arheart K. The Role of Artificial Intelligence in Diagnostic Radiology: A Survey at a Single Radiology Residency Training Program. *J Am Coll Radiol* 2018; **15**: 1753-1757 [PMID: 29477289 DOI: 10.1016/j.jacr.2017.12.021]
- 15 **Halevy A**, Norvig P, Pereira F. The Unreasonable Effectiveness of Data. *EEE Intell Syst* 2009; **24**:

- 8-12 [DOI: [10.1109/MIS.2009.36](https://doi.org/10.1109/MIS.2009.36)]
- 16 **Khan FM.** Semi-supervised transductive regression for survival analysis in medical prognostics, 2016. Available from: <https://rucore.libraries.rutgers.edu/rutgers-lib/51331/>
 - 17 **Zhou Y, Wang Y, Tang P, Bai S, Shen W, Fishman E, Yuille A.** Semi-Supervised 3D Abdominal Multi-Organ Segmentation Via Deep Multi-Planar Co-Training. In: 2019 IEEE Winter Conference on Applications of Computer Vision (WACV); 2019 Jan 7-11; Waikoloa, USA. IEEE, 2019: 121-140 [DOI: [10.1109/WACV.2019.00020](https://doi.org/10.1109/WACV.2019.00020)]
 - 18 **Chaitanya K, Karani N, Baumgartner CF, Becker A, Donati O, Konukoglu E.** Semi-supervised and Task-Driven Data Augmentation. In: Chung ACS, Gee JC, Yushkevich PA, Bao S. Information Processing in Medical Imaging. Cham: Springer International Publishing, 2019: 29-41
 - 19 **Sergio A, Cristofori C, Cardin R, Pivetta G, Ragazzi R, Baldan A, Girardi L, Cillo U, Burra P, Giacomini A, Farinati F.** Transcatheter arterial chemoembolization (TACE) in hepatocellular carcinoma (HCC): the role of angiogenesis and invasiveness. *Am J Gastroenterol* 2008; **103**: 914-921 [PMID: [18177453](https://pubmed.ncbi.nlm.nih.gov/18177453/) DOI: [10.1111/j.1572-0241.2007.01712.x](https://doi.org/10.1111/j.1572-0241.2007.01712.x)]
 - 20 **McGhana JP, Dodd GD 3rd.** Radiofrequency ablation of the liver: current status. *AJR Am J Roentgenol* 2001; **176**: 3-16 [PMID: [11133529](https://pubmed.ncbi.nlm.nih.gov/11133529/) DOI: [10.2214/ajr.176.1.1760003](https://doi.org/10.2214/ajr.176.1.1760003)]
 - 21 **Moore TJ, Peterson LM, Harrington DP, Smith RJ.** Successful arterial embolization of an insulinoma. *JAMA* 1982; **248**: 1353-1355 [PMID: [6287050](https://pubmed.ncbi.nlm.nih.gov/6287050/)]
 - 22 **Uflacker R.** Arterial embolization as definitive treatment for benign insulinoma of the pancreas. *J Vasc Interv Radiol* 1992; **3**: 639-44; discussion 644 [PMID: [1446125](https://pubmed.ncbi.nlm.nih.gov/1446125/) DOI: [10.1016/s1051-0443\(92\)72912-1](https://doi.org/10.1016/s1051-0443(92)72912-1)]
 - 23 **Peppas M, Brontzos E, Economopoulos N, Boutati E, Pikounis V, Patapis P, Economopoulos T, Raptis SA, Hadjidakis D.** Embolization as an alternative treatment of insulinoma in a patient with multiple endocrine neoplasia type 1 syndrome. *Cardiovasc Intervent Radiol* 2009; **32**: 807-811 [PMID: [19184198](https://pubmed.ncbi.nlm.nih.gov/19184198/) DOI: [10.1007/s00270-008-9499-x](https://doi.org/10.1007/s00270-008-9499-x)]
 - 24 **Girelli R, Frigerio I, Salvia R, Barbi E, Tinazzi Martini P, Bassi C.** Feasibility and safety of radiofrequency ablation for locally advanced pancreatic cancer. *Br J Surg* 2010; **97**: 220-225 [PMID: [20069610](https://pubmed.ncbi.nlm.nih.gov/20069610/) DOI: [10.1002/bjs.6800](https://doi.org/10.1002/bjs.6800)]
 - 25 **Hadjicostas P, Malakounides N, Varianos C, Kitiiris E, Lerni F, Symeonides P.** Radiofrequency ablation in pancreatic cancer. *HPB (Oxford)* 2006; **8**: 61-64 [PMID: [18333241](https://pubmed.ncbi.nlm.nih.gov/18333241/) DOI: [10.1080/136518205004666673](https://doi.org/10.1080/136518205004666673)]
 - 26 **Jones RL, McCall J, Adam A, O'Donnell D, Ashley S, Al-Muderis O, Thway K, Fisher C, Judson IR.** Radiofrequency ablation is a feasible therapeutic option in the multi modality management of sarcoma. *Eur J Surg Oncol* 2010; **36**: 477-482 [PMID: [20060679](https://pubmed.ncbi.nlm.nih.gov/20060679/) DOI: [10.1016/j.ejso.2009.12.005](https://doi.org/10.1016/j.ejso.2009.12.005)]
 - 27 **Ramaswamy RS, Choi HW, Mouser HC, Narsinh KH, McCammack KC, Treesit T, Kinney TB.** Role of interventional radiology in the management of acute gastrointestinal bleeding. *World J Radiol* 2014; **6**: 82-92 [PMID: [24778770](https://pubmed.ncbi.nlm.nih.gov/24778770/) DOI: [10.4329/wjr.v6.i4.82](https://doi.org/10.4329/wjr.v6.i4.82)]
 - 28 **Takeuchi N, Emori M, Yoshitani M, Soneda J, Takada M, Nomura Y.** Gastrointestinal Bleeding Successfully Treated Using Interventional Radiology. *Gastroenterology Res* 2017; **10**: 259-267 [PMID: [28912915](https://pubmed.ncbi.nlm.nih.gov/28912915/) DOI: [10.14740/gr851e](https://doi.org/10.14740/gr851e)]
 - 29 **Cura M, Haskal Z, Lopera J.** Diagnostic and interventional radiology for Budd-Chiari syndrome. *Radiographics* 2009; **29**: 669-681 [PMID: [19448109](https://pubmed.ncbi.nlm.nih.gov/19448109/) DOI: [10.1148/rg.293085056](https://doi.org/10.1148/rg.293085056)]
 - 30 **Ikeda O, Tamura Y, Nakasone Y, Yamashita Y.** Celiac artery stenosis/occlusion treated by interventional radiology. *Eur J Radiol* 2009; **71**: 369-377 [PMID: [18562143](https://pubmed.ncbi.nlm.nih.gov/18562143/) DOI: [10.1016/j.ejrad.2008.05.005](https://doi.org/10.1016/j.ejrad.2008.05.005)]
 - 31 **Rösch T, Lorenz R, Braig C, Feuerbach S, Siewert JR, Schusdziarra V, Classen M.** Endoscopic ultrasound in pancreatic tumor diagnosis. *Gastrointest Endosc* 1991; **37**: 347-352 [PMID: [2070987](https://pubmed.ncbi.nlm.nih.gov/2070987/) DOI: [10.1016/s0016-5107\(91\)70729-3](https://doi.org/10.1016/s0016-5107(91)70729-3)]
 - 32 **Kelly S, Harris KM, Berry E, Hutton J, Roderick P, Cullingworth J, Gathercole L, Smith MA.** A systematic review of the staging performance of endoscopic ultrasound in gastro-oesophageal carcinoma. *Gut* 2001; **49**: 534-539 [PMID: [11559651](https://pubmed.ncbi.nlm.nih.gov/11559651/) DOI: [10.1136/gut.49.4.534](https://doi.org/10.1136/gut.49.4.534)]
 - 33 **Williams DB, Sahai AV, Aabakken L, Penman ID, van Velse A, Webb J, Wilson M, Hoffman BJ, Hawes RH.** Endoscopic ultrasound guided fine needle aspiration biopsy: a large single centre experience. *Gut* 1999; **44**: 720-726 [PMID: [10205212](https://pubmed.ncbi.nlm.nih.gov/10205212/) DOI: [10.1136/gut.44.5.720](https://doi.org/10.1136/gut.44.5.720)]
 - 34 **Kahaleh M, Shami VM, Conaway MR, Tokar J, Rockoff T, De La Rue SA, de Lange E, Bassignani M, Gay S, Adams RB, Yeaton P.** Endoscopic ultrasound drainage of pancreatic pseudocyst: a prospective comparison with conventional endoscopic drainage. *Endoscopy* 2006; **38**: 355-359 [PMID: [16680634](https://pubmed.ncbi.nlm.nih.gov/16680634/) DOI: [10.1055/s-2006-925249](https://doi.org/10.1055/s-2006-925249)]
 - 35 **Clark K, Vendt B, Smith K, Freymann J, Kirby J, Koppel P, Moore S, Phillips S, Maffitt D, Pringle M, Tarbox L, Prior F.** The Cancer Imaging Archive (TCIA): maintaining and operating a public information repository. *J Digit Imaging* 2013; **26**: 1045-1057 [PMID: [23884657](https://pubmed.ncbi.nlm.nih.gov/23884657/) DOI: [10.1007/s10278-013-9622-7](https://doi.org/10.1007/s10278-013-9622-7)]
 - 36 **Roth H, Farag A, Turkbey EB, Lu L, Liu J, Summers RM.** Data From Pancreas-CT, 2016. Available from: <https://wiki.cancerimagingarchive.net/x/eIIXAQ>
 - 37 **Roth HR, Lu L, Farag A, Shin H-C, Liu J, Turkbey E, Summers RM.** DeepOrgan: Multi-level Deep Convolutional Networks for Automated Pancreas Segmentation. 2015 Preprint. Available from: arXiv:150606448
 - 38 **Xu Z, Lee CP, Heinrich MP, Modat M, Rueckert D, Ourselin S, Abramson RG, Landman BA.** Evaluation of Six Registration Methods for the Human Abdomen on Clinically Acquired CT. *IEEE*

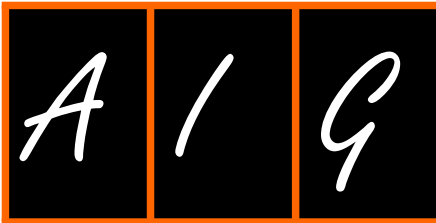
- Trans Biomed Eng* 2016; **63**: 1563-1572 [PMID: 27254856 DOI: 10.1109/TBME.2016.2574816]
- 39 **Synapse**. Multi-Atlas Labeling Beyond the Cranial Vault - Workshop and Challenge - syn3193805 - Wiki. Available from: <https://www.synapse.org/#!/Synapse:syn3193805/wiki/89480>
- 40 **Li X**, Jiang F, Guo Y, Jin Z, Wang Y. Computer-aided diagnosis of gastrointestinal stromal tumors: a radiomics method on endoscopic ultrasound image. *Int J Comput Assist Radiol Surg* 2019; **14**: 1635-1645 [PMID: 31049803 DOI: 10.1007/s11548-019-01993-3]
- 41 **Jaramillo M**, Ruano J, Gómez M, Romero E. Endoscopic ultrasound database of the pancreas. In: Proceedings Volume 11583, 16th International Symposium on Medical Information Processing and Analysis; 2020 Nov 3; Lima, Peru. International Society for Optics and Photonics, 2020: 115830G [DOI: 10.1117/12.2581321]
- 42 **Yan K**, Wang X, Lu L, Summers RM. DeepLesion: automated mining of large-scale lesion annotations and universal lesion detection with deep learning. *J Med Imaging (Bellingham)* 2018; **5**: 036501 [PMID: 30035154 DOI: 10.1117/1.JMI.5.3.036501]
- 43 **Li Z**, Zhang S, Zhang J, Huang K, Wang Y, Yu Y. MVP-Net: Multi-view FPN with Position-Aware Attention for Deep Universal Lesion Detection. In: Shen D, Liu T, Peters TM, Staib LH, Essert C, Zhou S, Yap RT, Khan A, editors. Medical Image Computing and Computer Assisted Intervention - MICCAI 2019. Cham: Springer International Publishing, 2019: 13-21
- 44 **Schellinger PD**, Jansen O, Fiebach JB, Hacke W, Sartor K. A standardized MRI stroke protocol: comparison with CT in hyperacute intracerebral hemorrhage. *Stroke* 1999; **30**: 765-768 [PMID: 10187876 DOI: 10.1161/01.str.30.4.765]
- 45 **Bammer R**. Basic principles of diffusion-weighted imaging. *Eur J Radiol* 2003; **45**: 169-184 [PMID: 12595101 DOI: 10.1016/s0720-048x(02)00303-0]
- 46 **Amit G**, Hadad O, Alpert S, Tlusty T, Gur Y, Ben-Ari R, Hashoul S. Hybrid Mass Detection in Breast MRI Combining Unsupervised Saliency Analysis and Deep Learning. In: Descoteaux M, Maier-Hein L, Franz A, Jannin P, Collins DL, Duchesne S, editors. Medical Image Computing and Computer Assisted Intervention - MICCAI 2017. Cham: Springer International Publishing, 2017: 594-602
- 47 **Kijowski R**, Liu F, Caliva F, Pedoia V. Deep Learning for Lesion Detection, Progression, and Prediction of Musculoskeletal Disease. *J Magn Reson Imaging* 2020; **52**: 1607-1619 [PMID: 31763739 DOI: 10.1002/jmri.27001]
- 48 **Su H**, Maji S, Kalogerakis E, Learned-Miller E. Multi-View Convolutional Neural Networks for 3D Shape Recognition, 2015. Available from: https://www.cv-foundation.org/openaccess/content_iccv_2015/html/Su_Multi-View_Convolutional_Neural_ICCV_2015_paper.html
- 49 **Setio AA**, Ciompi F, Litjens G, Gerke P, Jacobs C, van Riel SJ, Wille MM, Naqibullah M, Sanchez CI, van Ginneken B. Pulmonary Nodule Detection in CT Images: False Positive Reduction Using Multi-View Convolutional Networks. *IEEE Trans Med Imaging* 2016; **35**: 1160-1169 [PMID: 26955024 DOI: 10.1109/TMI.2016.2536809]
- 50 **Kang G**, Liu K, Hou B, Zhang N. 3D multi-view convolutional neural networks for lung nodule classification. *PLoS One* 2017; **12**: e0188290 [PMID: 29145492 DOI: 10.1371/journal.pone.0188290]
- 51 **El-Regaily SA**, Salem MAM, Abdel Aziz MH, Roushdy MI. Multi-view Convolutional Neural Network for lung nodule false positive reduction. *Expert Syst Appl* 2020; **162**: 113017
- 52 **Sun L**, Wang J, Hu Z, Xu Y, Cui Z. Multi-View Convolutional Neural Networks for Mammographic Image Classification. *IEEE Access* 2019; **7**: 126273-126282
- 53 **Birenbaum A**, Greenspan H. Longitudinal Multiple Sclerosis Lesion Segmentation Using Multi-view Convolutional Neural Networks. In: Carneiro G, Mateus D, Peter L, Bradley A, Tavares JMRS, Belagiannis V, Papa JP, Nascimento JC, Loog M, Lu Z, Cardoso JS, Cornebise J. Deep Learning and Data Labeling for Medical Applications. Cham: Springer International Publishing, 2016: 58-67
- 54 **Zlocha M**, Dou Q, Glocker B. Improving RetinaNet for CT Lesion Detection with Dense Masks from Weak RECISt Labels. In: Shen D, Liu T, Peters TM, Staib LH, Essert C, Zhou S, Yap RT, Khan A. Medical Image Computing and Computer Assisted Intervention - MICCAI 2019. Cham: Springer International Publishing, 2019: 402-410
- 55 **Lin TY**, Goyal P, Girshick R, He K, Dollar P. Focal Loss for Dense Object Detection. *IEEE Trans Pattern Anal Mach Intell* 2020; **42**: 318-327 [PMID: 30040631 DOI: 10.1109/TPAMI.2018.2858826]
- 56 **Tang Y**, Yan K, Tang Y, Liu J, Xiao J, Summers RM. Uldor: A Universal Lesion Detector For Ct Scans With Pseudo Masks And Hard Negative Example Mining. In: 2019 IEEE 16th International Symposium on Biomedical Imaging (ISBI 2019); 2019 Apr 8-11; Venice, Italy. IEEE, 2019: 833-836 [DOI: 10.1109/ISBI.2019.8759478]
- 57 **Harbin WP**, Mueller PR, Ferrucci JT Jr. Transhepatic cholangiography: complications and use patterns of the fine-needle technique: a multi-institutional survey. *Radiology* 1980; **135**: 15-22 [PMID: 6987704 DOI: 10.1148/radiology.135.1.6987704]
- 58 **Korman J**, Cosgrove J, Furman M, Nathan I, Cohen J. The role of endoscopic retrograde cholangiopancreatography and cholangiography in the laparoscopic era. *Ann Surg* 1996; **223**: 212-216 [PMID: 8597517 DOI: 10.1097/0000658-199602000-00015]
- 59 **Ney MV**, Maluf-Filho F, Sakai P, Zilberstein B, Gama-Rodrigues J, Rosa H. Echo-endoscopy versus endoscopic retrograde cholangiography for the diagnosis of choledocholithiasis: the influence of the size of the stone and diameter of the common bile duct. *Arq Gastroenterol* 2005; **42**: 239-243

- [PMID: 16444379 DOI: 10.1590/s0004-28032005000400009]
- 60 **Maranki J**, Hernandez AJ, Arslan B, Jaffan AA, Angle JF, Shami VM, Kahaleh M. Interventional endoscopic ultrasound-guided cholangiography: long-term experience of an emerging alternative to percutaneous transhepatic cholangiography. *Endoscopy* 2009; **41**: 532-538 [PMID: 19533558 DOI: 10.1055/s-0029-1214712]
 - 61 **Angulo P**, Lindor KD. Primary sclerosing cholangitis. *Hepatology* 1999; **30**: 325-332 [PMID: 10385674 DOI: 10.1002/hep.510300101]
 - 62 **O'Neill JA Jr.** Choledochal cyst. *Curr Probl Surg* 1992; **29**: 361-410 [PMID: 1582241 DOI: 10.1016/0011-3840(92)90025-x]
 - 63 **Sahni VA**, Mortelet KJ. Magnetic Resonance Cholangiopancreatography. In: Hawkey CJ, Bosch J, Richter JE, Garcia-Tsao G, Chan FKL. Textbook of Clinical Gastroenterology and Hepatology. John Wiley & Sons, 2012: 1021-1026 [DOI: 10.1002/9781118321386.ch135]
 - 64 **Fleischmann D**, Ringl H, Schöfl R, Pötzi R, Kontrus M, Henk C, Bankier AA, Kettenbach J, Mostbeck GH. Three-dimensional spiral CT cholangiography in patients with suspected obstructive biliary disease: comparison with endoscopic retrograde cholangiography. *Radiology* 1996; **198**: 861-868 [PMID: 8628884 DOI: 10.1148/radiology.198.3.8628884]
 - 65 **Varghese JC**, Liddell RP, Farrell MA, Murray FE, Osborne DH, Lee MJ. Diagnostic accuracy of magnetic resonance cholangiopancreatography and ultrasound compared with direct cholangiography in the detection of choledocholithiasis. *Clin Radiol* 2000; **55**: 25-35 [PMID: 10650107 DOI: 10.1053/crad.1999.0319]
 - 66 **Liang C**, Mao H, Wang Q, Han D, Li Yuxia L, Yue J, Cui H, Sun F, Yang R. Diagnostic performance of magnetic resonance cholangiopancreatography in malignant obstructive jaundice. *Cell Biochem Biophys* 2011; **61**: 383-388 [PMID: 21567133 DOI: 10.1007/s12013-011-9195-3]
 - 67 **McSweeney SE**, Kim TK, Jang HJ, Khalili K. Biliary anatomy in potential right hepatic lobe living donor liver transplantation (LDLT): the utility of CT cholangiography in the setting of inconclusive MRCP. *Eur J Radiol* 2012; **81**: 6-12 [PMID: 21041052 DOI: 10.1016/j.ejrad.2010.10.013]
 - 68 **De Castro VL**, Moura EG, Chaves DM, Bernardo WM, Matuguma SE, Artifon EL. Endoscopic ultrasound versus magnetic resonance cholangiopancreatography in suspected choledocholithiasis: A systematic review. *Endosc Ultrasound* 2016; **5**: 118-128 [PMID: 27080611 DOI: 10.4103/2303-9027.180476]
 - 69 **Guarise A**, Baltieri S, Mainardi P, Faccioli N. Diagnostic accuracy of MRCP in choledocholithiasis. *Radiol Med* 2005; **109**: 239-251 [PMID: 15775893]
 - 70 **de Jong K**, Nio CY, Mearadji B, Phoa SS, Engelbrecht MR, Dijkgraaf MG, Bruno MJ, Fockens P. Disappointing interobserver agreement among radiologists for a classifying diagnosis of pancreatic cysts using magnetic resonance imaging. *Pancreas* 2012; **41**: 278-282 [PMID: 22015970 DOI: 10.1097/MPA.0b013e31822899b6]
 - 71 **Uribarri-Gonzalez L**, Keane MG, Pereira SP, Iglesias-García J, Dominguez-Muñoz JE, Lariño-Noia J. Agreement among Magnetic Resonance Imaging/Magnetic Resonance Cholangiopancreatography (MRI-MRCP) and Endoscopic Ultrasound (EUS) in the evaluation of morphological features of Branch Duct Intraductal Papillary Mucinous Neoplasm (BD-IPMN). *Pancreatology* 2018; **18**: 170-175 [PMID: 29338919 DOI: 10.1016/j.pan.2018.01.002]
 - 72 **Ringe KI**, Vo Chieu VD, Wacker F, Lenzen H, Manns MP, Hundt C, Schmidt B, Winther HB. Fully automated detection of primary sclerosing cholangitis (PSC)-compatible bile duct changes based on 3D magnetic resonance cholangiopancreatography using machine learning. *Eur Radiol* 2021; **31**: 2482-2489 [PMID: 32974688 DOI: 10.1007/s00330-020-07323-5]
 - 73 **Tang Y**, Chen X, Wang W, Wu J, Zheng Y, Q Guo, Shu J, Su S. Identifying Periapillary Regions in MRI Images Using Deep Learning. 2020 Preprint. Available from: ResearchSquare:109396 [DOI: 10.21203/rs.3.rs-109369/v1]
 - 74 **AL-Oudat MA**, Oudat MA, Migdady H, Munaizel TA, Mahmoud MA, Jaafreh S. Automatic Intrahepatic Biliary Segmentation Based Image Processing Techniques using Magnetic Resonance Images. 2020 Preprint. Available from: ResearchSquare:106936 [DOI: 10.21203/rs.3.rs-106936/v1]
 - 75 **Huang L**, Lu X, Huang X, Zou X, Wu L, Zhou Z, Wu D, Tang D, Chen D, Wan X, Zhu Z, Deng T, Shen L, Liu J, Zhu Y, Gong D, Zhong Y, Liu F, Yu H. Intelligent difficulty scoring and assistance system for endoscopic extraction of common bile duct stones based on deep learning: multicenter study. *Endoscopy* 2020 [PMID: 32838430 DOI: 10.1055/a-1244-5698]
 - 76 **Zhang J**, Zhu L, Yao L, Ding X, Chen D, Wu H, Lu Z, Zhou W, Zhang L, An P, Xu B, Tan W, Hu S, Cheng F, Yu H. Deep learning-based pancreas segmentation and station recognition system in EUS: development and validation of a useful training tool (with video). *Gastrointest Endosc* 2020; **92**: 874-885. e3 [PMID: 32387499 DOI: 10.1016/j.gie.2020.04.071]
 - 77 **Chalasanani N**, Said A, Ness R, Hoen H, Lumeng L. Screening for hepatocellular carcinoma in patients with cirrhosis in the United States: results of a national survey. *Am J Gastroenterol* 1999; **94**: 2224-2229 [PMID: 10445554 DOI: 10.1111/j.1572-0241.1999.01297.x]
 - 78 **Boraschi P**, Tarantini G, Pacciardi F, Donati F. Dynamic and Multi-phase Contrast-Enhanced CT Scan. In: Radu-Ionita F, Pyrsopoulos NT, Jinga M, Tintoiu IC, Sun Z, Bontas E, editors. Liver Diseases: A Multidisciplinary Textbook. Cham: Springer International Publishing, 2020: 479-491 [DOI: 10.1007/978-3-030-24432-3_42]
 - 79 **Tejeda-Maldonado J**, García-Juárez I, Aguirre-Valadez J, González-Aguirre A, Vilatobá-Chapa M, Armengol-Alonso A, Escobar-Penagos F, Torre A, Sánchez-Ávila JF, Carrillo-Pérez DL. Diagnosis and treatment of hepatocellular carcinoma: An update. *World J Hepatol* 2015; **7**: 362-376 [PMID:

- 25848464 DOI: [10.4254/wjh.v7.i3.362](https://doi.org/10.4254/wjh.v7.i3.362)]
- 80 **Hussain SM**, Terkivatan T, Zondervan PE, Lanjouw E, de Rave S, Ijzermans JN, de Man RA. Focal nodular hyperplasia: findings at state-of-the-art MR imaging, US, CT, and pathologic analysis. *Radiographics* 2004; **24**: 3-17; discussion 18 [PMID: [14730031](https://pubmed.ncbi.nlm.nih.gov/14730031/) DOI: [10.1148/rg.241035050](https://doi.org/10.1148/rg.241035050)]
 - 81 **Choi JY**, Lee HC, Yim JH, Shim JH, Lim YS, Shin YM, Yu ES, Suh DJ. Focal nodular hyperplasia or focal nodular hyperplasia-like lesions of the liver: a special emphasis on diagnosis. *J Gastroenterol Hepatol* 2011; **26**: 1004-1009 [PMID: [21251063](https://pubmed.ncbi.nlm.nih.gov/21251063/) DOI: [10.1111/j.1440-1746.2011.06659.x](https://doi.org/10.1111/j.1440-1746.2011.06659.x)]
 - 82 **Mathieu D**, Bruneton JN, Drouillard J, Pointreau CC, Vasile N. Hepatic adenomas and focal nodular hyperplasia: dynamic CT study. *Radiology* 1986; **160**: 53-58 [PMID: [3520655](https://pubmed.ncbi.nlm.nih.gov/3520655/) DOI: [10.1148/radiology.160.1.3520655](https://doi.org/10.1148/radiology.160.1.3520655)]
 - 83 **Toft J**, Hadden WJ, Laurence JM, Lam V, Yuen L, Janssen A, Pleass H. Imaging modalities in the diagnosis of pancreatic adenocarcinoma: A systematic review and meta-analysis of sensitivity, specificity and diagnostic accuracy. *Eur J Radiol* 2017; **92**: 17-23 [PMID: [28624015](https://pubmed.ncbi.nlm.nih.gov/28624015/) DOI: [10.1016/j.ejrad.2017.04.009](https://doi.org/10.1016/j.ejrad.2017.04.009)]
 - 84 **Chakraborty J**, Midya A, Gazit L, Attiyeh M, Langdon-Embry L, Allen PJ, Do RKG, Simpson AL. CT radiomics to predict high-risk intraductal papillary mucinous neoplasms of the pancreas. *Med Phys* 2018; **45**: 5019-5029 [PMID: [30176047](https://pubmed.ncbi.nlm.nih.gov/30176047/) DOI: [10.1002/mp.13159](https://doi.org/10.1002/mp.13159)]
 - 85 **Li R**, Cai P, Ma KS, Ding SY, Guo DY, Yan XC. Dynamic enhancement patterns of intrahepatic cholangiocarcinoma in cirrhosis on contrast-enhanced computed tomography: risk of misdiagnosis as hepatocellular carcinoma. *Sci Rep* 2016; **6**: 26772 [PMID: [27226026](https://pubmed.ncbi.nlm.nih.gov/27226026/) DOI: [10.1038/srep26772](https://doi.org/10.1038/srep26772)]
 - 86 **Galassi M**, Iavarone M, Rossi S, Bota S, Vavassori S, Rosa L, Leoni S, Venerandi L, Marinelli S, Sangiovanni A, Veronese L, Fraquelli M, Granito A, Golfieri R, Colombo M, Bolondi L, Piscaglia F. Patterns of appearance and risk of misdiagnosis of intrahepatic cholangiocarcinoma in cirrhosis at contrast enhanced ultrasound. *Liver Int* 2013; **33**: 771-779 [PMID: [23445369](https://pubmed.ncbi.nlm.nih.gov/23445369/) DOI: [10.1111/liv.12124](https://doi.org/10.1111/liv.12124)]
 - 87 **Massarweh NN**, El-Serag HB. Epidemiology of Hepatocellular Carcinoma and Intrahepatic Cholangiocarcinoma. *Cancer Control* 2017; **24**: 1073274817729245 [PMID: [28975830](https://pubmed.ncbi.nlm.nih.gov/28975830/) DOI: [10.1177/1073274817729245](https://doi.org/10.1177/1073274817729245)]
 - 88 **Zhou XD**, Tang ZY, Fan J, Zhou J, Wu ZQ, Qin LX, Ma ZC, Sun HC, Qiu SJ, Yu Y, Ren N, Ye QH, Wang L, Ye SL. Intrahepatic cholangiocarcinoma: report of 272 patients compared with 5,829 patients with hepatocellular carcinoma. *J Cancer Res Clin Oncol* 2009; **135**: 1073-1080 [PMID: [19294418](https://pubmed.ncbi.nlm.nih.gov/19294418/) DOI: [10.1007/s00432-009-0547-y](https://doi.org/10.1007/s00432-009-0547-y)]
 - 89 **Neofytou K**, Chrysochos A, Charalambous N, Diets M, Petridis C, Andreou C, Petrou A. Hepatic epithelioid hemangi endothelioma and the danger of misdiagnosis: report of a case. *Case Rep Oncol Med* 2013; **2013**: 243939 [PMID: [23533870](https://pubmed.ncbi.nlm.nih.gov/23533870/) DOI: [10.1155/2013/243939](https://doi.org/10.1155/2013/243939)]
 - 90 **Mehrabi A**, Kashfi A, Fonouni H, Schemmer P, Schmiech BM, Hallscheidt P, Schirmacher P, Weitz J, Friess H, Buchler MW, Schmidt J. Primary malignant hepatic epithelioid hemangi endothelioma: a comprehensive review of the literature with emphasis on the surgical therapy. *Cancer* 2006; **107**: 2108-2121 [PMID: [17019735](https://pubmed.ncbi.nlm.nih.gov/17019735/) DOI: [10.1002/encr.22225](https://doi.org/10.1002/encr.22225)]
 - 91 **Yamada S**, Shimada M, Utsunomiya T, Morine Y, Imura S, Ikemoto T, Mori H, Hanaoka J, Iwahashi S, Saitoh Y, Asanoma M. Hepatic sclerosed hemangioma which was misdiagnosed as metastasis of gastric cancer: report of a case. *J Med Invest* 2012; **59**: 270-274 [PMID: [23037199](https://pubmed.ncbi.nlm.nih.gov/23037199/) DOI: [10.2152/jmi.59.270](https://doi.org/10.2152/jmi.59.270)]
 - 92 **Pitman A**, Cowan IA, Floyd RA, Munro PL. Measuring radiologist workload: Progressing from RVUs to study ascribable times. *J Med Imaging Radiat Oncol* 2018; **62**: 605-618 [PMID: [30070435](https://pubmed.ncbi.nlm.nih.gov/30070435/) DOI: [10.1111/1754-9485.12778](https://doi.org/10.1111/1754-9485.12778)]
 - 93 **Khan SH**, Hedges WP. Workload of consultant radiologists in a large DGH and how it compares to international benchmarks. *Clin Radiol* 2013; **68**: e239-e244 [PMID: [23261034](https://pubmed.ncbi.nlm.nih.gov/23261034/) DOI: [10.1016/j.crad.2012.10.016](https://doi.org/10.1016/j.crad.2012.10.016)]
 - 94 **Muhi A**, Ichikawa T, Motosugi U, Sou H, Sano K, Tsukamoto T, Fatima Z, Araki T. Mass-forming autoimmune pancreatitis and pancreatic carcinoma: differential diagnosis on the basis of computed tomography and magnetic resonance cholangiopancreatography, and diffusion-weighted imaging findings. *J Magn Reson Imaging* 2012; **35**: 827-836 [PMID: [22069025](https://pubmed.ncbi.nlm.nih.gov/22069025/) DOI: [10.1002/jmri.22881](https://doi.org/10.1002/jmri.22881)]
 - 95 **Zaheer A**, Singh VK, Akshintala VS, Kawamoto S, Tsai SD, Gage KL, Fishman EK. Differentiating autoimmune pancreatitis from pancreatic adenocarcinoma using dual-phase computed tomography. *J Comput Assist Tomogr* 2014; **38**: 146-152 [PMID: [24424563](https://pubmed.ncbi.nlm.nih.gov/24424563/) DOI: [10.1097/RCT.0b013e3182a9a431](https://doi.org/10.1097/RCT.0b013e3182a9a431)]
 - 96 **Chiou YY**, Chiang JH, Hwang JI, Yen CH, Tsay SH, Chang CY. Acinar cell carcinoma of the pancreas: clinical and computed tomography manifestations. *J Comput Assist Tomogr* 2004; **28**: 180-186 [PMID: [15091120](https://pubmed.ncbi.nlm.nih.gov/15091120/) DOI: [10.1097/00004728-200403000-00005](https://doi.org/10.1097/00004728-200403000-00005)]
 - 97 **Das A**, Acharya UR, Panda SS, Sabut S. Deep learning based liver cancer detection using watershed transform and Gaussian mixture model techniques. *Cogn Syst Res* 2019; **54**: 165-175 [DOI: [10.1016/j.cogsys.2018.12.009](https://doi.org/10.1016/j.cogsys.2018.12.009)]
 - 98 **Vorontsov E**, Cerny M, Régnier P, Di Jorio L, Pal CJ, Lapointe R, Vandenbroucke-Menu F, Turcotte S, Kadoury S, Tang A. Deep learning for automated segmentation of liver lesions at CT in patients with colorectal cancer liver metastases. *Radiol Artif Intell* 2019; **1**: 180014 [DOI: [10.1148/ryai.2019180014](https://doi.org/10.1148/ryai.2019180014)]
 - 99 **Kuo C**, Cheng S, Lin C, Hsiao K, Lee S. Texture-based treatment prediction by automatic liver

- tumor segmentation on computed tomography. In: 2017 International Conference on Computer, Information and Telecommunication Systems (CITS); 2017 July 21-23; Dalian, China. IEEE, 2017; 128-132 [DOI: [10.1109/CITS.2017.8035318](https://doi.org/10.1109/CITS.2017.8035318)]
- 100 **Huang W**, Li N, Lin Z, Huang G, Zong W, Zhou J, Duan Y. Liver tumor detection and segmentation using kernel-based extreme learning machine. In: 2013 35th Annual International Conference of the IEEE Engineering in Medicine and Biology Society (EMBC); 2013 July 3-7; Osaka, Japan. IEEE, 2013; 3662-3665 [DOI: [10.1109/EMBC.2013.6610337](https://doi.org/10.1109/EMBC.2013.6610337)]
- 101 **Li S**, Jiang H, Wang Z, Zhang G, Yao YD. An effective computer aided diagnosis model for pancreas cancer on PET/CT images. *Comput Methods Programs Biomed* 2018; **165**: 205-214 [PMID: [30337075](https://pubmed.ncbi.nlm.nih.gov/30337075/) DOI: [10.1016/j.cmpb.2018.09.001](https://doi.org/10.1016/j.cmpb.2018.09.001)]
- 102 **Liu SL**, Li S, Guo YT, Zhou YP, Zhang ZD, Lu Y. Establishment and application of an artificial intelligence diagnosis system for pancreatic cancer with a faster region-based convolutional neural network. *Chin Med J (Engl)* 2019; **132**: 2795-2803 [PMID: [31856050](https://pubmed.ncbi.nlm.nih.gov/31856050/) DOI: [10.1097/CM9.0000000000000544](https://doi.org/10.1097/CM9.0000000000000544)]
- 103 **Xu J**, Jing M, Wang S, Yang C, Chen X. A review of medical image detection for cancers in digestive system based on artificial intelligence. *Expert Rev Med Devices* 2019; **16**: 877-889 [PMID: [31530047](https://pubmed.ncbi.nlm.nih.gov/31530047/) DOI: [10.1080/17434440.2019.1669447](https://doi.org/10.1080/17434440.2019.1669447)]
- 104 **Zhen SH**, Cheng M, Tao YB, Wang YF, Juengpanich S, Jiang ZY, Jiang YK, Yan YY, Lu W, Lue JM, Qian JH, Wu ZY, Sun JH, Lin H, Cai XJ. Deep Learning for Accurate Diagnosis of Liver Tumor Based on Magnetic Resonance Imaging and Clinical Data. *Front Oncol* 2020; **10**: 680 [PMID: [32547939](https://pubmed.ncbi.nlm.nih.gov/32547939/) DOI: [10.3389/fonc.2020.00680](https://doi.org/10.3389/fonc.2020.00680)]
- 105 **Yasaka K**, Akai H, Abe O, Kiryu S. Deep Learning with Convolutional Neural Network for Differentiation of Liver Masses at Dynamic Contrast-enhanced CT: A Preliminary Study. *Radiology* 2018; **286**: 887-896 [PMID: [29059036](https://pubmed.ncbi.nlm.nih.gov/29059036/) DOI: [10.1148/radiol.2017170706](https://doi.org/10.1148/radiol.2017170706)]
- 106 **Wani S**, Keswani RN, Han S, Aagaard EM, Hall M, Simon V, Abidi WM, Banerjee S, Baron TH, Bartel M, Bowman E, Brauer BC, Buscaglia JM, Carlin L, Chak A, Chatrath H, Choudhary A, Confer B, Coté GA, Das KK, DiMaio CJ, Dries AM, Edmundowicz SA, El Chafic AH, El Hajj I, Ellert S, Ferreira J, Gamboa A, Gan IS, Gangarosa LM, Gannavarapu B, Gordon SR, Guda NM, Hammad HT, Harris C, Jalaj S, Jowell PS, Kenshil S, Klapman J, Kochman ML, Komanduri S, Lang G, Lee LS, Loren DE, Lukens FJ, Mullady D, Muthusamy VR, Nett AS, Olyaea MS, Pakserehet K, Perera P, Pfau P, Piraka C, Ponerros JM, Rastogi A, Razzak A, Riff B, Saligram S, Scheiman JM, Schuster I, Shah RJ, Sharma R, Spaete JP, Singh A, Sohail M, Sreenarasimhaiah J, Stevens T, Tabibian JH, Tzimas D, Uppal DS, Urayama S, Vitterbo D, Wang AY, Wassef W, Yachimski P, Zepeda-Gomez S, Zuchelli T, Early D. Competence in Endoscopic Ultrasound and Endoscopic Retrograde Cholangiopancreatography, From Training Through Independent Practice. *Gastroenterology* 2018; **155**: 1483-1494. e7 [PMID: [30056094](https://pubmed.ncbi.nlm.nih.gov/30056094/) DOI: [10.1053/j.gastro.2018.07.024](https://doi.org/10.1053/j.gastro.2018.07.024)]
- 107 **Levy MJ**, Wiersema MJ. EUS-guided Trucut biopsy. *Gastrointest Endosc* 2005; **62**: 417-426 [PMID: [16111962](https://pubmed.ncbi.nlm.nih.gov/16111962/) DOI: [10.1016/j.gie.2005.04.044](https://doi.org/10.1016/j.gie.2005.04.044)]
- 108 **Patel R**, Varadarajulu S, Wilcox CM. Endoscopic ampullectomy: techniques and outcomes. *J Clin Gastroenterol* 2012; **46**: 8-15 [PMID: [22064552](https://pubmed.ncbi.nlm.nih.gov/22064552/) DOI: [10.1097/MCG.0b013e318233a844](https://doi.org/10.1097/MCG.0b013e318233a844)]
- 109 **Tonozuka R**, Mukai S, Itoi T. The Role of Artificial Intelligence in Endoscopic Ultrasound for Pancreatic Disorders. *Diagnostics (Basel)* 2020; **11** [PMID: [33374181](https://pubmed.ncbi.nlm.nih.gov/33374181/) DOI: [10.3390/diagnostics11010018](https://doi.org/10.3390/diagnostics11010018)]
- 110 **Kikuchi D**, Iizuka T, Hoteya S, Yamada A, Furuhashi T, Yamashita S, Domon K, Nakamura M, Matsui A, Mitani T, Ogawa O, Kaise M. Prospective Study about the Utility of Endoscopic Ultrasound for Predicting the Safety of Endoscopic Submucosal Dissection in Early Gastric Cancer (T-HOPE 0801). *Gastroenterol Res Pract* 2013; **2013**: 329385 [PMID: [23606832](https://pubmed.ncbi.nlm.nih.gov/23606832/) DOI: [10.1155/2013/329385](https://doi.org/10.1155/2013/329385)]
- 111 **Cho BJ**, Bang CS, Lee JJ, Seo CW, Kim JH. Prediction of Submucosal Invasion for Gastric Neoplasms in Endoscopic Images Using Deep-Learning. *J Clin Med* 2020; **9** [PMID: [32549190](https://pubmed.ncbi.nlm.nih.gov/32549190/) DOI: [10.3390/jcm9061858](https://doi.org/10.3390/jcm9061858)]
- 112 **Tonozuka R**, Itoi T, Nagata N, Kojima H, Sofuni A, Tsuchiya T, Ishii K, Tanaka R, Nagakawa Y, Mukai S. Deep learning analysis for the detection of pancreatic cancer on endosonographic images: a pilot study. *J Hepatobiliary Pancreat Sci* 2021; **28**: 95-104 [PMID: [32910528](https://pubmed.ncbi.nlm.nih.gov/32910528/) DOI: [10.1002/jhbp.825](https://doi.org/10.1002/jhbp.825)]
- 113 **Scott IA**, Cook D, Coiera EW, Richards B. Machine learning in clinical practice: prospects and pitfalls. *Med J Aust* 2019; **211**: 203-205. e1 [PMID: [31389031](https://pubmed.ncbi.nlm.nih.gov/31389031/) DOI: [10.5694/mja2.50294](https://doi.org/10.5694/mja2.50294)]
- 114 **Goyal S**. An Overview of Current Trends, Techniques, Prospects, and Pitfalls of Artificial Intelligence in Breast Imaging. *RMI* 2021; **14**: 15-25 [DOI: [10.2147/RMI.S295205](https://doi.org/10.2147/RMI.S295205)]
- 115 **Mazurowski MA**, Buda M, Saha A, Bashir MR. Deep learning in radiology: An overview of the concepts and a survey of the state of the art with focus on MRI. *J Magn Reson Imaging* 2019; **49**: 939-954 [PMID: [30575178](https://pubmed.ncbi.nlm.nih.gov/30575178/) DOI: [10.1002/jmri.26534](https://doi.org/10.1002/jmri.26534)]
- 116 **Ahmad R**. Reviewing the relationship between machines and radiology: the application of artificial intelligence. *Acta Radiol Open* 2021; **10**: 2058460121990296 [PMID: [33623711](https://pubmed.ncbi.nlm.nih.gov/33623711/) DOI: [10.1177/2058460121990296](https://doi.org/10.1177/2058460121990296)]
- 117 **Goodfellow IJ**, Pouget-Abadie J, Mirza M, Xu B, Warde-Farley D, Ozair S, Aaron Courville A, Bengio Y. Generative Adversarial Networks. 2014 Preprint. Available from: arxiv:1406.2661
- 118 **Sun Y**, Wong AKC, Kamel MS. Classification of imbalanced data: a review. *Int J Patt Recogn Artif Intell* 2009; **23**: 687-719 [DOI: [10.1142/S0218001409007326](https://doi.org/10.1142/S0218001409007326)]

- 119 **Roberts M**, Driggs D, Thorpe M, Gilbey J, Yeung M, Ursprung S, Aviles-Rivero AI, Etmann C, McCague C, Beer L, Weir-McCall JR, Teng Z, Gkrania-Klotsas E, Covnet A, Rudd JHF, Sala E, Schönlieb CB. Common pitfalls and recommendations for using machine learning to detect and prognosticate for COVID-19 using chest radiographs and CT scans. *Nat Mach Intell* 2021; **3**: 199-217 [DOI: [10.1038/s42256-021-00307-0](https://doi.org/10.1038/s42256-021-00307-0)]
- 120 **Yeung BP**, Chiu PW. Application of robotics in gastrointestinal endoscopy: A review. *World J Gastroenterol* 2016; **22**: 1811-1825 [PMID: [26855540](https://pubmed.ncbi.nlm.nih.gov/26855540/) DOI: [10.3748/wjg.v22.i5.1811](https://doi.org/10.3748/wjg.v22.i5.1811)]
- 121 **Quaglia C**, Buselli E, Webster RJ, Valdastri P, Menciassi A, Dario P. An endoscopic capsule robot: a meso-scale engineering case study. *J Micromech Microeng* 2009; **19**: 105007 [DOI: [10.1088/0960-1317/19/10/105007](https://doi.org/10.1088/0960-1317/19/10/105007)]
- 122 **Turan M**, Almalioglu Y, Araujo H, Konukoglu E, Sitti M. A non-rigid map fusion-based direct SLAM method for endoscopic capsule robots. *Int J Intell Robot Appl* 2017; **1**: 399-409 [PMID: [29250588](https://pubmed.ncbi.nlm.nih.gov/29250588/) DOI: [10.1007/s41315-017-0036-4](https://doi.org/10.1007/s41315-017-0036-4)]
- 123 **Turan M**, Almalioglu Y, Araujo H, Konukoglu E, Sitti M. Deep EndoVO: A recurrent convolutional neural network (RCNN) based visual odometry approach for endoscopic capsule robots. *Neurocomputing* 2018; **275**: 1861-1870 [DOI: [10.1016/j.neucom.2017.10.014](https://doi.org/10.1016/j.neucom.2017.10.014)]
- 124 **Cheng PM**, Malhi HS. Transfer Learning with Convolutional Neural Networks for Classification of Abdominal Ultrasound Images. *J Digit Imaging* 2017; **30**: 234-243 [PMID: [27896451](https://pubmed.ncbi.nlm.nih.gov/27896451/) DOI: [10.1007/s10278-016-9929-2](https://doi.org/10.1007/s10278-016-9929-2)]
- 125 **de Groof AJ**, Struyvenberg MR, Fockens KN, van der Putten J, van der Sommen F, Boers TG, Zinger S, Bisschops R, de With PH, Pouw RE, Curvers WL, Schoon EJ, Bergman JJGHM. Deep learning algorithm detection of Barrett's neoplasia with high accuracy during live endoscopic procedures: a pilot study (with video). *Gastrointest Endosc* 2020; **91**: 1242-1250 [PMID: [31926965](https://pubmed.ncbi.nlm.nih.gov/31926965/) DOI: [10.1016/j.gie.2019.12.048](https://doi.org/10.1016/j.gie.2019.12.048)]
- 126 **Lecun Y**, Bottou L, Bengio Y, Haffner P. Gradient-based learning applied to document recognition. *Proc IEEE Inst Electr Electron Eng* 1998; **86**: 2278-2324 [DOI: [10.1109/5.726791](https://doi.org/10.1109/5.726791)]



Clinical value of artificial intelligence in hepatocellular carcinoma: Current status and prospect

Peng-Sheng Yi, Chen-Jun Hu, Chen-Hui Li, Fei Yu

ORCID number: Peng-Sheng Yi 0000-0002-5240-1127; Chen-Jun Hu 0000-0002-3355-7783; Chen-Hui Li 0000-0002-0702-9223; Fei Yu 0000-0003-1557-5993.

Author contributions: Yu F proposed the idea; Yi PS and Hu CJ wrote the manuscript; Yi PS and Hu CJ contributed equally to this work; Li CH performed the electronic searching and abstracted the data.

Supported by Project of Science and Technology Department of Sichuan Province, No. 2018JY050; and Nanchong Science and Technology Bureau Project, No. 18SXHZ0336.

Conflict-of-interest statement: The authors declare that they have no competing interests.

Open-Access: This article is an open-access article that was selected by an in-house editor and fully peer-reviewed by external reviewers. It is distributed in accordance with the Creative Commons Attribution NonCommercial (CC BY-NC 4.0) license, which permits others to distribute, remix, adapt, build upon this work non-commercially, and license their derivative works on different terms, provided the original work is properly cited and the use is non-commercial. See: <http://creativecommons.org/licenses/by-nc/4.0/>

Peng-Sheng Yi, Chen-Jun Hu, Department of Hepato-Biliary-Pancreas II, Affiliated Hospital of North Sichuan Medical College, Nanchong 637000, Sichuan Province, China

Chen-Hui Li, Department of Obstetrics and Gynecology, Nanchong Traditional Chinese Medicine Hospital, Nanchong 637000, Sichuan Province, China

Fei Yu, Department of Radiology, Yingshan County People's Hospital, Nanchong 610041, Sichuan Province, China

Corresponding author: Fei Yu, MD, Professor, Department of Radiology, Yingshan County People's Hospital, No. 100 Danan Street, Yingshan County, Nanchong 610041, Sichuan Province, China. 358496734@qq.com

Abstract

Hepatocellular carcinoma (HCC) is the most commonly diagnosed type of liver cancer and the fourth leading cause of cancer-related mortality worldwide. The early identification of HCC and effective treatments for it have been challenging. Due to the sufficient compensatory ability of early patients and its nonspecific symptoms, HCC is more likely to escape diagnosis in the incipient stage, during which patients can achieve a more satisfying overall survival if they undergo resection or liver transplantation. Patients at advanced stages can profit from radical therapies in a limited way. In order to improve the unfavorable prognosis of HCC, diagnostic ability and treatment efficiency must be improved. The past decade has seen rapid advancements in artificial intelligence, underlying its unique usefulness in almost every field, including that of medicine. Herein, we sought and reviewed studies that put emphasis on artificial intelligence and HCC.

Key Words: Hepatocellular carcinoma; Artificial intelligence; Diagnosis; Prognosis; Therapy; Genomic

©The Author(s) 2021. Published by Baishideng Publishing Group Inc. All rights reserved.

Core Tip: We performed electronic searching in PubMed, Web of Science and EMBASE. Artificial intelligence (AI) or in-depth learning and hepatocellular carcinoma were used as mesh terms. We found that AI showed favorable results in

[p://creativecommons.org/licenses/by-nc/4.0/](https://creativecommons.org/licenses/by-nc/4.0/)

Manuscript source: Unsolicited manuscript

Specialty type: Gastroenterology and hepatology

Country/Territory of origin: China

Peer-review report's scientific quality classification

Grade A (Excellent): 0

Grade B (Very good): 0

Grade C (Good): C

Grade D (Fair): 0

Grade E (Poor): 0

Received: January 6, 2021

Peer-review started: January 6, 2021

First decision: February 14, 2021

Revised: February 25, 2021

Accepted: March 15, 2021

Article in press: March 15, 2021

Published online: April 28, 2021

P-Reviewer: Simsek H

S-Editor: Wang JL

L-Editor: Filipodia

P-Editor: Li JH



early diagnosis and treatment response prediction and prognosis estimation in patients with hepatocellular carcinoma. The past decade has seen rapid advancements in AI, underlying its unique usefulness in almost every field, including that of medicine. Herein, we sought and reviewed studies, and we expect that AI will be an important complement to traditional diagnosis, treatment and prognosis estimation of hepatocellular carcinoma.

Citation: Yi PS, Hu CJ, Li CH, Yu F. Clinical value of artificial intelligence in hepatocellular carcinoma: Current status and prospect. *Artif Intell Gastroenterol* 2021; 2(2): 42-55

URL: <https://www.wjgnet.com/2644-3236/full/v2/i2/42.htm>

DOI: <https://dx.doi.org/10.35712/aig.v2.i2.42>

INTRODUCTION

According to GLOBOCAN 2018^[1], liver cancer was the sixth most commonly diagnosed (4.7%) type of cancer and the fourth leading cause (8.2%) of cancer-related mortality. It has been estimated that there are approximately 841000 new liver cancer cases and 782000 liver cancer-related deaths annually. Hepatocellular carcinoma (HCC) accounts for the majority of primary liver carcinoma^[1]. The widely accepted risks of HCC include chronic hepatitis B virus/hepatitis C virus infection, alcohol consumption, cirrhosis, aflatoxin intake as well as nonalcoholic fatty liver disease. Due to its atypical radiological appearance and the possibility of false-negative biopsy results, early-stage HCC is likely to be missed. Only a few HCC patients are suitable for radical resection, and even fewer can receive a liver transplant due to the limited availability. The high recurrence rate of HCC also undermines the benefits of surgery. Patients in intermediate and advanced stages can only benefit from noncurative treatments, including transarterial chemoembolization (TACE), radiofrequency ablation (RFA), targeted agents and systemic therapies, albeit in a limited way^[2]. Managing HCC is a major challenge in the clinic.

In the past few years, rapid progress has been made in artificial intelligence (AI) due to improvements in computer science. AI techniques, including machine learning (ML), artificial neural networks (ANNs) and computer vision, were combined with surgery, radiology, bioinformatics and pharmaceuticals and played an innovative role in boosting the development of those techniques^[3,4]. At present, AI is applied in drug design, patient monitoring, diagnostics and imaging, risk prediction and management, wearables and virtual assistants^[5].

As AI is now frequently used in diagnosis, treatment and patient managing of many types of cancer, including lung, gastric, prostate and colon cancers^[6-17], the assistance of AI in enhancing our diagnostic, therapeutic and prognostic ability to control HCC was not unexpected. In addition, the combination of AI and big data also performed much better than traditional methods^[18].

Recent studies have exhibited promising applications of AI in HCC. In the present study, the latest developments in the use of AI in HCC were studied, and both methods and improvements were reviewed.

DIAGNOSTIC ASSISTANCE FROM AI

An HCC diagnosis is based mostly on imaging and laboratory tests. Radiological and nonradiological imaging holds a dominant position in the diagnosis, staging, therapeutic decisions and management of patients, while laboratory biomarkers [e.g., α -fetoprotein (AFP)] offer some support. For certain patients, histological examination is recommended^[19]. By introducing AI into the evidence-based diagnostic procedure, more accurate classification was provided to assist clinical determination. Recent developments were summarized in [Table 1](#).

In a study in 2010, a total of 250 HCC patients, including 200 patients who underwent hepatectomy and 50 who underwent liver transplantation, were randomly divided into a test group ($n = 75$; 30%) and a training group ($n = 175$; 70%)^[20]. Factors including serum AFP, preoperative tumor number, maximum tumor size and tumor volume were found by univariate analysis to be strongly related to tumor grade

Table 1 Recent developments in artificial intelligence assisted diagnosis

AI category	Data adopted	Advantages	Control	Ref.
ANN	Preoperative serum AFP, tumor number, size and volume	The ANN showed higher AUCs in identifying tumor grade (0.94) and MVI (0.92)	LR model (0.85 and 0.85)	[20]
CNN	Enhanced MRI	The CNN showed comparable accuracy (90%)	Traditional multiphase MRI (89%)	[24,25]
Open-source framework "caffe" based CNN model	DWI	CNN trained with three sets of b-values found better grading accuracy (80%)	CNN trained with different b-values (65%, 68%, 70%)	[26]
CNN	Nonenhanced MRI	The deeply supervised and pretrained CNN model performed better in characterizing HCC (accuracy 77.00 ± 1.00%)	CNN-based method pretrained by ImageNet (65.00 ± 1.58%)	[27]
DL-based segmentation model	Contrast-enhanced CT	The model with a combination of 2D multiphase strategy showed higher ability of segmenting active part from the tumors	Traditional CT estimation	[28-30]
RF based ML model	HE-stained histopathological images	The classifying model showed an AUC of 0.988 in the test set and 0.886 in the external validation set	-	[31]
1D CNN	Hyperspectral and HE-stained images	The models had a higher average AUC of 0.950	RF (0.939) and SVM (0.930) models	[33]
Shiny and Caret packages-based prediction model	Clinical and laboratorial information	The optimal model had an AUC of 0.943	Single factor-based predictors (0.766, 0.644 and 0.683)	[34]

1D: One-dimensional; 2D: Two-dimensional; AFP: α-fetoprotein; AI: Artificial intelligence; ANN: Artificial neural network; AUC: Area under the curve; CNN: Convolutional neural network; CT: Computed tomography; DL: Deep learning; DWI: Diffusion-weighted imaging; HE: Hematoxylin and eosin; LR: Logistic regression; ML: Machine learning; MRI: Magnetic resonance imaging; MVI: Microvascular invasion; SVM: Support vector machine; RF: Random forest.

and/or microvascular invasion. Those four factors were used to build both a traditionally used logistic regression (LR) model and an ANN, which was set as a 3-layer feedforward neural network with a learning rule of backpropagation of error, endowing the ANN with a capacity of reducing overall error. It was clear that ANN [area under the curve (AUC) = 0.94; 95% confidence interval (CI): 0.89-0.97] had a notably higher ($P < 0.001$) predictive ability for tumor grade than LR analysis (AUC = 0.85; 95% CI: 0.78-0.89). At the same time, its ability to predict microvascular invasion was also significantly stronger (AUC = 0.92, 0.85; 95% CI: 0.86-0.96, 0.74-0.89; $P < 0.001$). Compared with single factor prediction, which cannot effectively predict tumor grade and microvascular invasion^[21-23], ANN provided a significantly improved ability to stratify tumors in a multidimensional way.

Magnetic resonance imaging (MRI) is highly valued in clinical diagnosis due to its outstanding ability to locate lesions. Recent research has shown the potential of deep-learning systems to distinguish HCC from other hepatic diseases, in which all 494 typical imaging features of six types of hepatic lesions were divided into a training set ($n = 434$) and a test set ($n = 60$)^[24]. An AI model was used to classify hepatic lesions through multiphase contrast-enhanced MRI scans. A custom convolutional neural network (CNN) with iteratively optimized architecture was trained by 43400 samples generated from 434 patients of the training set *via* augmentation techniques. The test set included 60 lesions (10 lesions from each category) randomly selected by Monte Carlo cross-validation. Eventually, the CNN consisted of three convolutional layers for generating filtered images, two maximum pooling layers for providing spatial invariance and two fully connected layers for outputting matched lesion types. As a result, a 90% sensitivity and an AUC of 0.992 for HCC classifying were observed in the test set, with an average 90% sensitivity and 98% specificity for a total of six classes of lesions. It had comparable efficiency to traditional multiphase MRI, which was reported to have an overall sensitivity of 89% and specificity of 96% for HCC^[25].

Another recent study, in which imaging data was partitioned into a training and validation set (60 HCCs) and a fixed test set (40 HCCs), paid attention to the tumor grading potential of diffusion-weighted imaging^[26]. An AI model was constructed based on an open-source deep-learning framework, "caffe", to grade HCC by diffusion-weighted imaging. Edmondson grade I and II HCCs were defined as low-grade ($n = 47$), while Edmondson grade III and IV HCCs were defined as high-grade (

$n = 53$). Diffusion-weighted imaging was performed with three sets of b-values (0, 100, 600 s/mm²), logarithmically transformed into log maps and then extracted by a specifically designed two-dimensional CNN to collect spatially deep features for grading tumors. The two-dimensional CNN was established with two convolutional layers, two pooling layers, two fully connected layers and a softmax layer. A deeply supervised loss functioned as the cross-entropy loss of the proposed CNN, which combined the three loss functions of CNN in the three b-value images and the loss function of the concatenated deep features. In terms of grading accuracy, the proposed CNN (80%; AUC, 0.83) performed better than other CNNs derived from original b 0 (65%), b 100 (68%), b 600 (70%) images and an apparent diffusion coefficient map (72.5%).

Jian *et al.*^[27] reported a novel method of training a deep-learning HCC diagnosis model with nonenhanced MRI scans. A total of 112 HCC patients (115 HCC tissue samples) with histological HCC proofs and enhanced MRI scans (including precontrast phase, arterial phase, portal vein phase and delayed phase) were classified into four Edmondson grades and further defined as low-grade (Edmondson grades I and II) and high-grade (Edmondson grades III and IV) HCCs. A deep-learning framework was established in two steps. The first step was the pretraining process, in which the relationship between precontrast (nonenhanced) and enhanced MRI scans was identified in order to find out malignant characterizations of nonenhanced MRI scans. The identified characterizations were transferring-learned using a supervised cross modal method in the second step. Results showed that the CNN-based method performed better in characterization than the traditional way, and the deeply supervised model pretrained by the cross modal from the three phases (precontrast, arterial and portal vein phase) performed the best compared with nonsupervised CNN and deeply supervised methods pretrained by the cross modal from two out of three phases (precontrast + arterial phase and precontrast + portal vein phase). This result revealed a new diagnostic approach for patients not receptive to enhanced imaging.

A deep-learning automatic segmentation model was built on multiphase computed tomography (CT) images to discriminate tumors from healthy liver tissue and further identify between active and necrotic tumor areas^[28]. A total of 13 contrast-enhanced CT sequences from 7 HCC patients were manually segmented by four experts into 104 labeled CT scan slices, containing images captured before contrast agent injection and images reflecting the arterial phase and the portal venous phase. The U-Net architecture was configured in a hierarchical method to specially segment by applying separate networks for each type of specific tissue. Two opposite strategies were investigated: Dimensional MultiPhase strategy, in which single-phase images were processed in a multi-dimensional feature map and the MultiPhase Fusion strategy, in which each phase was independently processed and then merged into the final segmentation. The softmax was introduced in the final layers of the different networks. The weighted cross-entropy functioned as the cost to optimize the weights and balance classes problem. Finally, a commonly used Dice similarity coefficient was used to estimate segmentation quality. Results indicated a better competency of multiphase methods in segmenting the liver and active part of tumors as compared with single phase ones. Between the two multiphase methods, Dimensional MultiPhase outperformed MultiPhase Fusion in the segmentation of the liver ($P = 0.004$) and active part of the tumors ($P = 0.005$). Furthermore, the combination of two Dimensional MultiPhase methods displayed the highest ability in spotting active areas from tumor tissues, making it reliable (mean error rate = 13.0%) in estimating the necrosis rate in which traditional CT estimation is not^[29,30]. With a more accurate assessment method, more beneficial clinical decisions may be made.

Histological examination provides solid evidence for the diagnosis, grading and prognosis analysis of HCC. Hematoxylin and eosin staining is the most common method used for biopsy. A total of 491 whole-slide hematoxylin and eosin-stained histopathological images of HCC and adjacent normal tissues downloaded from the Genomic Data Commons data portal were used for supervised training of ML classifier based on Breiman's random forest (RF)^[31]. The 31 most valuable image features (IFs) identified from the training set by principal component-based analysis (PCA) were used during the establishment of the classification model. An external validation set of tissue microarray images from the West China Hospital was employed in addition to the randomly partitioned training (70%) and test (30%) sets. The IF classification model showed an AUC of 0.988 (95%CI: 0.975-1.000) in the test set, while that of the external validation set was 0.886 (95%CI: 0.844-0.929). This outstanding performance of the IF model indicates its possible applications in the future.

Hyperspectral imaging (HSI) was regarded as a promising diagnostic technique^[32]. A one-dimensional CNN was designed to discriminate HCC from normal tissues through HSI images^[33]. HCC samples were cut into two adjacent slices, one of which was hematoxylin and eosin-stained and the other one underwent HSI. A total of 14 sets of HSI images, each containing 107 images photographed under different wavelengths, were used in a leave-one-out cross-validation approach, resulting in 14 different models. The framework consisted of a convolution layer, a max-pooling layer and a fully connected layer. The convolution layer could extract features from HSI images supervised by annotated tumor areas on the paired hematoxylin and eosin-stained slice, with a rectified linear unit that was shown to avoid gradient vanishing and accelerate the training process. Extracted features were processed in the max-pooling layer to reduce dimension and classified afterward in the fully connected layer. The average accuracy, sensitivity, specificity and AUC of those models was 0.881, 0.871, 0.888 and 0.950, respectively. Further evaluation was carried out and exhibited a salient capacity of the one-dimensional CNN model as compared with the RF and support vector machine (SVM) models.

Information was extracted from 539 HCC patients and 1043 non-HCC patients to train and test a predictive ML framework developed using R version 3.4.3 and the Shiny and Caret packages^[34]. Patients were randomly divided into the training (80%), development and test sets. Clinical information, including AFP, AFP-L3, des-g-carboxy prothrombin (commonly referred to as DCP), aspartate aminotransferase, alanine transaminase, platelet count, alkaline phosphatase, gamma-glutamyl transferase, albumin, total bilirubin, age, sex, height, body weight, hepatitis B surface antigen and hepatitis C virus antibody, was obtained for ML. The framework had several classifiers and two components. In the first component, a grid search was performed to select the best classifier and its specific hyperparameter, which would be introduced in the second component to output probabilities of HCC. Among a total of seven classifiers, gradient boosting showed an AUC of 0.940 as the highest one, with that of the optimal, based on the framework, classifier at 0.943; single-factor prediction using thresholds of 200 ng/mL for AFP, 40 mAu/mL for DCP and 15% for AFP-L325 performed AUCs of 0.766, 0.644 and 0.683, respectively.

THErapy RESPONSE PREDICTION BY AI

Surgical resection remains the first-line treatment for early-stage patients, with 5-year survival in appropriately selected cases exceeding 70%. However, it has been reported that HCC diagnosis is usually delayed, especially in countries with limited screening resources^[9]. Out of patients who miss the optimum surgical time window or are unsuitable for operative therapy, only a few benefit from loco-regional (*e.g.*, RFA), intra-arterial (*e.g.*, TACE), systemic and targeted therapies^[2]. Thus, enhancing the accuracy of surgical indications and promoting treatment benefits of nonoperative therapies would effectively improve the clinical prognosis of patients. In the past years, some AI models with great potential were built, as referred in [Table 2](#).

HCC has been estimated as the fourth highest cause of all cancer-related mortality worldwide^[1], indicating a high malignancy and poor prognosis of HCC. Accurate prognostic prediction of tumor resection is needed to identify high-risk patients and enable more favorable clinical decisions. As Qiao *et al*^[35] reported, the independent risk factors (including tumor size, number, AFP, microvascular invasion and tumor capsule) found by linear regression to be significantly related to survival were selected to assist in predicting the prognosis of early HCC after partial hepatectomy, both in a Cox model and using an ANN method. A feed-forward neural network was built as a perceptron with several layers, outputting a prognosis condition (survival or death) for certain time points. In addition to the training and cross-validation cohort in which patients from the Eastern Hepatobiliary Surgery Hospital were randomly selected, an external validation cohort was obtained from the First Affiliated Hospital of Fujian Medical University. AUCs demonstrated that the ANN (0.855) outperformed the Cox model (0.826), Tumor, Node, Metastasis 6th (0.639), Barcelona Clinic Liver Cancer (BCLC) (0.612) and HepatoPancreato-Biliary Association system (0.711), and consistent results were observed in the external validation cohort. It drew attention to the potential of the ANN model to provide clinical assistance and improve benefits of early-stage HCC patients.

AI models can also help identify predictive factors of surgery outcomes. In a multicenter retrospective study that included 976 BCLC 0-B HCC patients who underwent hepatectomy, Tsilimigras *et al*^[36] generated homogeneous groups of

Table 2 Artificial intelligence models that can help in predicting therapy responses

AI	Data adopted	Advantages	Control	Ref.
ANN	Cox-identified risk factors	The ANN had the highest AUC (0.855)	Cox model, TNM 6 th , BCLC and HPBA system (0.826, 0.639, 0.612, 0.711)	[35]
CART model	Clinical and laboratorial parameters	The model successfully identified pre- and postoperative prognosis predictive factors	-	[36]
Weka-based ANNs	Cox-identified risk factors (15 factors for DFS and 21 for OS)	The ANNs showed higher abilities of predicting DFS and OS	LR and decision tree model	[37,38]
Radiomics-based DL CEUS model	Contrast-enhanced ultrasound	The model showed an AUC of 0.93 in predicting therapy response to TACE	Radiomics-based time-intensity curve of CEUS model (0.80) and radiomics-based B-Mode images model (0.81)	[40]
Pretrained CNN "ResNet50"	Manually segmented CT images	The model showed AUCs for predicting CR, PR, SD and PD in training (0.97, 0.96, 0.95, 0.96) and validation (0.98, 0.96, 0.95, 0.94) cohorts	-	[41]
Automatic predictive CNN model	Quantitative CT and BCLC stage	The model had a better prediction accuracy of 74.2%	ML model based on BCLC stage (62.9%)	[42]
ANN	Clinical features	The models showed higher AUCs in predicting 1- and 2-yr DFS (0.94, 0.88) after RFA	Model built with 8 features for 1-yr DFS (0.80), and model built with 6 features for 2-yr DFS (0.76)	[45]

AI: Artificial intelligence; ANN: Artificial neural network; AUC: Area under the curve; BCLC: Barcelona Clinic Liver Cancer; CART: Classification and Regression Tree; CEUS: Contrast-enhanced ultrasound; CNN: Convolutional neural network; CR: Complete response; CT: Computed tomography; DFS: Disease-free survival; DL: Deep learning; HPBA: HepatoPancreato-Biliary Association; LR: Logistic regression; ML: Machine learning; OS: Overall survival; PD: Progressive disease; PR: Partial response; RFA: Radiofrequency ablation; SD: Stable disease; TACE: Transarterial chemoembolization; TNM: Tumor, Node, Metastasis; Weka: Waikato Environment for Knowledge Analysis.

patients based on their 5-year overall survival (OS) and identified clinical factors, which can be used to predict OS after resection using the nonparametric Classification and Regression Tree (CART) model based on pre- (preoperative CART model) and postoperative (postoperative CART model) factors. CART is a risk prediction model with a performance to recursively partition the 'covariate space'. As a result, the CART model successfully identified several prognosis predictive factors. Among BCLC-0/A patients, the CART model selected AFP and Charlson comorbidity score as the first and second most important preoperative factors and lymph vascular invasion as the best postoperative predictor of OS. Radiological tumor burden score and pathologic tumor burden score were selected as the best pre- and postoperative factors for predicting surgical outcomes for BCLC-B HCC patients.

Consecutive studies of Ho *et al* [37,38] have been reported in which AI models were predictively capable of classifying patients into different groups with distinctive disease-free survival (DFS) and OS after hepatic resection. Data from HCC patients who underwent liver resection were examined and merged for further construction of survival predictive models. The input variables were identified by the univariate Cox proportional hazard model to be closely related (log-rank test; $P < 0.05$) to DFS or OS. Eighty percent of the data were used for training, and the other 20% for validation, while no significantly different effect of input variables was observed between training and validation ($P > 0.05$). The proposed ANNs in both studies, which shared homologous structures based on the Waikato Environment for Knowledge Analysis software using a backpropagation algorithm, were framed with input, hidden and output layers. Each of the identified variables was inputted into one of the input neurons, and then a trial-and-error process was performed in the hidden layer to optimize its neuron numbers before generating DFS and OS status in the output layer, which contained only one neuron.

In the first reported study showing the capacity of the ANN to predict DFS based on 15 statistically significantly associated variables, two comparative models were tested: An LR and a decision tree model. The receiver operating characteristics curves and AUCs for the 1-, 3- and 5-year DFS models constructed using ANN, LR and decision tree demonstrated an acceptable and exceeding performance of the ANN model as compared with the LR and decision tree models.

In another study, attention was paid to OS after resection with 21 potential variables serving as inputs. An LR model was used for performance comparison. The accuracy, sensitivity, specificity and AUC of the ANN and LR models were calculated. As a result, the prediction performance of the ANN model was significantly stronger than that of the LR model. In both studies, the possible usage of the ANN as a clinical supplementary tool for decision-making was emphasized, suggesting it might be able to enhance the profit-risk ratio of HCC resection.

TACE has been widely accepted as the standard and effective treatment for HCC patients at the intermediate stage^[39]. Recent studies have paid considerable attention to deep-learning and TACE, highlighting treatment response prediction and AI-assisted clinical decision-making.

Contrast-enhanced ultrasound (CEUS) and B-mode ultrasound images of 130 HCC patients who received first-time TACE treatment were obtained for retrospective analysis using AI, which was trained to predict patient response (objective-response and nonresponse) to TACE^[40]. A total of three models were framed by applying CEUS images (deep-learning radiomics-based CEUS model), the time-intensity curve of CEUS (ML radiomics-based time-intensity curve of CEUS model) and B-mode images (ML radiomics-based B-Mode images model). AUCs were compared between the three models, and the hepatoma arterial-embolization prognostic score was used to predict the outcomes of patients with HCC undergoing TACE. In the training ($n = 89$; 68.5%) and validation ($n = 41$; 31.5%) cohorts, the three models markedly outperformed the hepatoma arterial-embolization prognostic score [AUC = 0.98 (0.92-0.99), 0.84 (0.74-0.90), 0.82 (0.73-0.91) and 0.623 in the training and 0.93 (0.80-0.98), 0.80 (0.64-0.90), 0.81 (0.67-0.95) and 0.617 in the validation cohorts for deep-learning radiomics-based CEUS model, ML radiomics-based time-intensity curve of CEUS model, ML radiomics-based B-Mode images model and hepatoma arterial-embolization prognostic score, respectively]. A high reproducibility of this predictive accuracy was displayed by robustness experiments performed in triplicate in both the training and validation cohorts. The predictive capability of human readers with a deep-learning feature map showed an advantage over that of ML radiomics-based time-intensity curve of CEUS model or ML radiomics-based B-Mode images model but not over that of deep-learning radiomics-based CEUS model.

In two analogous studies, the ML network displayed a strong ability to predict TACE therapy outcomes using CT images. Peng *et al*^[41] trained a pretrained deep CNN, ResNet50, with manually segmented CT images to predict treatment response to TACE. Tumor regions of interest segmented by experienced radiologists were divided into one training set ($n = 562$) and two validation sets ($n = 89$; 138). The weights of earlier layers (1-174) in this network were frozen to prevent overfitting and speed up the training process. The trained model showed AUCs of 0.97 (0.97-0.98), 0.96 (0.96-0.97), 0.95 (0.94-0.96) and 0.96 (0.96-0.97) in the training cohort ($n = 562$), 0.98 (0.97-0.99), 0.96 (0.95-0.98), 0.95 (0.93-0.98) and 0.94 (0.90-0.98) in the validation cohort 1 ($n = 89$), and 0.97 (0.96-0.98) and 0.96 (0.94-0.98), 0.94 (0.92-0.97), 0.97 (0.95-0.98) in the validation cohort 2 ($n = 138$) for complete response, partial response, stable disease and progressive disease, respectively. Morshid *et al*^[42] built a fully automated ML algorithm that can predict response to TACE using quantitative CT scan features and BCLC stage. A total of 105 HCC patients who had received TACE were defined by time to progression as TACE-susceptible (time to progression ≥ 14 wk) or TACE-refractory (time to progression < 14 wk). A total of five imaging features that were different between background liver and tumor were extracted, including tumor volume, maximum two-dimensional axial diameter of the background liver, small area low gray-level emphasis within the background liver, maximal correlation coefficient within the background liver and long-run high gray-level emphasis within the tumor. Those features were added to the AI model to promote prediction accuracy. Compared with the model based on the BCLC stage alone (prediction accuracy = 62.9%, 95%CI: 0.52-0.72), the model based on CT scan features and BCLC stage showed a better prediction accuracy of 74.2% (95%CI: 0.64-0.82).

Abajian *et al*^[43] established an LR and an RF model to predict TACE treatment response using MRI scans. The quantitative European Association for the Study of the Liver response criteria were used to measure TACE response. A total of 36 patients were defined as treatment responders (8/36; 22.2%) and nonresponders (28/36; 77.8%) using a cut-off value of 65% changes in quantitative European Association for the Study of the Liver response criteria. During the training process of both models, five features, including cirrhosis, pre-TACE tumor signal intensity, pre-TACE number of tumors, performing method of TAC and existence of sorafenib treatment, were used in 30 different combinations to identify the most accurate predictive model. A leave-one-out cross-validation method was used for a predictive accuracy test. When trained on

all five features, the LR model displayed an accuracy of 72.0%, sensitivity of 50.0% and specificity of 78.6%, while an accuracy of 66.0%, sensitivity of 62.5% and specificity of 67.9% were validated for the RF model. Notably, these two models shared a best performance (accuracy 78%, sensitivity 62.5% and specificity 82.1%) when trained using only two (pre-TACE tumor signal intensity > 27.0 and presence of cirrhosis) of those five features but still remained inferior to that of MR scan using a baseline apparent diffusion coefficients value threshold of $0.83 \times 10^{-3} \text{mm}^2/\text{s}$, which demonstrated 91% sensitivity and 96% specificity to predict TACE response at 1 mo after treatment and an AUC of 0.965^[44].

RFA is considered a viable option for HCC patients who are unsuitable for resection or on the waiting list for a liver transplant. A prognostic prediction ANN model was reported to be promising for clinical practice^[45]. Patients were divided into a 1- ($n = 252$) and a 2-year (179) DFS group. A total of eight and six variables from a total of fifteen potential variables (total bilirubin, aspartate aminotransferase, alanine transaminase, albumin, platelet, age, gender, tumor size, tumor number, AFP, HCC treatment history, TACE, recurrence events after TACE, BCLC stages and liver cirrhosis events) were found to be significantly associated with 1- and 2-year DFS and were used as inputs for building prediction models, which was based on a multiple-layer perceptron structure and a backpropagation learning rule. This ANN model was designed with the ability of selecting structure depending on its predictive performance. Between two 1-year DFS models, the one built with 15 features (the accuracy, sensitivity, specificity, and AUC were 0.92, 0.87, 0.94 and 0.94, respectively) was better than the one with 8 significant features (the accuracy, sensitivity, specificity and AUC were 0.78, 0.37, 0.96 and 0.80, respectively). Consistently, a 2-year DFS model with 15 features (the accuracy, sensitivity, specificity and AUC were 0.86, 0.79, 0.91 and 0.88, respectively) showed a considerable advantage over that with 6 significant features (the accuracy, sensitivity, specificity and AUC were 0.68, 0.47, 0.84 and 0.76, respectively) and traditional methods including acoustic radiation force impulse elastography (AUC = 0.821; 95%CI: 0.747-0.895) and transient elastography (AUC 0.793; 95%CI: 0.712-0.874)^[46,47]. Although some of the 15 features were evaluated by χ^2 test to be nonsignificantly related with 1- or 2-year DFS, the better outcome of models with all 15 features might have prompted their implicit roles in RFA response prediction.

PROGNOSIS ESTIMATION USING AI

In order to correctly identify the development characteristics and improve the outcomes of existing therapies, accurate prognostic information is indispensable. Individualized precise treatment based on risk and prognostic data would substantially enhance curing efficiency in HCC^[48]. Table 3 displayed some of the effective models which can provide prognosis estimation.

Two deep-learning algorithms, CHOWDER and SCHMOWDER, which adopted whole-slide digitized histological slides of HCC patients that had undergone surgery were set up to predict OS after resection^[49]. CHOWDER could automatically recognize survival-related patterns on the tiles derived from the slides and assess the risk score for each whole-slide digitized histological slide in three steps: Preprocessing, tile-scoring and prediction. SCHMOWDER has an identical preprocessing step as CHOWDER and a two-branch tile-scoring and predicting pipeline. The upper branch, which generated a representation of highly-probably tumoral tiles with an attention mechanism used, was trained by annotations from pathologists; the lower branch, which generated a representation of only a few tiles, was weakly supervised. Representations from the two branches were merged to calculate a survival risk score. The discriminatory capacities of the two models assessed by cross-validation were demonstrated as better than baseline factors (including microvascular invasion, serum AFP, largest nodule diameter and satellite nodules) and composite score by combining survival-related clinical, biological and pathological features.

In a prospective study including 442 patients with Child A or B cirrhosis, an HCC development prediction model based on ML algorithms, known as RF, was compared using conventional regression analysis^[50]. Previously determined clinically relevant parameters (age, body mass index and presence of diabetes) and those identified by univariate analysis (AFP level, bilirubin, male gender, aspartate aminotransferase, alanine transaminase, Child-Pugh score and viral etiology) were selected to build a predictive regression model and an ML classifier. Multiple decision trees were constructed and used as “votes” to create the final classification prediction model. Cross-validated accuracy estimation and external validation in the hepatitis C antiviral

Table 3 Prognosis prediction models built with artificial intelligence algorithms

AI category	Data adopted	Advantages	Control	Ref.
DL algorithms CHOWDER and SCHMOWDER	Whole-slide digitized histological slide	C-indexes for survival prediction of SCHMOWDER and CHOWDER reached 0.78 and 0.75	Baseline factors and composite score	[49]
ML classifier	Previously determined relevant parameters and those identified by univariate analysis	The ML algorithm performed a c-statistic of 0.64 for HCC development prediction	Regression model (0.61) and the model built on the HALT-C cohort (0.60)	[50]
DL survival prediction model	RNA, miRNA and methylation data from TCGA	The DL model showed better potential in classifying HCC patients into two subgroups with different survival	PCA and the model built with manually inputted features	[51]
OS prediction model based on SVM-RFE algorithm	134 methylation sites identified using Cox regression and SVM-RFE algorithm	This algorithm showed a higher accuracy of classifying HCC patients	Traditionally set classifying methods based on DNA methylation	[54-56]
ANN	Mortality-related variables	The ANN showed higher AUCs (0.84 and 0.89) in predicting in-hospital and long-term mortality	LR model (0.76 and 0.77)	[57,58]

AI: Artificial intelligence; ANN: Artificial neural network; AUC: Area under the curve; DL: Deep learning; HALT-C: Hepatitis C antiviral long-term treatment against cirrhosis; HCC: Hepatocellular carcinoma; LR: Logistic regression; ML: Machine learning; OS: Overall survival; PCA: Principal component-based analysis; RFE: Recursive feature elimination; SVM: Support vector machine; TCGA: The Cancer Genome Atlas.

long-term treatment against cirrhosis trial cohort, which included 1050 patients, was conducted. The ML algorithm performed the best classifying characteristics with a c-statistic of 0.64 (95%CI: 0.60-0.69) compared with the regression model (0.61; 95%CI: 0.56-0.67) and the model built on the hepatitis C antiviral long-term treatment against cirrhosis cohort (0.60; 95%CI: 0.50-0.70), raising the possibility of prospectively predictive HCC development by ML.

Two HCC subgroups were found to have a notably discrepant prognosis by survival analysis and were focused on to build a deep-learning survival prediction model^[51]. RNA, miRNA and methylation data from 360 HCC patients were collected from The Cancer Genome Atlas (TCGA) and were split to train an SVM model. Five additional confirmation datasets were obtained to estimate the predictive accuracy. TCGA HCC omics data were regarded as the input of the proposed autoencoder, in which three hidden layers with different numbers of nodes were implemented using the Python Keras library. The autoencoder was trained for ten epochs with a 50% dropout in the gradient descent algorithm. A total of 37 features of the TCGA omics data significantly (log-rank test, $P < 0.05$) associated with survival were identified by the autoencoder. With those features, a classification model using the SVM algorithm was built and validated in the test group and five additional groups of HCC patients. C-index, Brier score and log-rank test were carried out to evaluate the performance of the AI model, and two alternative methods, including PCA and a model based on 37 manually identified features from the omics data. The proposed model showed a clearly better potential than that of PCA and the model with manually-inputted features, and intended prediction robustness was validated in additional datasets.

Anomalous DNA methylation was found to be highly related to HCC^[52,53] and able to predict survival in HCC patients that had undergone surgery^[54]. DNA methylation data from 377 HCC samples and 50 adjacent normal tissue samples were obtained and analyzed using the ChAMP tool in R software. A total of 2785 sites from 40799 sites that had been methylated differently between HCC tissue and adjacent normal tissue were assessed *via* Cox regression and found to be significantly related to OS ($P < 0.05$). The SVM-recursive feature elimination algorithm behaved as a classifier to identify valuable sites that could be used to build a predictive model. Finally, 134 methylation sites were used to build the predictive model. A total of 163 patients were divided into a “high-risk” (died within 1 year after surgery, $n = 58$), “intermediate-risk” (survived 1-5 years after surgery, $n = 64$) and “low-risk” (survived > 5 years after surgery, $n = 41$) groups and were separated into a training ($n = 130$) and a test ($n = 33$) set. A total of 26 (78.8%) patients were successfully classified into the test set. Further validation of 19 paired HCC and normal tissue samples from the GSE77269 dataset in the Gene Expression Omnibus database demonstrated no incorrect classification of normal tissues and a similar ratio of HCC samples classified as “high-risk.” Although this algorithm showed a higher accuracy of classifying HCC patients than some traditionally-set classifying methods based on DNA methylation^[55,56], validation in a

larger sample size was needed.

Liao *et al.*^[51] built an IF-based prognosis prediction model (IF model) that can divide HCC patients who underwent resection into two groups, the high- and low-score groups, with a different OS according to the cut-off value of the training set. A total of 46 informative IFs, identified by Cox proportional hazard regression and an RF minimal depth algorithm, were found to be significantly ($P < 0.05$) associated with OS and were used to train the IF model. As a result, the IF model successfully distinguished patients with higher scores from those with lower scores in all three sets (log-rank test; $P < 0.0001$ in the training set, $P = 0.013$ in both the test and external validation sets), exhibiting a well-performed prognosis prediction ability. Furthermore, time-dependent receiver operating characteristics curves were used to compare the prognosis performance between the IF model and the Tumor, Node, Metastasis staging system, with no significant difference observed (adjusted $P = 0.848$ - 1.000) at each time point (1-9 years after treatment), indicating that the IF model may have a comparable predictive accuracy with that of the Tumor, Node, Metastasis staging system.

Two similarly framed ANN models, expected to respectively predict in-hospital and 5-year mortality in HCC, were trained with data from a large population of 22926 patients who had been diagnosed with HCC and had undergone resection^[57,58]. The structure of ANNs consists of an input layer, a hidden layer and an output layer. To identify related variables, continuous and categorical variables were respectively tested by one-way analysis of variance and Fisher's exact test, and significant predictors ($P < 0.05$) were verified by univariate analysis. The following steps were repeated 1000 times: (1) Data were randomly divided into a training set ($n = 18341$; 80%) and a test set ($n = 4585$; 20%); (2) the LR and ANN models were established based on the training dataset; and (3) Paired *t*-tests were used to compare indices between the two models. Statistically in-hospital mortality-related variables, including age, gender, comorbidity (estimated by Charlson comorbidity index), hospital volume, surgeon volume and length of stay) were extracted by the ANN, and an outcome (death/survival) was generated. Compared to the LR model, the ANN showed a substantial advantage with a higher accuracy rate (97.28 vs 88.29, $P < 0.001$), a lower Hosmer-Lemeshow statistic (41.18 vs 54.53, $P < 0.001$) and a higher AUC (0.84 vs 0.76, $P < 0.001$). The other ANN model was built and tested similarly with six identical variables to predict 5-year mortality, and ANN was found to significantly outperform the LR model (accuracy rate 96.57% vs 87.96%; Hosmer-Lemeshow statistic 0.34 vs 0.45; AUC 88.51% vs 77.23%). Those two models combined with the deep-learning technique showed unique prognosis prediction performance, revealing their possible applicability in the prediction of in-hospital and long-term mortality.

OMICS RESEARCH PERFORMED WITH AI

Genomic data have exhibited efficient and unique advantages in both research and clinical experience. A recent study managed to correlate tumor samples and their original tissue types using an ML prediction model^[59]. RNA-seq data of 14 tumors and at least 10 corresponding adjacent normal tissue samples for each tumor were downloaded from TCGA, Therapeutically Applicable Research to Generate Effective Treatments and the Genotype-Tissue Expression. An autoencoder neural network based on Pytorch with a rectifying activation function, dropout and normalization between layers was built. The mean squared error between the input and output was introduced as the loss function. After 10000 iterations for converging loss, the autoencoder demonstrated an outstanding ability to identify tissue sites for cancers with increasing accuracy in parallel with the mounting number of varying genes, noticeably surpassing the predominant PCA method, which identified only 8/14 cancers. In the distinction of HCC samples, the autoencoder with all features utilized showed a highly specific capacity of capturing biological information. This study provided a solid reference for further research in HCC and might be able to promote sample usage in a precise way.

A novel approach of seeking HCC-related genes by ML was established^[60]. Gene expression profiles of 43 tumor and 52 normal tissue samples were downloaded from NCBI Gene Expression Omnibus. A maximum relevance-minimum redundancy (mRMR) method, referred to as mRMRe, was used to rank the features. The mRMR is a proven ML approach for phenotype classification; it can classify transcriptional features based on both the redundancy between features and their relevance to the target. An incremental feature selection method was combined with the mRMRe

algorithm, generating a possible feature subset for further analysis. A subset consisting of 117 features with a satisfying accuracy of 0.895 was finally selected as the criteria to distinguish HCC from non-HCC samples, in which several previously identified HCC-related genes (such as *MT1X*, *BMI1* and *CAP2*) were found, justifying the rationality of this model. Furthermore, some genes, such as *TACSTD2*, that were not considered to be HCC-related before (one of which was identified by protein-protein interaction) might be crucial during the pathogenesis of HCC, namely ubiquitin C was identified by this model.

CONCLUSION

AI showed a substantial enhancement throughout the pre- and postclinical process of HCC in terms of both investigation and treatment. Due to the low diagnostic rate of early-stage patients, its high recurrence rate and unsatisfactory treatment effectiveness, HCC is one of the deadliest types of cancer worldwide. The emerging and fast-developing techniques of AI offer the possibility of improving the survival of HCC patients. Brought by deep-learning methods, a higher accuracy of diagnosis and treatment response prediction combined with individual prognosis assessment could potentially improve the time and quality of survival for HCC patients to a considerable extent.

AI has also been used in a wider range of clinical practice. Hyer *et al*^[61] released an ML approach to predict postsurgical prognosis. The novel method referred to as Complexity Score outperformed several currently used indices of prognosis estimation. Mueller-Breckenridge *et al*^[62] identified two hepatitis B virus quasispecies by ultra-deep sequencing and developed a ML model to determine the viral variants and assist clinical decision-making with regards to anti-hepatitis B virus strategies. A newly-established ML model was reported as an alternative method in the prediction of liver fibrosis caused by chronic hepatitis C virus infection^[63]. While none of those studies were directly related to HCC, their findings might significantly help preclinical prevention, early diagnosis and surgical planning.

REFERENCES

- 1 **Bray F**, Ferlay J, Soerjomataram I, Siegel RL, Torre LA, Jemal A. Global cancer statistics 2018: GLOBOCAN estimates of incidence and mortality worldwide for 36 cancers in 185 countries. *CA Cancer J Clin* 2018; **68**: 394-424 [PMID: 30207593 DOI: 10.3322/caac.21492]
- 2 **Llovet JM**, Zucman-Rossi J, Pikarsky E, Sangro B, Schwartz M, Sherman M, Gores G. Hepatocellular carcinoma. *Nat Rev Dis Primers* 2016; **2**: 16018 [PMID: 27158749 DOI: 10.1038/nrdp.2016.18]
- 3 **Hashimoto DA**, Rosman G, Rus D, Meireles OR. Artificial Intelligence in Surgery: Promises and Perils. *Ann Surg* 2018; **268**: 70-76 [PMID: 29389679 DOI: 10.1097/SLA.0000000000002693]
- 4 **Min S**, Lee B, Yoon S. Deep learning in bioinformatics. *Brief Bioinform* 2017; **18**: 851-869 [PMID: 27473064 DOI: 10.1093/bib/bbw068]
- 5 **Hosny A**, Parmar C, Quackenbush J, Schwartz LH, Aerts HJWL. Artificial intelligence in radiology. *Nat Rev Cancer* 2018; **18**: 500-510 [PMID: 29777175 DOI: 10.1038/s41568-018-0016-5]
- 6 **Christie JR**, Lang P, Zelko LM, Palma DA, Abdelrazek M, Mattonen SA. Artificial Intelligence in Lung Cancer: Bridging the Gap Between Computational Power and Clinical Decision-Making. *Can Assoc Radiol J* 2021; **72**: 86-97 [PMID: 32735493 DOI: 10.1177/0846537120941434]
- 7 **Wan YL**, Wu PW, Huang PC, Tsay PK, Pan KT, Trang NN, Chuang WY, Wu CY, Lo SB. The Use of Artificial Intelligence in the Differentiation of Malignant and Benign Lung Nodules on Computed Tomograms Proven by Surgical Pathology. *Cancers (Basel)* 2020; **12** [PMID: 32784681 DOI: 10.3390/cancers12082211]
- 8 **Su HH**, Pan HW, Lu CP, Chuang JJ, Yang T. Automatic Detection Method for Cancer Cell Nucleus Image Based on Deep-Learning Analysis and Color Layer Signature Analysis Algorithm. *Sensors (Basel)* 2020; **20** [PMID: 32784663 DOI: 10.3390/s20164409]
- 9 **Ueyama H**, Kato Y, Akazawa Y, Yatagai N, Komori H, Takeda T, Matsumoto K, Ueda K, Hojo M, Yao T, Nagahara A, Tada T. Application of artificial intelligence using a convolutional neural network for diagnosis of early gastric cancer based on magnifying endoscopy with narrow-band imaging. *J Gastroenterol Hepatol* 2021; **36**: 482-489 [PMID: 32681536 DOI: 10.1111/jgh.15190]
- 10 **Murakami D**, Yamato M, Amano Y, Tada T. Challenging detection of hard-to-find gastric cancers with artificial intelligence-assisted endoscopy. *Gut* 2020 [PMID: 32816967 DOI: 10.1136/gutjnl-2020-322453]
- 11 **Song Z**, Zou S, Zhou W, Huang Y, Shao L, Yuan J, Gou X, Jin W, Wang Z, Chen X, Ding X, Liu J, Yu C, Ku C, Liu C, Sun Z, Xu G, Wang Y, Zhang X, Wang D, Wang S, Xu W, Davis RC, Shi H.

- Clinically applicable histopathological diagnosis system for gastric cancer detection using deep learning. *Nat Commun* 2020; **11**: 4294 [PMID: 32855423 DOI: 10.1038/s41467-020-18147-8]
- 12 **Deding U**, Herp J, Havshoei AL, Kobaek-Larsen M, Buijs MM, Nadimi ES, Baatrup G. Colon capsule endoscopy vs CT colonography after incomplete colonoscopy. Application of artificial intelligence algorithms to identify complete colonic investigations. *United European Gastroenterol J* 2020; **8**: 782-789 [PMID: 32731841 DOI: 10.1177/2050640620937593]
 - 13 **Zheng L**, Zhang X, Hu J, Gao Y, Zhang M, Li S, Zhou X, Niu T, Lu Y, Wang D. Establishment and Applicability of a Diagnostic System for Advanced Gastric Cancer T Staging Based on a Faster Region-Based Convolutional Neural Network. *Front Oncol* 2020; **10**: 1238 [PMID: 32850373 DOI: 10.3389/fonc.2020.01238]
 - 14 **Ellmann S**, Schlicht M, Dietzel M, Janka R, Hammon M, Saake M, Ganslandt T, Hartmann A, Kunath F, Wullich B, Uder M, Bäuerle T. Computer-Aided Diagnosis in Multiparametric MRI of the Prostate: An Open-Access Online Tool for Lesion Classification with High Accuracy. *Cancers (Basel)* 2020; **12** [PMID: 32825612 DOI: 10.3390/cancers12092366]
 - 15 **Shao L**, Yan Y, Liu Z, Ye X, Xia H, Zhu X, Zhang Y, Zhang Z, Chen H, He W, Liu C, Lu M, Huang Y, Ma L, Sun K, Zhou X, Yang G, Lu J, Tian J. Radiologist-like artificial intelligence for grade group prediction of radical prostatectomy for reducing upgrading and downgrading from biopsy. *Theranostics* 2020; **10**: 10200-10212 [PMID: 32929343 DOI: 10.7150/thno.48706]
 - 16 **Gupta P**, Chiang SF, Sahoo PK, Mohapatra SK, You JF, Onthoni DD, Hung HY, Chiang JM, Huang Y, Tsai WS. Prediction of Colon Cancer Stages and Survival Period with Machine Learning Approach. *Cancers (Basel)* 2019; **11** [PMID: 31842486 DOI: 10.3390/cancers11122007]
 - 17 **Chao WL**, Manickavasagan H, Krishna SG. Application of Artificial Intelligence in the Detection and Differentiation of Colon Polyps: A Technical Review for Physicians. *Diagnostics (Basel)* 2019; **9** [PMID: 31434208 DOI: 10.3390/diagnostics9030099]
 - 18 **Chen B**, Garmire L, Calvisi DF, Chua MS, Kelley RK, Chen X. Harnessing big 'omics' data and AI for drug discovery in hepatocellular carcinoma. *Nat Rev Gastroenterol Hepatol* 2020; **17**: 238-251 [PMID: 31900465 DOI: 10.1038/s41575-019-0240-9]
 - 19 **Dimitroulis D**, Damaskos C, Valsami S, Davakis S, Garmis N, Spartalis E, Athanasiou A, Moris D, Sakellariou S, Kykalos S, Tsourouflis G, Garmis A, Delladetsima I, Kontzoglou K, Kouraklis G. From diagnosis to treatment of hepatocellular carcinoma: An epidemic problem for both developed and developing world. *World J Gastroenterol* 2017; **23**: 5282-5294 [PMID: 28839428 DOI: 10.3748/wjg.v23.i29.5282]
 - 20 **Cucchetti A**, Piscaglia F, Grigioni AD, Ravaioli M, Cescon M, Zanella M, Grazi GL, Golfieri R, Grigioni WF, Pinna AD. Preoperative prediction of hepatocellular carcinoma tumour grade and micro-vascular invasion by means of artificial neural network: a pilot study. *J Hepatol* 2010; **52**: 880-888 [PMID: 20409605 DOI: 10.1016/j.jhep.2009.12.037]
 - 21 **Özdemir F**, Baskiran A. The Importance of AFP in Liver Transplantation for HCC. *J Gastrointest Cancer* 2020; **51**: 1127-1132 [PMID: 32845425 DOI: 10.1007/s12029-020-00486-w]
 - 22 **Liu H**, Yang Y, Chen C, Wang L, Huang Q, Zeng J, Lin K, Zeng Y, Guo P, Zhou W, Liu J. Reclassification of tumor size for solitary HBV-related hepatocellular carcinoma by minimum p value method: a large retrospective study. *World J Surg Oncol* 2020; **18**: 185 [PMID: 32709254 DOI: 10.1186/s12957-020-01963-z]
 - 23 **Bhatti ABH**, Qureshi AI, Tahir R, Dar FS, Khan NY, Zia HH, Riyaz S, Rana A. When to call it off: defining transplant candidacy limits in liver donor liver transplantation for hepatocellular carcinoma. *BMC Cancer* 2020; **20**: 754 [PMID: 32787864 DOI: 10.1186/s12885-020-07238-w]
 - 24 **Hamm CA**, Wang CJ, Savic LJ, Ferrante M, Schobert I, Schlachter T, Lin M, Duncan JS, Weinreb JC, Chapiro J, Letzen B. Deep learning for liver tumor diagnosis part I: development of a convolutional neural network classifier for multi-phasic MRI. *Eur Radiol* 2019; **29**: 3338-3347 [PMID: 31016442 DOI: 10.1007/s00330-019-06205-9]
 - 25 **Marrero JA**, Hussain HK, Nghiem HV, Umar R, Fontana RJ, Lok AS. Improving the prediction of hepatocellular carcinoma in cirrhotic patients with an arterially-enhancing liver mass. *Liver Transpl* 2005; **11**: 281-289 [PMID: 15719410 DOI: 10.1002/Lt.20357]
 - 26 **Zhou W**, Wang G, Xie G, Zhang L. Grading of hepatocellular carcinoma based on diffusion weighted images with multiple b-values using convolutional neural networks. *Med Phys* 2019; **46**: 3951-3960 [PMID: 31169907 DOI: 10.1002/mp.13642]
 - 27 **Jian W**, Ju H, Cen X, Cui M, Zhang H, Zhang L, Wang G, Gu L, Zhou W. Improving the malignancy characterization of hepatocellular carcinoma using deeply supervised cross modal transfer learning for non-enhanced MR. *Conf Proc IEEE Eng Med Biol Soc* 2019; **2019**: 853-856
 - 28 **Ouhmich F**, Agnus V, Noblet V, Heitz F, Pessaux P. Liver tissue segmentation in multiphase CT scans using cascaded convolutional neural networks. *Int J Comput Assist Radiol Surg* 2019; **14**: 1275-1284 [PMID: 31041697 DOI: 10.1007/s11548-019-01989-z]
 - 29 **Arslanoglu A**, Chalian H, Sodagari F, Seyal AR, Töre HG, Salem R, Yaghmai V. Threshold for Enhancement in Treated Hepatocellular Carcinoma on MDCT: Effect on Necrosis Quantification. *AJR Am J Roentgenol* 2016; **206**: 536-543 [PMID: 26901009 DOI: 10.2214/AJR.15.15339]
 - 30 **Najmi Varzaneh F**, Pandey A, Aliyari Ghasabeh M, Shao N, Khoshpouri P, Pandey P, Zarghampour M, Fouladi D, Liddell R, Anders RA, Kamel IR. Prediction of post-TACE necrosis of hepatocellular carcinoma using volumetric enhancement on MRI and volumetric oil deposition on CT, with pathological correlation. *Eur Radiol* 2018; **28**: 3032-3040 [PMID: 29383518 DOI: 10.1007/s00330-017-5198-9]

- 31 **Liao H**, Xiong T, Peng J, Xu L, Liao M, Zhang Z, Wu Z, Yuan K, Zeng Y. Classification and Prognosis Prediction from Histopathological Images of Hepatocellular Carcinoma by a Fully Automated Pipeline Based on Machine Learning. *Ann Surg Oncol* 2020; **27**: 2359-2369 [PMID: 31916093 DOI: 10.1245/s10434-019-08190-1]
- 32 **Lu G**, Fei B. Medical hyperspectral imaging: a review. *J Biomed Opt* 2014; **19**: 10901 [PMID: 24441941 DOI: 10.1117/1.JBO.19.1.010901]
- 33 **Wang R**, He Y, Yao C, Wang S, Xue Y, Zhang Z, Wang J, Liu X. Classification and Segmentation of Hyperspectral Data of Hepatocellular Carcinoma Samples Using 1-D Convolutional Neural Network. *Cytometry A* 2020; **97**: 31-38 [PMID: 31403260 DOI: 10.1002/cyto.a.23871]
- 34 **Sato M**, Morimoto K, Kajihara S, Tateishi R, Shiina S, Koike K, Yatomi Y. Machine-learning Approach for the Development of a Novel Predictive Model for the Diagnosis of Hepatocellular Carcinoma. *Sci Rep* 2019; **9**: 7704 [PMID: 31147560 DOI: 10.1038/s41598-019-44022-8]
- 35 **Qiao G**, Li J, Huang A, Yan Z, Lau WY, Shen F. Artificial neural networking model for the prediction of post-hepatectomy survival of patients with early hepatocellular carcinoma. *J Gastroenterol Hepatol* 2014; **29**: 2014-2020 [PMID: 24989634 DOI: 10.1111/jgh.12672]
- 36 **Tsilimigras DI**, Mehta R, Moris D, Sahara K, Bagante F, Paredes AZ, Farooq A, Ratti F, Marques HP, Silva S, Soubrane O, Lam V, Poultsides GA, Popescu I, Grigorie R, Alexandrescu S, Martel G, Workneh A, Guglielmi A, Hugh T, Aldrighetti L, Endo I, Pawlik TM. Utilizing Machine Learning for Pre- and Postoperative Assessment of Patients Undergoing Resection for BCLC-0, A and B Hepatocellular Carcinoma: Implications for Resection Beyond the BCLC Guidelines. *Ann Surg Oncol* 2020; **27**: 866-874 [PMID: 31696396 DOI: 10.1245/s10434-019-08025-z]
- 37 **Ho WH**, Lee KT, Chen HY, Ho TW, Chiu HC. Disease-free survival after hepatic resection in hepatocellular carcinoma patients: a prediction approach using artificial neural network. *PLoS One* 2012; **7**: e29179 [PMID: 22235270 DOI: 10.1371/journal.pone.0029179]
- 38 **Chiu HC**, Ho TW, Lee KT, Chen HY, Ho WH. Mortality predicted accuracy for hepatocellular carcinoma patients with hepatic resection using artificial neural network. *ScientificWorldJournal* 2013; **2013**: 201976 [PMID: 23737707 DOI: 10.1155/2013/201976]
- 39 **Sieghart W**, Huckle F, Peck-Radosavljevic M. Transarterial chemoembolization: modalities, indication, and patient selection. *J Hepatol* 2015; **62**: 1187-1195 [PMID: 25681552 DOI: 10.1016/j.jhep.2015.02.010]
- 40 **Liu D**, Liu F, Xie X, Su L, Liu M, Kuang M, Huang G, Wang Y, Zhou H, Wang K, Lin M, Tian J. Accurate prediction of responses to transarterial chemoembolization for patients with hepatocellular carcinoma by using artificial intelligence in contrast-enhanced ultrasound. *Eur Radiol* 2020; **30**: 2365-2376 [PMID: 31900703 DOI: 10.1007/s00330-019-06553-6]
- 41 **Peng J**, Kang S, Ning Z, Deng H, Shen J, Xu Y, Zhang J, Zhao W, Li X, Gong W, Huang J, Liu L. Residual convolutional neural network for predicting response of transarterial chemoembolization in hepatocellular carcinoma from CT imaging. *Eur Radiol* 2020; **30**: 413-424 [PMID: 31332558 DOI: 10.1007/s00330-019-06318-1]
- 42 **Morshid A**, Elsayes KM, Khalaf AM, Elmohr MM, Yu J, Kaseb AO, Hassan M, Mahvash A, Wang Z, Hazle JD, Fuentes D. A machine learning model to predict hepatocellular carcinoma response to transcatheter arterial chemoembolization. *Radiol Artif Intell* 2019; **1** [PMID: 31858078 DOI: 10.1148/ryai.2019180021]
- 43 **Abajian A**, Murali N, Savic LJ, Laage-Gaupp FM, Nezami N, Duncan JS, Schlachter T, Lin M, Geschwind JF, Chapiro J. Predicting Treatment Response to Intra-arterial Therapies for Hepatocellular Carcinoma with the Use of Supervised Machine Learning-An Artificial Intelligence Concept. *J Vasc Interv Radiol* 2018; **29**: 850-857. e1 [PMID: 29548875 DOI: 10.1016/j.jvir.2018.01.769]
- 44 **Kokabi N**, Ludwig JM, Camacho JC, Xing M, Mittal PK, Kim HS. Baseline and Early MR Apparent Diffusion Coefficient Quantification as a Predictor of Response of Unresectable Hepatocellular Carcinoma to Doxorubicin Drug-Eluting Bead Chemoembolization. *J Vasc Interv Radiol* 2015; **26**: 1777-1786 [PMID: 26603497 DOI: 10.1016/j.jvir.2015.08.023]
- 45 **Wu CF**, Wu YJ, Liang PC, Wu CH, Peng SF, Chiu HW. Disease-free survival assessment by artificial neural networks for hepatocellular carcinoma patients after radiofrequency ablation. *J Formos Med Assoc* 2017; **116**: 765-773 [PMID: 28117199 DOI: 10.1016/j.jfma.2016.12.006]
- 46 **Kim CG**, Lee HW, Choi HJ, Lee JI, Kim SU, Park JY, Kim DY, Ahn SH, Han KH, Kim HS, Kim KH, Choi SJ, Kim Y, Lee KS, Kim GM, Kim MD, Won JY, Lee DY, Kim BK. Development and validation of a prognostic model for patients with hepatocellular carcinoma undergoing radiofrequency ablation. *Cancer Med* 2019; **8**: 5023-5032 [PMID: 31290618 DOI: 10.1002/cam4.2417]
- 47 **Yoon JS**, Lee YR, Kweon YO, Tak WY, Jang SY, Park SY, Hur K, Park JG, Lee HW, Chun JM, Han YS, Lee WK. Comparison of acoustic radiation force impulse elastography and transient elastography for prediction of hepatocellular carcinoma recurrence after radiofrequency ablation. *Eur J Gastroenterol Hepatol* 2018; **30**: 1230-1236 [PMID: 29794814 DOI: 10.1097/MEG.0000000000001170]
- 48 **Fujiwara N**, Friedman SL, Goossens N, Hoshida Y. Risk factors and prevention of hepatocellular carcinoma in the era of precision medicine. *J Hepatol* 2018; **68**: 526-549 [PMID: 28989095 DOI: 10.1016/j.jhep.2017.09.016]
- 49 **Saillard C**, Schmauch B, Laifa O, Moarii M, Toldo S, Zaslavskiy M, Pronier E, Laurent A, Amaddeo G, Regnault H, Sommacale D, Ziol M, Pawlowsky JM, Mulé S, Luciani A, Wainrib G, Clozel T,

- Courtiol P, Calderaro J. Predicting Survival After Hepatocellular Carcinoma Resection Using Deep Learning on Histological Slides. *Hepatology* 2020; **72**: 2000-2013 [PMID: [32108950](#) DOI: [10.1002/hep.31207](#)]
- 50 **Singal AG**, Mukherjee A, Elmunzer BJ, Higgins PD, Lok AS, Zhu J, Marrero JA, Waljee AK. Machine learning algorithms outperform conventional regression models in predicting development of hepatocellular carcinoma. *Am J Gastroenterol* 2013; **108**: 1723-1730 [PMID: [24169273](#) DOI: [10.1038/ajg.2013.332](#)]
- 51 **Chaudhary K**, Poirion OB, Lu L, Garmire LX. Deep Learning-Based Multi-Omics Integration Robustly Predicts Survival in Liver Cancer. *Clin Cancer Res* 2018; **24**: 1248-1259 [PMID: [28982688](#) DOI: [10.1158/1078-0432.CCR-17-0853](#)]
- 52 **Qiu J**, Peng B, Tang Y, Qian Y, Guo P, Li M, Luo J, Chen B, Tang H, Lu C, Cai M, Ke Z, He W, Zheng Y, Xie D, Li B, Yuan Y. CpG Methylation Signature Predicts Recurrence in Early-Stage Hepatocellular Carcinoma: Results From a Multicenter Study. *J Clin Oncol* 2017; **35**: 734-742 [PMID: [28068175](#) DOI: [10.1200/JCO.2016.68.2153](#)]
- 53 **Hinrichsen I**, Kemp M, Peveling-Oberhag J, Passmann S, Plotz G, Zeuzem S, Brieger A. Promoter methylation of MLH1, PMS2, MSH2 and p16 is a phenomenon of advanced-stage HCCs. *PLoS One* 2014; **9**: e84453 [PMID: [24400091](#) DOI: [10.1371/journal.pone.0084453](#)]
- 54 **Dong RZ**, Yang X, Zhang XY, Gao PT, Ke AW, Sun HC, Zhou J, Fan J, Cai JB, Shi GM. Predicting overall survival of patients with hepatocellular carcinoma using a three-category method based on DNA methylation and machine learning. *J Cell Mol Med* 2019; **23**: 3369-3374 [PMID: [30784182](#) DOI: [10.1111/jcmm.14231](#)]
- 55 **Liao LE**, Hu DD, Zheng Y. A Four-Methylated lncRNAs-Based Prognostic Signature for Hepatocellular Carcinoma. *Genes (Basel)* 2020; **11** [PMID: [32784402](#) DOI: [10.3390/genes11080908](#)]
- 56 **Li GX**, Ding ZY, Wang YW, Liu TT, Chen WX, Wu JJ, Xu WQ, Zhu P, Zhang BX. Integrative analysis of DNA methylation and gene expression identify a six epigenetic driver signature for predicting prognosis in hepatocellular carcinoma. *J Cell Physiol* 2019; **234**: 11942-11950 [PMID: [30536816](#) DOI: [10.1002/jcp.27882](#)]
- 57 **Shi HY**, Lee KT, Lee HH, Ho WH, Sun DP, Wang JJ, Chiu CC. Comparison of artificial neural network and logistic regression models for predicting in-hospital mortality after primary liver cancer surgery. *PLoS One* 2012; **7**: e35781 [PMID: [22563399](#) DOI: [10.1371/journal.pone.0035781](#)]
- 58 **Shi HY**, Lee KT, Wang JJ, Sun DP, Lee HH, Chiu CC. Artificial neural network model for predicting 5-year mortality after surgery for hepatocellular carcinoma: a nationwide study. *J Gastrointest Surg* 2012; **16**: 2126-2131 [PMID: [22878787](#) DOI: [10.1007/s11605-012-1986-3](#)]
- 59 **Zeng WZD**, Glicksberg BS, Li Y, Chen B. Selecting precise reference normal tissue samples for cancer research using a deep learning approach. *BMC Med Genomics* 2019; **12**: 21 [PMID: [30704474](#) DOI: [10.1186/s12920-018-0463-6](#)]
- 60 **Gui T**, Dong X, Li R, Li Y, Wang Z. Identification of hepatocellular carcinoma-related genes with a machine learning and network analysis. *J Comput Biol* 2015; **22**: 63-71 [PMID: [25247452](#) DOI: [10.1089/cmb.2014.0122](#)]
- 61 **Hyer JM**, White S, Cloyd J, Dillhoff M, Tsung A, Pawlik TM, Ejaz A. Can We Improve Prediction of Adverse Surgical Outcomes? *J Am Coll Surg* 2020; **230**: 43-52.e1 [PMID: [31672674](#) DOI: [10.1016/j.jamcollsurg.2019.09.015](#)]
- 62 **Mueller-Breckenridge AJ**, Garcia-Alcalde F, Wildum S, Smits SL, de Man RA, van Campenhout MJH, Brouwer WP, Niu J, Young JAT, Najera I, Zhu L, Wu D, Racek T, Hundie GB, Lin Y, Boucher CA, van de Vijver D, Haagmans BL. Machine-learning based patient classification using Hepatitis B virus full-length genome quasispecies from Asian and European cohorts. *Sci Rep* 2019; **9**: 18892 [PMID: [31827222](#) DOI: [10.1038/s41598-019-55445-8](#)]
- 63 **Hashem S**, Esmat G, Elakel W, Habashy S, Raouf SA, Elhefnawi M, Eladawy M, Elhefnawi M. Comparison of Machine Learning Approaches for Prediction of Advanced Liver Fibrosis in Chronic Hepatitis C Patients. *IEEE/ACM Trans Comput Biol Bioinform* 2018; **15**: 861-868 [PMID: [28391204](#) DOI: [10.1109/TCBB.2017.2690848](#)]



Artificial intelligence for pancreatic cancer detection: Recent development and future direction

Passisd Laoveeravat, Priya R Abhyankar, Aaron R Brenner, Moamen M Gabr, Fadlallah G Habr, Amporn Atsawarungrangkit

ORCID number: Passisd Laoveeravat 0000-0001-6855-0437; Priya R Abhyankar 0000-0003-4835-6439; Aaron R Brenner 0000-0001-8816-9182; Moamen M Gabr 0000-0002-0069-5047; Fadlallah G Habr 0000-0001-7954-1413; Amporn Atsawarungrangkit 0000-0003-0622-6839.

Author contributions: Laoveeravat P, Abhyankar PR, and Brenner AR equally contributed to this paper with conception and design of the study, literature review and analysis, drafting the manuscript; Gabr MM, Habr FG, and Atsawarungrangkit A provided critical revision, editing, and final approval of the final version.

Conflict-of-interest statement: No conflict of interest exists.

Open-Access: This article is an open-access article that was selected by an in-house editor and fully peer-reviewed by external reviewers. It is distributed in accordance with the Creative Commons Attribution NonCommercial (CC BY-NC 4.0) license, which permits others to distribute, remix, adapt, build upon this work non-commercially, and license their derivative works on different terms, provided the original work is properly cited and the use is non-commercial. See: <http://creativecommons.org/licenses/by-nc/4.0/>

Passisd Laoveeravat, Moamen M Gabr, Division of Digestive Diseases and Nutrition, University of Kentucky College of Medicine, Lexington, KY 40536, United States

Priya R Abhyankar, Aaron R Brenner, Department of Internal Medicine, University of Kentucky College of Medicine, Lexington, KY 40536, United States

Fadlallah G Habr, Amporn Atsawarungrangkit, Division of Gastroenterology, Warren Alpert Medical School of Brown University, Providence, RI 02903, United States

Corresponding author: Amporn Atsawarungrangkit, MD, Academic Fellow, Instructor, Research Fellow, Division of Gastroenterology, Warren Alpert Medical School of Brown University, 593 Eddy Street, Providence, RI 02903, United States.

amporn_atsawarungrangkit@brown.edu

Abstract

Artificial intelligence (AI) has been increasingly utilized in medical applications, especially in the field of gastroenterology. AI can assist gastroenterologists in imaging-based testing and prediction of clinical diagnosis, for examples, detecting polyps during colonoscopy, identifying small bowel lesions using capsule endoscopy images, and predicting liver diseases based on clinical parameters. With its high mortality rate, pancreatic cancer can highly benefit from AI since the early detection of small lesion is difficult with conventional imaging techniques and current biomarkers. Endoscopic ultrasound (EUS) is a main diagnostic tool with high sensitivity for pancreatic adenocarcinoma and pancreatic cystic lesion. The standard tumor markers have not been effective for diagnosis. There have been recent research studies in AI application in EUS and novel biomarkers to early detect and differentiate malignant pancreatic lesions. The findings are impressive compared to the available traditional methods. Herein, we aim to explore the utility of AI in EUS and novel serum and cyst fluid biomarkers for pancreatic cancer detection.

Key Words: Artificial intelligence; Machine learning; Deep learning; Endoscopic ultrasound; microRNA; Pancreatic cancer; Pancreatic cyst

©The Author(s) 2021. Published by Baishideng Publishing Group Inc. All rights reserved.

[p://creativecommons.org/licenses/by-nc/4.0/](https://creativecommons.org/licenses/by-nc/4.0/)

Manuscript source: Invited manuscript

Specialty type: Gastroenterology and hepatology

Country/Territory of origin: United States

Peer-review report's scientific quality classification

Grade A (Excellent): 0

Grade B (Very good): B, B

Grade C (Good): 0

Grade D (Fair): 0

Grade E (Poor): E

Received: January 26, 2021

Peer-review started: January 26, 2021

First decision: February 27, 2021

Revised: March 31, 2021

Accepted: April 20, 2021

Article in press: April 20, 2021

Published online: April 28, 2021

P-Reviewer: Jiménez Pérez M, Marescaux J, Vishnoi S

S-Editor: Wang JL

L-Editor: A

P-Editor: Li JH



Core Tip: Artificial intelligence (AI) aided endoscopic ultrasound (EUS) and microRNA analyses are sensitive and effective for pancreatic cancer detection with sensitivity of more than 95%. The size of pancreatic lesion does not affect the diagnostic performance by artificial intelligence. This will help overcome the delayed diagnosis and high mortality of pancreatic cancer. Recent studies showed that the speed of AI system in EUS can be performed in real time fashion. This will be adjunctive to the conventional EUS examination for future utility.

Citation: Laoveeravat P, Abhyankar PR, Brenner AR, Gabr MM, Habr FG, Atsawarungruangkit A. Artificial intelligence for pancreatic cancer detection: Recent development and future direction. *Artif Intell Gastroenterol* 2021; 2(2): 56-68

URL: <https://www.wjgnet.com/2644-3236/full/v2/i2/56.htm>

DOI: <https://dx.doi.org/10.35712/aig.v2.i2.56>

INTRODUCTION

Pancreatic cancer has been notorious for late detection and high mortality rate^[1,2]. The main contributing factor is the difficulty of diagnosis from imaging studies^[3]. Differentiation between benign disease like chronic pancreatitis and malignancy is challenging^[4]. Malignant pancreatic diseases [*i.e.*, pancreatic ductal carcinoma, intraductal papillary mucinous neoplasms (IPMN), and mucinous cystic neoplasm] can present differently in radiologic imaging^[5]. Endoscopic ultrasound (EUS) has been recognized as an effective method for detecting pancreatic cancer with a reasonable sensitivity but low specificity^[6]. Compared to computed tomography (CT) and magnetic resonance imaging (MRI), EUS had a superior performance in small pancreatic tumors^[6,7].

The use of computer aided diagnosis for cancer detection has been introduced since 1960^[8]. In the past 10 years, the use of artificial intelligence (AI) has been exponentially increased in every field, including medicine^[9-11]. Machine learning and deep learning are two major techniques in AI used for analyzing a large dataset and creating a predictive model^[12-14]. The advance of AI in gastroenterology field has played an important role in pancreatic cancer regarding detection and survival prediction^[15-17].

Given the emerging role of AI in this field, we conducted the systematic review on AI and pancreatic cancer with keywords of "artificial intelligence" and "pancreatic cancer" from PubMed and Institute of Electrical and Electronics Engineers databases. We aim to elaborate the advancement of AI application in pancreatic cancer detection by imaging studies focusing on endoscopic ultrasound and novel serum and cyst fluid marker analysis.

AI CONCEPT AND TERMINOLOGY

AI is the use of mathematical models and computer algorithms to mimic human intelligence. It has been increasingly used to predict risk and diagnose pancreatic cancer with imaging and personal health features^[15,18-20]. Most medical AI is considered narrow AI, which focuses on single or limited tasks^[19]. There are different AI techniques for creating predictive models, including machine learning and deep learning.

Machine learning is a subfield of AI that uses mathematical techniques to create a predictive model by recognizing patterns in the dataset without being explicitly programmed^[18,19]. There are many machine learning algorithms available such as regression, decision trees, k-nearest neighbors, and neural network^[21]. Machine learning shows great promise in medical research as it can detect complex patterns in a large dataset that human doctors would likely miss^[22,23].

Deep learning, a subfield of machine learning, is basically a neural network with multiple hidden layers (usually a large number) to automatically detect higher-level features of input data. A neural network is also known as artificial neural network. As shown in **Figure 1**, neural network is a system of interconnected neurons with three type of layers: (1) Input layer; (2) Hidden layer; and (3) Output layer. Each layer

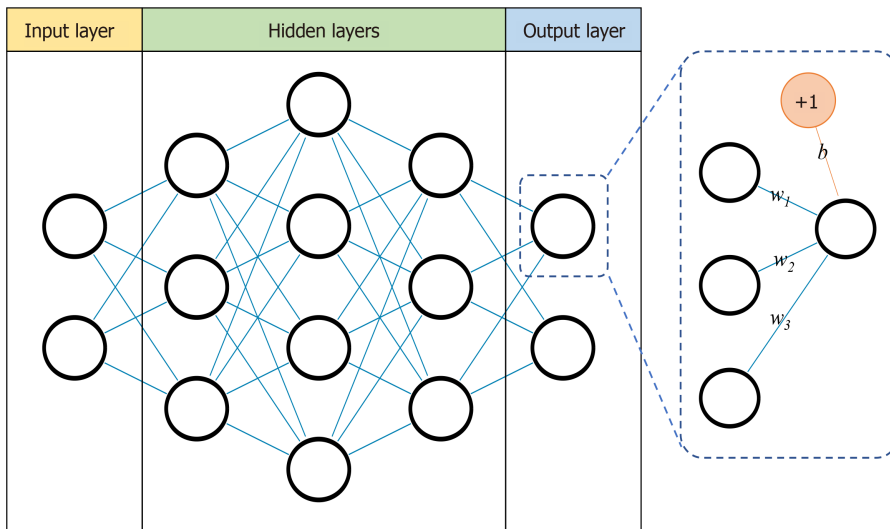


Figure 1 Neural network with input layer, hidden layers, and output layer. Each circle represents a neuron within the network. Within each neuron, weights and bias are applied to the input values to produce an output value. w: Weight; b: Bias.

amplifies certain aspects of the input that are important for discrimination by applying a weight to each input^[24,25]. Besides requiring a large and well-annotated dataset, the major drawback of deep learning is a long training time, which could take hours or days. One method that can significantly improve the training time of deep learning is the use specialized hardware such as graphic processing unit or tensor processing unit^[26].

A convolutional neural network (CNN) is a class of deep learning that apply a filter to capture the characteristic of the data. In image analysis, CNN use different filters to capture various aspects of the image^[27,28]. The most significant advantage of CNN in the medical field is its ability to detect image features automatically and objectively, for instance, the detection of pancreatic cancer based on EUS images^[19,29].

Three major types of machine learning problems are supervised learning, unsupervised learning, and reinforcement learning. Most machine learning problems in medicine are supervised learning, in which the response variable must be already known or labeled. To create a predictive model for solving supervised learning problem, the first step is the collection and annotation (label) of input data. The data is then divided into training and testing sets. The training data is used for training machine learning models, including applying different learning algorithms or architectures, optimizing model parameters, and selecting a final predictive model. Once the final predictive model is selected, the model will be evaluated using the testing data to assess the model performance on the data that has not been used before. These are common steps used to create a predictive model for both machine learning and deep learning^[21,30]. In fact, the choice of using machine learning or deep learning usually depends on the type of inputs. Typically, CNN-based deep learning is the preferred choice for image classification. Additionally, deep learning model had a higher diagnostic ability than the subjective measurement of tumor feature values (tumor width, shape, and color) by doctors because of its objectivity^[31-33].

APPLICATION OF AI IN IMAGING STUDIES FOR PANCREATIC CANCER DETECTION

Modern imaging modalities, including CT scan, MRI, ultrasound, and endoscopy, contain far more visual information than humans can distinguish with the naked eye^[18]. Since 2010, significant progress has been achieved in applying AI to the gastroenterology imaging^[15]. The pancreas is one of the most challenging organs in CT segmentation. Each patient produces more than 300 images that a radiologist must discern, creating intense reading efforts that sometimes succumb to unavoidable misdiagnosis^[34]. Many machine learning and deep learning models have been created to aid physicians in making diagnosis based on medical imaging, including the detection of pancreatic neoplasms. There are two major types of AI systems used in the

detection of cancer: Computer-assisted detection (CADe) and computer-assisted diagnosis (CADx) and they serve different purposes. CADe systems are used for locating lesions in medical images. CADx systems characterize lesions and can distinguish between benign and malignant^[35].

COMPUTED TOMOGRAPHY

CADx AI systems have been created with the analysis of segmented CT images of the pancreas. These systems work by creating an experimental group of image data and a control group of image data which are imported into a program. The data is fed through two matrices and a filter, statistics, and other data are applied. Then the pancreatic cancer and the normal control images are distinguished by data processing and statistical analysis^[36].

An extension of CADx systems is the use of radiomics in CT images. Radiomics is an AI process that not only answers simple clinical questions (*e.g.*, benign or malignant), but can also be used to extract quantitative imaging features from radiology images to produce more detailed information about the areas of interest (*e.g.*, determining risk of malignancy in pre-malignant lesions)^[18]. A study by Wei *et al.*^[37] used a machine learning based model to determine serous cystic neoplasms from non-serous cystic neoplasms based on 409 quantitative radiomic features from preoperative CT images. The model outperformed clinicians with an area under the receiver operating characteristic curve (AUC) of 0.84.

Segmentation of the pancreas in CT imaging is a difficult but essential task for a successful diagnosis of pancreatic cancer. The main challenges lie in its close proximity to other organs, shape variance and low contrast blurring^[27,38-40]. Notably, the ideal type of CT imaging in patients with suspected pancreatic cancer is a contrast-enhanced, multidetector CT, which has sensitivity of 70% to 100% whereas traditional CT has an accuracy of 83.3%, sensitivity of 81.4%, and specificity of 43% for pancreatic adenocarcinoma detection^[41].

Liu *et al.*^[42] used a faster region-based CNN (faster R-CNN) model to form a CADx to solve the challenging pancreas segmentation problem in CT images. Their faster R-CNN model assisted had an AUC of 0.96 and mean average precision of 0.7664, indicating a high discriminating ability and precision. Consequently, the time required to establish a diagnosis using their model was 3 s compared to 8 min by an imaging specialist. Another study used multi-scale segmentation-for-classification to detect pancreatic ductal adenocarcinoma (PDAC). This method functioned by performing tumor segmentation at the same time as tumor classification. This information was helpful for radiologists when determining tumor location. Their method reported a sensitivity of 94.1% and a specificity of 98.5%, implying that their model for tumor segmentation was strong in screening for PDAC^[43]. Interestingly, Chu *et al.*^[44] used random forest algorithm to classify PDAC based on CT images. The overall accuracy, AUC, sensitivity, and specificity were 99.2%, 0.999, 100%, and 98.5%, respectively.

To classify pancreatic cancer, a custom method using a combination of support vector machine and random forest technology was applied to PET/CT images^[45]. Their proposed model achieved accuracy of 96.47%, sensitivity of 95.23%, and specificity of 97.51%. They demonstrated that their model outperformed other models based on an external dataset.

MAGNETIC RESONANCE IMAGING

It is challenging to obtain multi-modal MRI images and then effectively fuse the information from these images due to the heterogeneity of the pancreas and the ill-defined tumor boundary^[46-48]. PDAC diagnostic value by traditional MRI has an accuracy of 89.1%, sensitivity of 89.5%, and specificity of 63.4%^[41].

Barriers to machine learning algorithm development for MRI include limited availability of MRI data, reduced image quality, and unstandardized nature of MRI^[49]. In addition, overfitting can be an issue due to small datasets in MRI and CNN studies^[48]. However, CADx systems for the diagnosis of pancreatic cancer have been developed with MRI images. One study used a CNN was used for feature representation for IPMN diagnosis with MRI^[47]. This approach led to a 30% improvement in specificity of IPMN diagnosis compared to single modality-based approaches (T1 or T2 imaging). The multi-modal fusion approach for IPMN detection had an accuracy of 82.80%, sensitivity of 83.55%, and specificity of 81.67%. It is only

needed to identify a single slice where pancreatic tissues could be obviously observed. Zhang *et al.*^[54] used support vector machine in combination with MRI detection to classify pediatric pancreatic cancer; their proposed model achieved a higher accuracy when compared to the normal detection algorithm. Corral *et al.*^[50] created a CNN which diagnosed intraductal papillary mucinous neoplasm (IPMN) on MRI images in 1.82 s with a sensitivity of 75% and specificity of 78%. Another study by Gao *et al.*^[51] created a deep learning model that graded pancreatic neuroendocrine tumors using MRI images, reaching an accuracy of 81.1% and AUC of 0.89. In a 2020 retrospective study, the research group assessed baseline CT images from 207 patients with proven PDAC and developed a machine learning model that used radiomics to predict molecular subtypes. The classification algorithm achieved a sensitivity, specificity and ROC-AUC of 0.84, 0.92, and 0.93, respectively^[49]. **Table 1** demonstrates the studies on CT and MRI of pancreatic cancer.

ULTRASONOGRAPHY

AI is used in transabdominal ultrasonography and endoscopic ultrasonography. In transabdominal ultrasonography, AI is used primarily for detecting liver fibrosis stage and chronic liver disease by using the histogram analysis and RGB-to-stiffness inverse mapping technique^[49]. The role of transabdominal ultrasonography for pancreatic cancer detection is very minimal because the pancreas visualization is obscured by bowel gas. Due to this, there are no available studies in the evaluation of pancreatic cancer with transabdominal ultrasound.

ENDOSCOPIC ULTRASOUND

Among MRI, CT, and EUS, only EUS enables observation of the pancreas with high spatial resolution. EUS has higher tumor detection rates than contrast enhanced CT by allowing detection of the echo structure in lesions as small as 1 cm^[52]. The sensitivity of EUS is superior to CT scan, 94% and 74%, respectively^[5]. However, the accuracy of EUS is currently highly operator dependent.

There are previous studies on the application of AI in EUS for pancreatic cancer detection (**Table 2**). The overall accuracy of AI based approach were 80%-97% with sensitivity of 83%-100%. The findings are comparable to a sensitivity of 94% by endoscopist driven EUS according to the meta-analysis^[5]. The first study of AI based EUS analyzed a single EUS image per patient obtained from the total of 21 patients^[53]. Machine and human demonstrated a similar diagnostic performance. However, this study was done before the introduction of modern deep learning framework, which has demonstrated much better performance in general than earlier neural network architecture. Based on the observation that there is an age-related change of pancreas shape, Ozkan *et al.*^[54] used three different neural network models to classify pancreatic cancer in three age groups: Below 40, 40 to 60, and above 60. As a result, a higher performance was achieved by using a different model for each age group.

There were different techniques being used for image analyses and creating classification models in pancreatic cancer studies, including deep pocket inspection^[55], support vector machine^[56], region of interest, principal component analysis^[57], neural network, and deep learning. We noticed that these requires were evolved with the major progress of AI development; machine learning techniques were used at the beginning and gradually evolved to CNN-based models (deep learning).

Interfering factors associated with misdetection of pancreatic cancer include chronic pancreatitis with more false negative results^[4]. The compromised ability of pancreatic cancer detection in patients with chronic pancreatitis decreased to 54%-75%. Tonozuka *et al.*^[33] found that non-PDAC is the significant factor of misdetection which means the system tends to work towards preventing the overlooking of tumors than overdiagnosis of tumors. On the other hand, tumor size is not associated with misdetection. Thus, AI guided diagnosis can help with early detection of small tumor and prevent the progression of pancreatic cancer. Another consideration is that the control group with a few cases of mass forming pancreatitis makes the results not generalizable to the group of focal pancreatitis (pseudotumorous pancreatitis) as more included in Norton *et al.*^[53]. The main limitations of prior studies on AI-guided EUS diagnosis are small sample size. Data augmentation has been used to increase the number of images in later study^[33]. Slow processing time and low-quality image are other constraints. They hinder the development of this approach to be real time

Table 1 Summary of studies assessing computed tomography and magnetic resonance using artificial intelligence-based approach for pancreatic cancer

Ref.	Overall dataset	Testing data	Model	Model performance on testing data					
				Accuracy (%)	AUC	Sensitivity (%)	Specificity (%)	PPV (%)	NPV (%)
CT									
Zhu <i>et al</i> ^[43] , 2019 (United States)	439 cases	23 cases	CNN	NA	NA	94.1	98.5	NA	NA
Liu <i>et al</i> ^[42] , 2019 (China)	338 patients	100 patients	CNN	NA	0.9632	NA	NA	NA	NA
Chu <i>et al</i> ^[44] , 2019 (China)	380 patients	125 patients	ML	99.2%	0.999	100	98.5	NA	NA
Li <i>et al</i> ^[75] , 2018 (China)	206 patients	No separate testing data (10-fold CV)	CNN	72.8% ¹	NA	NA	NA	NA	NA
Wei <i>et al</i> ^[57] , 2018 (China)	260 patients	60 patients	SVM	NA	0.837	66.7	81.8	NA	NA
MR									
Kaissis <i>et al</i> ^[49] , 2020 (Germany)	207 patients	26 patients	ML	NA	0.93	84	92	NA	NA
Corral <i>et al</i> ^[50] , 2019 (United States)	139 cases	No separate testing data (10-fold CV)	DL	NA	0.78 ¹	92 ¹	52% ¹	NA	NA
Gao <i>et al</i> ^[51] , 2019 (China)	96 patients	No separate testing data (5-fold CV)	DL	85.13 ¹	0.9117 ¹	NA	NA	NA	NA

¹The performance was based on n-fold cross-validation on training data.

AUC: Area under the curve; CNN: Convolutional neural network; CT: Computed tomography; CV: Cross-validation; DL: Deep learning; IPMN: Intraductal papillary mucinous neoplasm; MR: Magnetic resonance; NA: Not available; NN: Neural network; NPV: Negative predictive value; PCA: Principal component analysis; PPV: Positive predictive value; SVM: Support vector machine.

analysis. Interestingly, real time EUS video using CNN for pancreas segmentation and station recognition has been studied^[56]. The real-time system works as a monitoring safety net and remind endoscopist to make up the unobserved part. It can also increase trainee performance in learning how to detect pancreatic cancer using EUS, which can lead to the reduction of training time and cost.

AI also plays important role in two new EUS techniques, including contrast enhancing EUS (CE-EUS) and EUS elastography. CE-EUS is a technique that uses gas-containing contrast agents intravenously injected for better visualization and differential diagnosis of focal pancreatic lesions. A study found machine learning assisted CE-EUS provided higher sensitivity of 94% compared to 87.5% of qualitative CE-EUS without machine learning aid^[59]. EUS elastography is a technique that measure the tissue stiffness, which help differentiate a mass from normal or inflammatory area. The real-time performance of neural network provided comparable efficacy to standard EUS elastography. The predictive performance of EUS elastography is similar to the b-mode EUS with AUCs of 0.94-0.965^[60,61].

Regarding a real-time application, Marya *et al*^[62] demonstrated the high accuracy of PDAC detection from other pancreatic diseases with AUC of 0.98. The author claimed that the speed of image processing is eligible for real-time system but it was not performed. Future application is warranted which can guide biopsy in patients with diffuse inflammation as chronic pancreatitis to avoid unnecessary biopsies.

AI has not only been studies in PDAC, but also in pancreatic cystic lesions. One study on the differentiation of malignant *vs* benign IPMN by EUS revealed the superior accuracy in identifying malignancy; 94% by AI *vs* 56% by the physician diagnosis performing EUS. However, the AI's prediction on EUS images was not performed during the EUS procedure in a real time. The real-time integration will help aid clinicians to make a clinical judgement^[63]. EUS guided needle confocal laser endomicroscopy is a novel technique for pancreatic cystic lesions. A study was conducted in 15027 videos from 35 subjects with IPMN. The CNN algorithm for high grade dysplasia or adenocarcinoma diagnosis had higher sensitivity (83.3% *vs* 55.6%)

Table 2 Summary of endoscopic ultrasound using artificial intelligence-based approach studies pancreatic cancer and malignant pancreatic cyst detection

Ref.	Overall dataset	Testing data	Model	Model performance on testing data					
				Accuracy (%)	AUC	Sensitivity (%)	Specificity (%)	PPV (%)	NPV (%)
Marya <i>et al</i> ^[62] , 2020 (United States)	583 patients (1174461 images)	123 patients	CNN	NA	0.976	95	91	87	97
Tonozuka <i>et al</i> ^[33] , 2020 (Japan)	139 patients (920 images)	47 patients (470 images)	CNN	NA	0.94	92.4	84.1	86.8	90.7
Ozkan <i>et al</i> ^[54] , 2016 (Turkey)	332 images	72 images	NN	87.5	NA	83.3	93.33	NA	NA
Saftoiu <i>et al</i> ^[59] , 2015 (Multicenter in Europe)	167 cases	15% of cases	NN	NA	NA	94.64	94.44	97.24	89.47
Zhu <i>et al</i> ^[56] , 2013 (China)	388 images	50% of all data (200 trials)	SVM	93.86	NA	92.52	93.03	91.75	94.39
Zhang <i>et al</i> ^[55] , 2010 (China)	216 patients	50% of all data (50 trials)	SVM	97.98	NA	94.32	99.45	98.65	97.77
Das <i>et al</i> ^[57] , 2008 (United States)	319 images	50% of all data	NN	NA	0.93	93	92	87	96
Norton <i>et al</i> ^[53] , 2001 (United States)	21 patients	4 patients	ML	80	NA	100	50	NA	NA
Elastography									
Saftoiu <i>et al</i> ^[61] , 2012 (Multicenter in Europe)	258 cases	No separate testing data (10-fold CV)	NN	84.27 ²	0.94 ²	87.59 ²	82.94 ²	96.25 ²	57.22 ²
Saftoiu <i>et al</i> ^[60] , 2008 (Denmark and Romania)	68 cases	No separate testing data (10-fold CV)	NN	NA	0.957 ²	NA	NA	NA	NA
IPMN									
Machicado <i>et al</i> ^[64] , 2021 (United States) ¹	35 cases of EUS-nCLE (15027 frames)	No separate testing data (5-fold CV)	(1) CNN (segmentation); and (2) CNN (holistic)	(1) 82.9 ² ; and (2) 85.7 ²	NA	(1) 83.3 ² ; and (2) 83.3 ²	(1) 82.4 ² ; and (2) 88.2 ²	(1) 83.3 ² ; and (2) 88.2 ²	(1) 82.4 ² ; and (2) 83.3 ²
Kuwahara <i>et al</i> ^[63] , 2019 (Japan)	50 cases	No separate testing data (10-fold CV)	CNN	94 ²	NA	95.7 ²	92.6 ²	91.7 ²	96.2 ²

¹Presented two designs of CNN algorithms: segmentation based model and holistic based model.

²The performance was based on n-fold cross-validation on training data.

AUC: Area under the receiver operating characteristic curve; CE-EUS: Contrast enhanced endoscopic ultrasound; CNN: Convolutional neural network; CV: Cross-validation; EUS-nCLE: Endoscopic ultrasound-guided needle based confocal laser endomicroscopy; IPMN: Intraductal papillary mucinous neoplasm; NA: Not available; NN: Neural network; NPV: Negative predictive value; PCA: Principal component analysis; PPV: Positive predictive value; SVM: Support vector machine.

and accuracy (82.9%-85.7% *vs* 68.6%-74.3%) than the Fukuoka and American Gastroenterology Association diagnostic criteria^[64].

APPLICATION OF AI IN BIOMARKER ANALYSIS FOR PANCREATIC CANCER DETECTION

Conventional markers

The most used biomarker in monitoring pancreatic cancer is currently carbohydrate antigen (CA) 19-9^[65]. It is usually used in monitoring progression and treatment of

pancreatic cancer due to the low specificity and sensitivity. The combined sensitivity and specificity were 78.2% and 82.8% respectively. The relatively low specificity and sensitivity, and low positive predictive value in asymptomatic patients, would indicate that CA19-9, would be a poor biomarker if applied as a screening test, causing unnecessary and wasteful workups for patients^[66]. Another biomarker that has been explored is carcinoembryonic antigen (CEA), which exhibits an even poorer sensitivity and specificity for classifying pancreatic cancer than the CA19-9^[65].

Some methods using more targeted screening have been suggested such as using multiple biomarkers together or screening only high-risk populations, but those have yet to be universally defined. A screening model was suggested to separate high risk populations into those with inherited pancreatic cancer and those who are at high risk for non-inherited. Even between those two categories non-inherited high-risk could only narrowed to individuals with new onset diabetes^[66]. Using this as an example would still provide for a very large screening population with low sensitivity and specificity if only using CA19-9^[67]. Other biomarkers have been identified that are present in early pancreatic adenocarcinoma but none of them alone have produced high enough quality data to prove even non-inferiority *vs* no screening, let alone CA19-9^[66,68].

A study utilized neural network for multiple tumor marker analysis (CA19-9, CEA, and CA125) for pancreatic cancer diagnosis in 913 serum specimens. AUCs of neural network derived model was superior to logistic regression model with AUCs of 0.905 and 0.812, respectively. The diagnostic performance of single marker is lower than the AI model with AUCs of CA19-9, CA125, and CEA of 0.845, 0.795, and 0.800, respectively^[69].

Kurita *et al*^[70] used AI to differentiate between malignant and cystic lesions of the pancreas using a dataset consisting of biomarkers, sex, characteristics of cystic lesion, and cytology. It is worth noting that the authors clearly stated that the deep learning was used, but it is technically a neural network with two hidden layers; each layer contains nine nodes. In terms of discriminating performance of classifiers, their AI approach with an AUC of 0.966 well outperformed CEA (AUC = 0.719) and cytology (AUC = 0.739). Although this study is limited by its low sample size and retrospective nature, it showed that a predictive model based on a combination of biomarkers and other factors could achieve a higher performance in classifying the malignancy status of pancreatic cyst fluid in comparison to the use of single biomarker.

Novel biomarkers

In the past, conventional markers like CEA, CA72-4, CA125, and CA19-9, have been used to identify, differentiate, and monitor pancreatic cyst fluid. CA19-9 and CA125 can be used to assess for if a cyst has mucinous characteristics, while CEA can help to differentiate a malignant cyst from benign cyst^[65,70]. Advances in genomic sequencing and identification have introduced the ability to isolate microRNA (miRNA) sequences in pancreatic cyst fluid and serum as potential biomarkers for pancreatic adenocarcinoma.

It was first suggested in 2010, that miRNA could be used as a marker for pancreatic adenocarcinoma. miRNA-21 and miRNA-155 in pancreatic juice were present in statistically significantly higher levels in pancreatic adenocarcinoma as compared to benign pancreatic cysts^[71]. miRNA are exosome sequences that, in the setting of pancreatic adenocarcinoma, encode for proteins that are oncogenic or have tumor suppressor function. Several specific miRNAs have been identified to have a higher expression in pancreatic ductal adenocarcinoma, including miRNA-21 and miRNA-155^[68]. These miRNAs are detected in the pancreatic juice. miRNAs are mostly expressed in pancreatic cyst fluid, but Yoshizawa *et al*^[72] have gone on to examine miRNA in the urine. Looking the ratio of miR-3940-5p/miR-8069 in the urine of patients with pancreatic ductal adenocarcinoma, they found that an elevated ratio with an elevated CA19-9 better predicts pancreatic ductal adenocarcinoma than CA19-9 alone. These studies all examine the viability of miRNA in various types of fluid to detect disease states of the pancreas, none though utilize AI to determine which miRNA may produce the highest yield results. A limitation is that they represent small sample sizes with limited application at a population level.

Several studies have identified several miRNAs that potentially represent significant value in determining malignancy of pancreatic cystic lesion or identifying pancreatic adenocarcinoma at an early stage by AI, but each study has decided which miRNAs to utilize based on identifying and isolating very few sequences. Alizadeh *et al*^[73], combined several AI and data mining techniques to best determine the miRNA sequences that have the greatest diagnostic and prognostic capabilities. Particle Swarm Optimization (PSO) and neural network, two forms of AI deep learning, identified a

set of five miRNAs: miR-663, miR-1469, miR-92a-2-5p, miR-125b-1-3p, and miR-532-5p. These were identified from 671 serum samples of patients with pancreatic ductal adenocarcinoma and healthy controls. This model had the greatest AUC score in differentiating pancreatic adenocarcinoma from controls with a sensitivity of 0.93, specificity of 0.92, and accuracy of 0.93.

Cao *et al.*^[74] employed machine learning to identify two panels of plasma miRNA to distinguish between chronic pancreatitis and pancreatic neoplasm from 361 plasma samples in China. Panel 1 consisted of miR-486-5p, miR-126-3p, and miR-106b-3p, and had an AUC of 0.891. Panel 2 consisted of miR-486-5p, miR-126-3p, miR-106b-3p, miR-938, miR26b-3p, and miR-1285, and had an AUC of 0.889. Both panels had a higher AUC than CA 19-9, which was 0.775.

The most robust path to create a new screening test for pancreatic adenocarcinoma must contain a combination of biomarkers and patient data to maximize both the sensitivity and specificity of the test^[68,70,71,74]. AI creates the potential to assess patient characteristics, miRNA, and classical biomarkers, which allows for a comprehensive screening analysis of a patient. With the use of neural network and PSO, AI thinks, acts, and analyzes data at much faster speed and in more depth pattern recognition that forms the perfect environment for the development of high yield screening tests that have previously evaded us in diagnosing and screening for pancreatic cancer. Pancreatic juice for multiple exosomes of miRNA that are known to be associated with increased risk for pancreatic cancer, like oncogenes and tumor suppressor mutations, provides the opportunity to examine multiple pancreatic adenocarcinoma biomarkers with one test.

FUTURE PROSPECT

Pancreatic cancer is notorious for late detection. The studies on this area have been conducted mainly to identify the best approach for early detection by imaging studies and biomarkers. The advancement of EUS and the application of AI technology showed a promising performance. The modes of EUS: B-mode and elastography do not provide different accuracy and predictive value for pancreatic cancer. However, no data is available for EUS with contrast enhancement. B-mode which is generally used among centers can be the first step of AI implication. Ultimately, the data of imaging studies, biomarkers, and clinical parameters will be combined to build the sophisticated algorithm and implemented in the electronic medical records where clinicians use it as the predictive tool. There are a few limitations of AI application for EUS. First, the collection of EUS images as the big data is difficult. The collaboration of gastroenterologists, radiologists, and hospital administration will help facilitate the retrieval of images into the system. Multicenter participation is required to create the large dataset of EUS images of which it will optimize the efficiency of AI. The platform of dataset in one institution can be the good example that other centers can adopt and join the group. Second, the root of clinical decision based on AI results is possibly affected by the black box issue (inability to identify the ground of decision). Although there are ways that enable AI to be more interpretable, it is still an active area of research in computer science. Third, the diagnosis is most often made by examination of static images after EUS procedure. Further research on real-time implication of pancreatic malignant lesion diagnosis by AI method is warranted to aid clinician at the examination time to avoid unnecessary biopsy. Regarding biomarkers, although still a mainstay of current practice, the use of singular biomarkers like CA19-9, CEA, and CA-125, may soon become a thing of the past for pancreatic cancer detection. Recent studies showed that moving toward AI aided multiple fluid and serum analysis for biomarkers, like miRNA, potentially provide more sensitive and specific detection. AI not only provides a pathway for the computational, multilayered analysis of multiple patient variables and biomarkers, but also can provide indications for which of those EUS and biomarkers will be highest yield. Combining the knowledge in the field of and the capability of AI introduces a new world of exploration into both screening and diagnosis of pancreatic cancer. AI capabilities allow research to be more finely tuned and the implementation of the most effective method for research into developing screening and diagnostics for pancreatic adenocarcinoma and malignant pancreatic cysts.

CONCLUSION

AI applications for pancreatic cancer has are emerging. New studies come out and showed the promising results of AI in radiological imaging and biomarkers for pancreatic cancer detection. There are still some limitations which need to be addressed in the future studies before incorporating this technology in the clinical practice. The accuracy of AI aided EUS for pancreatic cancer diagnosis is high. However, it has been derived from the small training dataset. The generalizability needs to be considered before using it. Larger studies with population of various pancreatic diseases and third-party validation will demonstrate a greater confidence for adopting AI. For novel biomarkers, our review demonstrated that AI guided analysis of combination of candidate miRNAs have high predictive performance compared to standard tumor markers. The availability of miRNA testing is not widespread in every medical facility. To adopt this implication, further studies on the diagnostic performance are warranted to strongly support the evidence of utility.

REFERENCES

- 1 **Xu Q**, Zhang TP, Zhao YP. Advances in early diagnosis and therapy of pancreatic cancer. *Hepatobiliary Pancreat Dis Int* 2011; **10**: 128-135 [PMID: 21459718 DOI: 10.1016/s1499-3872(11)60021-0]
- 2 **Vincent A**, Herman J, Schulick R, Hruban RH, Goggins M. Pancreatic cancer. *Lancet* 2011; **378**: 607-620 [PMID: 21620466 DOI: 10.1016/S0140-6736(10)62307-0]
- 3 **Dimastromatteo J**, Brentnall T, Kelly KA. Imaging in pancreatic disease. *Nat Rev Gastroenterol Hepatol* 2017; **14**: 97-109 [PMID: 27826137 DOI: 10.1038/nrgastro.2016.144]
- 4 **Fritscher-Ravens A**, Brand L, Knöfel WT, Bobrowski C, Topalidis T, Thonke F, de Werth A, Soehendra N. Comparison of endoscopic ultrasound-guided fine needle aspiration for focal pancreatic lesions in patients with normal parenchyma and chronic pancreatitis. *Am J Gastroenterol* 2002; **97**: 2768-2775 [PMID: 12425546 DOI: 10.1111/j.1572-0241.2002.07020.x]
- 5 **Kitano M**, Yoshida T, Itonaga M, Tamura T, Hatamaru K, Yamashita Y. Impact of endoscopic ultrasonography on diagnosis of pancreatic cancer. *J Gastroenterol* 2019; **54**: 19-32 [PMID: 30406288 DOI: 10.1007/s00535-018-1519-2]
- 6 **Kitano M**, Kudo M, Yamao K, Takagi T, Sakamoto H, Komaki T, Kamata K, Imai H, Chiba Y, Okada M, Murakami T, Takeyama Y. Characterization of small solid tumors in the pancreas: the value of contrast-enhanced harmonic endoscopic ultrasonography. *Am J Gastroenterol* 2012; **107**: 303-310 [PMID: 22008892 DOI: 10.1038/ajg.2011.354]
- 7 **Canto MI**, Hruban RH, Fishman EK, Kamel IR, Schulick R, Zhang Z, Topazian M, Takahashi N, Fletcher J, Petersen G, Klein AP, Axilbund J, Griffin C, Syngal S, Saltzman JR, Mortele KJ, Lee J, Tamm E, Vikram R, Bhosale P, Margolis D, Farrell J, Goggins M; American Cancer of the Pancreas Screening (CAPS) Consortium. Frequent detection of pancreatic lesions in asymptomatic high-risk individuals. *Gastroenterology* 2012; **142**: 796-804; quiz e14 [PMID: 22245846 DOI: 10.1053/j.gastro.2012.01.005]
- 8 **Doi K**. Computer-aided diagnosis in medical imaging: historical review, current status and future potential. *Comput Med Imaging Graph* 2007; **31**: 198-211 [PMID: 17349778 DOI: 10.1016/j.compmedimag.2007.02.002]
- 9 **Lee AY**, Yanagihara RT, Lee CS, Blazes M, Jung HC, Chee YE, Gencarella MD, Gee H, Maa AY, Cockerham GC, Lynch M, Boyko EJ. Multicenter, Head-to-Head, Real-World Validation Study of Seven Automated Artificial Intelligence Diabetic Retinopathy Screening Systems. *Diabetes Care* 2021 [PMID: 33402366 DOI: 10.2337/dc20-1877]
- 10 **Paydar S**, Parva E, Ghahramani Z, Pourahmad S, Shayan L, Mohammadkarimi V, Sabetian G. Do clinical and paraclinical findings have the power to predict critical conditions of injured patients after traumatic injury resuscitation? *Chin J Traumatol* 2021; **24**: 48-52 [PMID: 33358634 DOI: 10.1016/j.cjtee.2020.11.009]
- 11 **Hassan C**, Spadaccini M, Iannone A, Maselli R, Jovani M, Chandrasekar VT, Antonelli G, Yu H, Areia M, Dinis-Ribeiro M, Bhandari P, Sharma P, Rex DK, Rösch T, Wallace M, Repici A. Performance of artificial intelligence in colonoscopy for adenoma and polyp detection: a systematic review and meta-analysis. *Gastrointest Endosc* 2021; **93**: 77-85. e6 [PMID: 32598963 DOI: 10.1016/j.gie.2020.06.059]
- 12 **Huynh E**, Hosny A, Guthrie C, Bitterman DS, Petit SF, Haas-Kogan DA, Kann B, Aerts HJWL, Mak RH. Artificial intelligence in radiation oncology. *Nat Rev Clin Oncol* 2020; **17**: 771-781 [PMID: 32843739 DOI: 10.1038/s41571-020-0417-8]
- 13 **Tang X**. The role of artificial intelligence in medical imaging research. *BJR Open* 2020; **2**: 20190031 [PMID: 33178962 DOI: 10.1259/bjro.20190031]
- 14 **Ngiam KY**, Khor IW. Big data and machine learning algorithms for health-care delivery. *Lancet Oncol* 2019; **20**: e262-e273 [PMID: 31044724 DOI: 10.1016/S1470-2045(19)30149-4]
- 15 **Le Berre C**, Sandborn WJ, Aridhi S, Devignes MD, Fournier L, Smaïl-Tabbone M, Danese S, Peyrin-Biroulet L. Application of Artificial Intelligence to Gastroenterology and Hepatology.

- Gastroenterology* 2020; **158**: 76-94. e2 [PMID: 31593701 DOI: 10.1053/j.gastro.2019.08.058]
- 16 **Zhang Y**, Lobo-Mueller EM, Karanicolas P, Gallinger S, Haider MA, Khalvati F. CNN-based survival model for pancreatic ductal adenocarcinoma in medical imaging. *BMC Med Imaging* 2020; **20**: 11 [PMID: 32013871 DOI: 10.1186/s12880-020-0418-1]
 - 17 **Walczak S**, Velanovich V. An Evaluation of Artificial Neural Networks in Predicting Pancreatic Cancer Survival. *J Gastrointest Surg* 2017; **21**: 1606-1612 [PMID: 28776157 DOI: 10.1007/s11605-017-3518-7]
 - 18 **Gorris M**, Hoogenboom SA, Wallace MB, van Hooft JE. Artificial intelligence for the management of pancreatic diseases. *Dig Endosc* 2021; **33**: 231-241 [PMID: 33065754 DOI: 10.1111/den.13875]
 - 19 **Kuwahara T**, Hara K, Mizuno N, Haba S, Okuno N, Koda H, Miyano A, Fumihara D. Current status of artificial intelligence analysis for endoscopic ultrasonography. *Dig Endosc* 2021; **33**: 298-305 [PMID: 33098123 DOI: 10.1111/den.13880]
 - 20 **Almeida PP**, Cardoso CP, de Freitas LM. PDAC-ANN: an artificial neural network to predict pancreatic ductal adenocarcinoma based on gene expression. *BMC Cancer* 2020; **20**: 82 [PMID: 32005189 DOI: 10.1186/s12885-020-6533-0]
 - 21 **Deo RC**. Machine Learning in Medicine. *Circulation* 2015; **132**: 1920-1930 [PMID: 26572668 DOI: 10.1161/CIRCULATIONAHA.115.001593]
 - 22 **Chung WY**, Correa E, Yoshimura K, Chang MC, Dennison A, Takeda S, Chang YT. Using probe electrospray ionization mass spectrometry and machine learning for detecting pancreatic cancer with high performance. *Am J Transl Res* 2020; **12**: 171-179 [PMID: 32051746]
 - 23 **Mandrell CT**, Holland TE, Wheeler JF, Esmaceli SMA, Amar K, Chowdhury F, Sivakumar P. Machine Learning Approach to Raman Spectrum Analysis of MIA PaCa-2 Pancreatic Cancer Tumor Repopulating Cells for Classification and Feature Analysis. *Life (Basel)* 2020; **10** [PMID: 32899572 DOI: 10.3390/Life10090181]
 - 24 **LeCun Y**, Bengio Y, Hinton G. Deep learning. *Nature* 2015; **521**: 436-444 [PMID: 26017442 DOI: 10.1038/nature14539]
 - 25 **Esteva A**, Chou K, Yeung S, Naik N, Madani A, Mottaghi A, Liu Y, Topol E, Dean J, Socher R. Deep learning-enabled medical computer vision. *NPJ Digit Med* 2021; **4**: 5 [PMID: 33420381 DOI: 10.1038/s41746-020-00376-2]
 - 26 **Montagnon E**, Cerny M, Cadrin-Chênevert A, Hamilton V, Derennes T, Ilincă A, Vandenbroucke-Menu F, Turcotte S, Kadoury S, Tang A. Deep learning workflow in radiology: a primer. *Insights Imaging* 2020; **11**: 22 [PMID: 32040647 DOI: 10.1186/s13244-019-0832-5]
 - 27 **Ma H**, Liu ZX, Zhang JJ, Wu FT, Xu CF, Shen Z, Yu CH, Li YM. Construction of a convolutional neural network classifier developed by computed tomography images for pancreatic cancer diagnosis. *World J Gastroenterol* 2020; **26**: 5156-5168 [PMID: 32982116 DOI: 10.3748/wjg.v26.i34.5156]
 - 28 **Saraswathi HS**, Rafi M, Manjunath KG, Shankar A. Review on computer aided diagnosis of pancreatic cancer using Artificial Intelligence System. In: Proceedings of the 2020 10th International Conference on Cloud Computing, Data Science & Engineering (Confluence); 2020 Jan 29-31; Noida, India. IEEE, 2020: 623-628 [DOI: 10.1109/Confluence47617.2020.9057939]
 - 29 **Fassler DJ**, Abousamra S, Gupta R, Chen C, Zhao M, Paredes D, Batool SA, Knudsen BS, Escobar-Hoyos L, Shroyer KR, Samaras D, Kurc T, Saltz J. Deep learning-based image analysis methods for brightfield-acquired multiplex immunohistochemistry images. *Diagn Pathol* 2020; **15**: 100 [PMID: 32723384 DOI: 10.1186/s13000-020-01003-0]
 - 30 **Sidey-Gibbons JAM**, Sidey-Gibbons CJ. Machine learning in medicine: a practical introduction. *BMC Med Res Methodol* 2019; **19**: 64 [PMID: 30890124 DOI: 10.1186/s12874-019-0681-4]
 - 31 **Shen D**, Wu G, Suk HI. Deep Learning in Medical Image Analysis. *Annu Rev Biomed Eng* 2017; **19**: 221-248 [PMID: 28301734 DOI: 10.1146/annurev-bioeng-071516-044442]
 - 32 **Saffari N**, Rashwan HA, Abdel-Nasser M, Kumar Singh V, Arenas M, Mangina E, Herrera B, Puig D. Fully Automated Breast Density Segmentation and Classification Using Deep Learning. *Diagnostics (Basel)* 2020; **10** [PMID: 33238512 DOI: 10.3390/diagnostics10110988]
 - 33 **Tonozuka R**, Itoi T, Nagata N, Kojima H, Sofuni A, Tsuchiya T, Ishii K, Tanaka R, Nagakawa Y, Mukai S. Deep learning analysis for the detection of pancreatic cancer on endosonographic images: a pilot study. *J Hepatobiliary Pancreat Sci* 2021; **28**: 95-104 [PMID: 32910528 DOI: 10.1002/jhbp.825]
 - 34 **Zhang Y**, Wang S, Qu S, Zhang H. Support vector machine combined with magnetic resonance imaging for accurate diagnosis of paediatric pancreatic cancer. *IET Image Process* 2020; **14**: 1233-1239 [DOI: 10.1049/iet-ipr.2019.1041]
 - 35 **Firmino M**, Angelo G, Morais H, Dantas MR, Valentim R. Computer-aided detection (CADE) and diagnosis (CADx) system for lung cancer with likelihood of malignancy. *Biomed Eng Online* 2016; **15**: 2 [PMID: 26759159 DOI: 10.1186/s12938-015-0120-7]
 - 36 **Lin HM**, Xue XF, Wang XG, Dang SC, Gu M. Application of artificial intelligence for the diagnosis, treatment, and prognosis of pancreatic cancer. *Artif Intell Gastroenterol* 2020; **1**: 19-29 [DOI: 10.35712/aig.v1.i1.19]
 - 37 **Wei R**, Lin K, Yan W, Guo Y, Wang Y, Li J, Zhu J. Computer-Aided Diagnosis of Pancreas Serous Cystic Neoplasms: A Radiomics Method on Preoperative MDCT Images. *Technol Cancer Res Treat* 2019; **18**: 1533033818824339 [PMID: 30803366 DOI: 10.1177/1533033818824339]
 - 38 **Jadhav S**, Dmitriev K, Marino J, Barish M, Kaufman AE. 3D Virtual Pancreatography. *IEEE Trans Vis Comput Graph* 2020; Online ahead of print [PMID: 32870794 DOI: 10.1109/TVCG.2020.3020958]

- 39 **Liu S**, Yuan X, Hu R, Liang S, Feng S, Ai Y, Zhang Y. Automatic Pancreas Segmentation via Coarse Location and Ensemble Learning. *IEEE Access* 2020; **8**: 2906-2914 [DOI: [10.1109/ACCESS.2019.2961125](https://doi.org/10.1109/ACCESS.2019.2961125)]
- 40 **Xie L**, Yu Q, Zhou Y, Wang Y, Fishman EK, Yuille AL. Recurrent Saliency Transformation Network for Tiny Target Segmentation in Abdominal CT Scans. *IEEE Trans Med Imaging* 2020; **39**: 514-525 [DOI: [10.1109/TMI.2019.2930679](https://doi.org/10.1109/TMI.2019.2930679)]
- 41 **Costache MI**, Costache CA, Dumitrescu CI, Tica AA, Popescu M, Baluta EA, Anghel AC, Saftoiu A, Dumitrescu D. Which is the Best Imaging Method in Pancreatic Adenocarcinoma Diagnosis and Staging - CT, MRI or EUS? *Curr Health Sci J* 2017; **43**: 132-136 [PMID: [30595868](https://pubmed.ncbi.nlm.nih.gov/30595868/) DOI: [10.12865/CHSJ.43.02.05](https://doi.org/10.12865/CHSJ.43.02.05)]
- 42 **Liu SL**, Li S, Guo YT, Zhou YP, Zhang ZD, Lu Y. Establishment and application of an artificial intelligence diagnosis system for pancreatic cancer with a faster region-based convolutional neural network. *Chin Med J (Engl)* 2019; **132**: 2795-2803 [PMID: [31856050](https://pubmed.ncbi.nlm.nih.gov/31856050/) DOI: [10.1097/CM9.0000000000000544](https://doi.org/10.1097/CM9.0000000000000544)]
- 43 **Zhu Z**, Xia Y, Xie L, Fishman EK, Yuille AL. Multi-scale Coarse-to-Fine Segmentation for Screening Pancreatic Ductal Adenocarcinoma. In: Shen D, Liu T, Peters TM, Staib LH, Essert C, Zhou S, Yap PT, Khan A. Medical Image Computing and Computer Assisted Intervention – MICCAI 2019. Proceedings of the Medical Image Computing and Computer Assisted Intervention – MICCAI 2019; 2019 Oct 13-17; Shenzhen, China. Cham: Springer, 2019: 3-12
- 44 **Chu LC**, Park S, Kawamoto S, Fouladi DF, Shayesteh S, Zinreich ES, Graves JS, Horton KM, Hruban RH, Yuille AL, Kinzler KW, Vogelstein B, Fishman EK. Utility of CT Radiomics Features in Differentiation of Pancreatic Ductal Adenocarcinoma From Normal Pancreatic Tissue. *AJR Am J Roentgenol* 2019; **213**: 349-357 [PMID: [31012758](https://pubmed.ncbi.nlm.nih.gov/31012758/) DOI: [10.2214/AJR.18.20901](https://doi.org/10.2214/AJR.18.20901)]
- 45 **Li S**, Jiang H, Wang Z, Zhang G, Yao YD. An effective computer aided diagnosis model for pancreas cancer on PET/CT images. *Comput Methods Programs Biomed* 2018; **165**: 205-214 [PMID: [30337075](https://pubmed.ncbi.nlm.nih.gov/30337075/) DOI: [10.1016/j.cmpb.2018.09.001](https://doi.org/10.1016/j.cmpb.2018.09.001)]
- 46 **Chen X**, Lin X, Shen Q, Qian X. Combined Spiral Transformation and Model-Driven Multi-Modal Deep Learning Scheme for Automatic Prediction of TP53 Mutation in Pancreatic Cancer. *IEEE Trans Med Imaging* 2021; **40**: 735-747 [PMID: [33147142](https://pubmed.ncbi.nlm.nih.gov/33147142/) DOI: [10.1109/TMI.2020.3035789](https://doi.org/10.1109/TMI.2020.3035789)]
- 47 **Hussein S**, Kandel P, Bolan CW, Wallace MB, Bagci U. Lung and Pancreatic Tumor Characterization in the Deep Learning Era: Novel Supervised and Unsupervised Learning Approaches. *IEEE Trans Med Imaging* 2019; **38**: 1777-1787 [PMID: [30676950](https://pubmed.ncbi.nlm.nih.gov/30676950/) DOI: [10.1109/TMI.2019.2894349](https://doi.org/10.1109/TMI.2019.2894349)]
- 48 **Liang Y**, Schott D, Zhang Y, Wang Z, Nasief H, Paulson E, Hall W, Knechtges P, Erickson B, Li XA. Auto-segmentation of pancreatic tumor in multi-parametric MRI using deep convolutional neural networks. *Radiother Oncol* 2020; **145**: 193-200 [PMID: [32045787](https://pubmed.ncbi.nlm.nih.gov/32045787/) DOI: [10.1016/j.radonc.2020.01.021](https://doi.org/10.1016/j.radonc.2020.01.021)]
- 49 **Kaassis GA**, Ziegelmayr S, Lohöfer FK, Harder FN, Jungmann F, Sasse D, Muckenhuber A, Yen HY, Steiger K, Siveke J, Friess H, Schmid R, Weichert W, Makowski MR, Braren RF. Image-Based Molecular Phenotyping of Pancreatic Ductal Adenocarcinoma. *J Clin Med* 2020; **9** [PMID: [32155990](https://pubmed.ncbi.nlm.nih.gov/32155990/) DOI: [10.3390/jcm9030724](https://doi.org/10.3390/jcm9030724)]
- 50 **Corral JE**, Hussein S, Kandel P, Bolan CW, Bagci U, Wallace MB. Deep Learning to Classify Intraductal Papillary Mucinous Neoplasms Using Magnetic Resonance Imaging. *Pancreas* 2019; **48**: 805-810 [PMID: [31210661](https://pubmed.ncbi.nlm.nih.gov/31210661/) DOI: [10.1097/MPA.0000000000001327](https://doi.org/10.1097/MPA.0000000000001327)]
- 51 **Gao X**, Wang X. Deep learning for World Health Organization grades of pancreatic neuroendocrine tumors on contrast-enhanced magnetic resonance images: a preliminary study. *Int J Comput Assist Radiol Surg* 2019; **14**: 1981-1991 [PMID: [31555998](https://pubmed.ncbi.nlm.nih.gov/31555998/) DOI: [10.1007/s11548-019-02070-5](https://doi.org/10.1007/s11548-019-02070-5)]
- 52 **Yamaguchi K**, Okusaka T, Shimizu K, Furuse J, Ito Y, Hanada K, Shimosegawa T, Okazaki K; Committee for Revision of Clinical Guidelines for Pancreatic Cancer of the Japan Pancreas Society. Clinical Practice Guidelines for Pancreatic Cancer 2016 From the Japan Pancreas Society: A Synopsis. *Pancreas* 2017; **46**: 595-604 [PMID: [28426492](https://pubmed.ncbi.nlm.nih.gov/28426492/) DOI: [10.1097/MPA.0000000000000816](https://doi.org/10.1097/MPA.0000000000000816)]
- 53 **Norton ID**, Zheng Y, Wiersma MS, Greenleaf J, Clain JE, Dimagno EP. Neural network analysis of EUS images to differentiate between pancreatic malignancy and pancreatitis. *Gastrointest Endosc* 2001; **54**: 625-629 [PMID: [11677484](https://pubmed.ncbi.nlm.nih.gov/11677484/) DOI: [10.1067/mge.2001.118644](https://doi.org/10.1067/mge.2001.118644)]
- 54 **Ozkan M**, Cakiroglu M, Kocaman O, Kurt M, Yilmaz B, Can G, Korkmaz U, Dandil E, Eksi Z. Age-based computer-aided diagnosis approach for pancreatic cancer on endoscopic ultrasound images. *Endosc Ultrasound* 2016; **5**: 101-107 [PMID: [27080608](https://pubmed.ncbi.nlm.nih.gov/27080608/) DOI: [10.4103/2303-9027.180473](https://doi.org/10.4103/2303-9027.180473)]
- 55 **Zhang MM**, Yang H, Jin ZD, Yu JG, Cai ZY, Li ZS. Differential diagnosis of pancreatic cancer from normal tissue with digital imaging processing and pattern recognition based on a support vector machine of EUS images. *Gastrointest Endosc* 2010; **72**: 978-985 [PMID: [20855062](https://pubmed.ncbi.nlm.nih.gov/20855062/) DOI: [10.1016/j.gie.2010.06.042](https://doi.org/10.1016/j.gie.2010.06.042)]
- 56 **Zhu M**, Xu C, Yu J, Wu Y, Li C, Zhang M, Jin Z, Li Z. Differentiation of pancreatic cancer and chronic pancreatitis using computer-aided diagnosis of endoscopic ultrasound (EUS) images: a diagnostic test. *PLoS One* 2013; **8**: e63820 [PMID: [23704940](https://pubmed.ncbi.nlm.nih.gov/23704940/) DOI: [10.1371/journal.pone.0063820](https://doi.org/10.1371/journal.pone.0063820)]
- 57 **Das A**, Nguyen CC, Li F, Li B. Digital image analysis of EUS images accurately differentiates pancreatic cancer from chronic pancreatitis and normal tissue. *Gastrointest Endosc* 2008; **67**: 861-867 [PMID: [18179797](https://pubmed.ncbi.nlm.nih.gov/18179797/) DOI: [10.1016/j.gie.2007.08.036](https://doi.org/10.1016/j.gie.2007.08.036)]
- 58 **Zhang J**, Zhu L, Yao L, Ding X, Chen D, Wu H, Lu Z, Zhou W, Zhang L, An P, Xu B, Tan W, Hu S, Cheng F, Yu H. Deep learning-based pancreas segmentation and station recognition system in EUS:

- development and validation of a useful training tool (with video). *Gastrointest Endosc* 2020; **92**: 874-885. e3 [PMID: 32387499 DOI: 10.1016/j.gie.2020.04.071]
- 59 **Săftoiu A**, Vilmann P, Dietrich CF, Iglesias-Garcia J, Hocke M, Seicean A, Ignee A, Hassan H, Streba CT, Ioncică AM, Gheonea DI, Ciurea T. Quantitative contrast-enhanced harmonic EUS in differential diagnosis of focal pancreatic masses (with videos). *Gastrointest Endosc* 2015; **82**: 59-69 [PMID: 25792386 DOI: 10.1016/j.gie.2014.11.040]
- 60 **Săftoiu A**, Vilmann P, Gorunescu F, Gheonea DI, Gorunescu M, Ciurea T, Popescu GL, Iordache A, Hassan H, Iordache S. Neural network analysis of dynamic sequences of EUS elastography used for the differential diagnosis of chronic pancreatitis and pancreatic cancer. *Gastrointest Endosc* 2008; **68**: 1086-1094 [PMID: 18656186 DOI: 10.1016/j.gie.2008.04.031]
- 61 **Săftoiu A**, Vilmann P, Gorunescu F, Janssen J, Hocke M, Larsen M, Iglesias-Garcia J, Arcidiacono P, Will U, Giovannini M, Dietrich CF, Havre R, Gheorghe C, McKay C, Gheonea DI, Ciurea T; European EUS Elastography Multicentric Study Group. Efficacy of an artificial neural network-based approach to endoscopic ultrasound elastography in diagnosis of focal pancreatic masses. *Clin Gastroenterol Hepatol* 2012; **10**: 84-90. e1 [PMID: 21963957 DOI: 10.1016/j.cgh.2011.09.014]
- 62 **Marya NB**, Powers PD, Chari ST, Gleeson FC, Leggett CL, Abu Dayyeh BK, Chandrasekhara V, Iyer PG, Majumder S, Pearson RK, Petersen BT, Rajan E, Sawas T, Storm AC, Vege SS, Chen S, Long Z, Hough DM, Mara K, Levy MJ. Utilisation of artificial intelligence for the development of an EUS-convolutional neural network model trained to enhance the diagnosis of autoimmune pancreatitis. *Gut* 2020 [PMID: 33028668 DOI: 10.1136/gutjnl-2020-322821]
- 63 **Kuwahara T**, Hara K, Mizuno N, Okuno N, Matsumoto S, Obata M, Kurita Y, Koda H, Toriyama K, Onishi S, Ishihara M, Tanaka T, Tajika M, Niwa Y. Usefulness of Deep Learning Analysis for the Diagnosis of Malignancy in Intraductal Papillary Mucinous Neoplasms of the Pancreas. *Clin Transl Gastroenterol* 2019; **10**: 1-8 [PMID: 31117111 DOI: 10.14309/ctg.0000000000000045]
- 64 **Machicado JD**, Chao WL, Carlyn DE, Pan TY, Poland S, Alexander VL, Maloof TG, Dubay K, Ueltschi O, Middendorf DM, Jajeh MO, Vishwanath AB, Porter K, Hart PA, Papachristou GI, Cruz-Monserrate Z, Conwell DL, Krishna SG. High performance in risk stratification of intraductal papillary mucinous neoplasms by confocal laser endomicroscopy image analysis with convolutional neural networks (with video). *Gastrointest Endosc* 2021 [PMID: 33465354 DOI: 10.1016/j.gie.2020.12.054]
- 65 **Pereira SP**, Oldfield L, Ney A, Hart PA, Keane MG, Pandol SJ, Li D, Greenhalf W, Jeon CY, Koay EJ, Almario CV, Halloran C, Lennon AM, Costello E. Early detection of pancreatic cancer. *Lancet Gastroenterol Hepatol* 2020; **5**: 698-710 [PMID: 32135127 DOI: 10.1016/S2468-1253(19)30416-9]
- 66 **Poruk KE**, Gay DZ, Brown K, Mulvihill JD, Boucher KM, Scaife CL, Firpo MA, Mulvihill SJ. The clinical utility of CA 19-9 in pancreatic adenocarcinoma: diagnostic and prognostic updates. *Curr Mol Med* 2013; **13**: 340-351 [PMID: 23331006 DOI: 10.2174/1566524011313030003]
- 67 **Keane MG**, Shah A, Pereira SP, Joshi D. Novel biomarkers and endoscopic techniques for diagnosing pancreaticobiliary malignancy. *F1000Res* 2017; **6**: 1643 [PMID: 28944047 DOI: 10.12688/f1000research.11371.1]
- 68 **Ideno N**, Mori Y, Nakamura M, Ohtsuka T. Early Detection of Pancreatic Cancer: Role of Biomarkers in Pancreatic Fluid Samples. *Diagnostics (Basel)* 2020; **10** [PMID: 33291257 DOI: 10.3390/diagnostics10121056]
- 69 **Yang Y**, Chen H, Wang D, Luo W, Zhu B, Zhang Z. Diagnosis of pancreatic carcinoma based on combined measurement of multiple serum tumor markers using artificial neural network analysis. *Chin Med J (Engl)* 2014; **127**: 1891-1896 [PMID: 24824251]
- 70 **Kurita Y**, Kuwahara T, Hara K, Mizuno N, Okuno N, Matsumoto S, Obata M, Koda H, Tajika M, Shimizu Y, Nakajima A, Kubota K, Niwa Y. Diagnostic ability of artificial intelligence using deep learning analysis of cyst fluid in differentiating malignant from benign pancreatic cystic lesions. *Sci Rep* 2019; **9**: 6893 [PMID: 31053726 DOI: 10.1038/s41598-019-43314-3]
- 71 **Sadakari Y**, Ohtsuka T, Ohuchida K, Tsutsumi K, Takahata S, Nakamura M, Mizumoto K, Tanaka M. MicroRNA expression analyses in preoperative pancreatic juice samples of pancreatic ductal adenocarcinoma. *JOP* 2010; **11**: 587-592 [PMID: 21068491]
- 72 **Yoshizawa N**, Sugimoto K, Tameda M, Inagaki Y, Ikejiri M, Inoue H, Usui M, Ito M, Takei Y. miR-3940-5p/miR-8069 ratio in urine exosomes is a novel diagnostic biomarker for pancreatic ductal adenocarcinoma. *Oncol Lett* 2020; **19**: 2677-2684 [PMID: 32218818 DOI: 10.3892/ol.2020.11357]
- 73 **Alizadeh Savareh B**, Asadzadeh Aghdaie H, Behmanesh A, Bashiri A, Sadeghi A, Zali M, Shams R. A machine learning approach identified a diagnostic model for pancreatic cancer through using circulating microRNA signatures. *Pancreatol* 2020; **20**: 1195-1204 [PMID: 32800647 DOI: 10.1016/j.pan.2020.07.399]
- 74 **Cao Z**, Liu C, Xu J, You L, Wang C, Lou W, Sun B, Miao Y, Liu X, Wang X, Zhang T, Zhao Y. Plasma microRNA panels to diagnose pancreatic cancer: Results from a multicenter study. *Oncotarget* 2016; **7**: 41575-41583 [PMID: 27223429 DOI: 10.18632/oncotarget.9491]
- 75 **Li H**, Shi K, Reichert M, Lin K, Tselousov N, Braren R, Fu D, Schmid R, Li J, Menze B. Differential Diagnosis for Pancreatic Cysts in CT Scans Using Densely-Connected Convolutional Networks. *Annu Int Conf IEEE Eng Med Biol Soc* 2019; **2019**: 2095-2098 [PMID: 31946314 DOI: 10.1109/EMBC.2019.8856745]



Published by **Baishideng Publishing Group Inc**
7041 Koll Center Parkway, Suite 160, Pleasanton, CA 94566, USA

Telephone: +1-925-3991568

E-mail: bpgoffice@wjgnet.com

Help Desk: <https://www.f6publishing.com/helpdesk>

<https://www.wjgnet.com>

